Date: November 19th 2015

Literature evaluation of stimulation techniques worldwide & Modeling Thermal Stimulation

GeoCap WP 2.05

Authors:
Joost van den Broek
Nick Buik

Document number: GEOCAP/2015/REP/IF/WP2.05/20151119

COOPERATING COMPANIES & UNIVERSITIES

GEOCAP

Geothermal Capacity Building Program Indonesia - Netherlands

INAGA

University of Twente, Faculty ITC

IF technology

University of Indonesia

DNV GL

Gadjah Mada University

Technical University Bandung

Utrecht University, Faculty of Geosciences, Department of Earth Sciences

Delft University of Technology, Department of Geotechnology

Netherlands Organisation for Applied Scientific Research

Consultant	IF Technology bv
	P.O. Box 605
	6800 AP ARNHEM
	The Netherlands
	T +31 26 35 35 555 | N.Buik@iftechnology.nl
Contact person:	Mr Nick Buik

Colophon	Author:	Mr J.M. van den Broek
	Version:	1.0
	Checked by:	Mr N. Buik
	Released by:	Mr B. Pittens

TABLE OF CONTENTS

ABSTRACT

GEOCAP is a collaboration between Indonesia and the Netherlands aiming to increase and improve the amount of geothermal energy produced in Indonesia. The geothermal potential of Indonesia is regarded as one of the largest in the world, the country is therefore often dubbed a 'sleeping giant' in terms of geothemal energy production.

Workpackage 2.05: Hydro-fracturing and acidizing, is part of the GEOCAP project, it concerns reservoir stimulation and its use to enhance productivity of geothermal wells.

There are three main stimulation techniques in use today; hydraulic stimulation uses high fluid pressures to overcome rock strength and create fractures, increasing permeability and conductivity. Chemical stimulation uses acids to dissolve material and increase permeability and conductivity. Thermal stimulation involves the injection of cold fluids into a hot reservoir, inducing a thermal shock which lowers the effective strength of the rock creating fractures.

This report contains a literature evaluation of different techniques, their application worldwide and the success rate of these treatments. Literature on the Indonesian situation is rather limited, with only the Gunung Salak field being properly described in literature. Therefore the scope was increased to include any stimulated high enthalpy geothermal field.

Results from 97 treatments indicate that chemical stimulation was most widely utilised (51%) and had the highest average improvement rate (167%). However, thermal stimulation had a higher success rate than chemical stimulation (85% versus 72% respectively) and a decent average improvement (155%). It should be noted that improvement values for both techniques showed a large spread. Only 11 hydraulic stimulation treatments where found, therefore due to insufficient data no real conclusions are drawn for hydraulic stimulation.

Thermal stimulation was very effective but not as widely utilised (37% thermal stimulation treatments versus 51% chemical stimulation treatments). As to provide operators and planners with a viable alternative to chemical stimulation, an analytical model for thermal stimulation was (partly) constructed. The model is a first order approximation and can be utilised as a quick scan tool in order to evaluate the possible effectiveness of thermal stimulation treatments. It is not yet finished as completion requires an iterative procedure,

although initial results do look promising. One of the main observations from the modelling is that, for high reservoir temperatures, thermal stimulation can be a very effective stimulation technique due to the large thermal shock induced in the system.

In conclusion, it seems that under the right conditions, thermal stimulation can be very effective and as such can be utilised in combination with or alternative to other techniques.

1 INTRODUCTION

The Geothermal Capacity Building Programme – Indonesia-Netherlands (GEOCAP) is an international collaboration program between Universities, Knowledge Institutes and Industry, with IF Technology being one of the partners. It aims to develop geothermal programmes for education and training, research and subsurface databases (https://www.geocap.nl/) and is funded by the Dutch Ministry of Foreign affairs. This report will focus on parts of work package 2.05 of the GEOCAP programme: Hydro-fracturing and acidizing.

Drilling is a major expense in geothermal projects and reduction of these costs will lead to a significant increase in project economy. By increasing well production or injectivity, significant amounts of money can be saved resulting in a more financially efficient venture. Increasing the production of the reservoir is usually accomplished by applying stimulation to the well and/ or reservoir. It leads to an increase in permeability directly around the well by removing or lowering of the skin. Lowering of the skin results in an increase in the injectivity or productivity indexes.

There are three general methods available for stimulation which are briefly outlined below and discussed in more detail in chapter 2.

- Hydraulic stimulation uses a (special) fracturing fluid, often a high density and- or viscosity liquid, to increase the pore fluid pressure around the well and fracture the surrounding rock (figure 1).
- Thermal stimulation is a technique where low temperature fluids (mainly water) are injected into the well. The resulting, thermal shock causes the rock to shrink, increasing the tension present in the rocks eventually resulting in fracture formation.
- Chemical stimulation uses acid to dissolve the rock or rock matrix surrounding the well and thus increasing the permeability.

The best type and method of stimulation depends on the local, in this case Indonesian, parameters such as geological setting, rock type and properties, state of stress in the reservoir, the current status, initial design and history of the well.

1.1 Objectives and approach

The main goal of GEOCAP WP 2.05 is to enhance productivity of geothermal wells by applying stimulation techniques. This report will cover part of this package and aims to investigate which stimulation techniques are available and which is most suitable for increasing the productivity of geothermal wells in Indonesia. In chapters 2, 3 and 4 evaluation of the current available literature on stimulation techniques and their uses worldwide as well as limited evaluation of literature and results of previous stimulated geothermal projects in Indonesia are presented. The evaluation shows that thermal stimulation has considerable potential as a stimulation method to increase geothermal energy production.

Chapter 5 provides a detailed review of an analytical model for thermal stimulation which aims to provide operators and planners with a quick way of estimating the possible potential of a thermal stimulation treatment. The model will incorporate thermo-elastic and poro-elastic stress changes which result from cold fluid injection. The purpose of the final model is to perform indicative calculations in the first phases of stimulation treatment planning. It will give a rough first order approximation of the effectiveness of a thermal stimulation treatment. For more detailed analysis of the stimulation job and actual planning, more advanced (e.g. commercial) software should be utilised.

Other types of stimulation, such as hydraulic, chemical and acoustic stimulation will not be modelled because either there is already (commercial) software available (e.g. MFrac, commercial software for modelling of hydraulic stimulation), the process is difficult to model (e.g. chemical stimulation) or the technique is hardly used (e.g. acoustic stimulation). For details regarding the various numerical models regarding geothermal reservoir simulation, the reader is referred to (O'Sullivan et al., 2001).

It is important to note that this rapport defines two types of stimulation, wellbore and reservoir stimulation.

- Wellbore stimulation concerns stimulation of the wellbore itself. This often involves removal of scaling or other wellbore damage.
- Reservoir stimulation concerns stimulation of the reservoir outside the wellbore. This can include near wellbore formation damage, but also newly formed fractures.

This report only deals with reservoir stimulation.

2 Overview of stimulation techniques

The different kinds of stimulation of any reservoir, be it of a hydrocarbon or a geothermal system, can (generally) be grouped into three general types: hydraulic, thermal and chemical stimulation. Stimulation based on other physical principles are, in this report, grouped under unconventional stimulation techniques. They have seen limited use or are in development, but these are not as widespread as the three main techniques they are only briefly mentioned in this report.

The three general stimulation techniques have been (partly) developed by the hydrocarbon industry. However, applying them to high temperature geothermal systems involves different processes as reservoir temperature in these geothermal systems is (generally) much higher than the reservoir temperature of a hydrocarbon reservoir. Also, water has different flow properties than oil or gas.

2.1 Hydraulic stimulation

Hydraulic stimulation is the most widely used stimulation technique in the oil and gas industry for improvements in productivity rates. It is based on the principles of rock failure, if the pressure inside the reservoir is larger than the tensile strength plus the minimal horizontal stress, fracturing will occur (equation 2.1). The pressure required to keep the fracture open is the pore fluid pressure (the sum of the in-situ and the applied pressure at the reservoir) minus the tensile strength of the rock and the minimal principal stress (equation 2.1)

$$(\mathrm{P_{ini}} + \Delta\mathrm{P_{tot}}) - (\sigma_{\mathrm{Ten}} + \sigma_{\mathrm{h,min}} + \Delta\sigma_{\mathrm{inj}}) > 0 \qquad [2.1]$$

$\mathrm{P_{ini}}$ = Initial reservoir pressure (generally assumed to be hydrostatic) [Pa]
$\Delta\mathrm{P_{tot}}$ = Pressure change due to injection [Pa]
σ_{Ten} = Tensile rock strength [Pa]
$\sigma_{\mathrm{h,min}}$ = Minimal horizontal stress [Pa]
$\Delta\sigma_{\mathrm{inj}}$ = Stress change due to injection [Pa]

figure 1
Schematic overview of a reservoir which is being hydraulically stimulated. Note that this is a schematic for a shale gas/ thight gas reservoir. The principles and procedures, however, remain the same (from: *http://en.skifergas.dk/technical-guide/what-is-hydraulic-fracturing.aspx*)

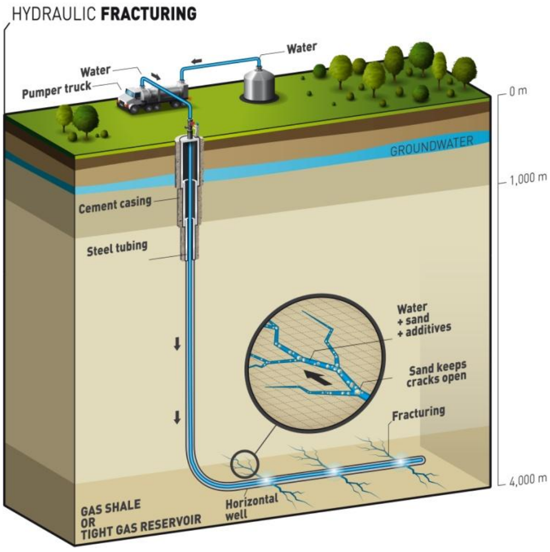

These fractures increase the permeability and conductivity of the reservoir and thus improve the productivity/ injectivity of a well (figure 1). Practically, these fractures are formed by injecting a fracturing fluid into the reservoir at a high rate. This leads to an increase in reservoir pressure, as the reservoir cannot absorb the amount of injected fluid. Details on these frac fluids are beyond the scope of this report and many service companies have designed their own fluids.

Formed fractures are generally assumed to be mode I cracks (

figure 2) as all modelling software available is based on mode I cracks initiating fractures. Although there is often a (small) shear stress component, this is only deemed relevant for shear fracs, in EGS or shale gas reservoirs.

When fractures are initiated and opened, most often a proppant is injected into the fractures to prevent closing. The materials used are mainly natural sand and man-made ceramic or bauxite. Many different (sub) types exist and for further information the reader is referred to other literature (e.g. Economides and Martin, 2007). Sand is generally used at closure pressures below ~ 400 bars and the ceramic or bauxite proppants are used above such pressures. These ceramic or bauxite proppants are generally very expensive, often comprising a third to half of the total costs of a hydraulic 'frac' job.

figure 2
The three different fracture modes by which fractures are initiated. This report assumes all fractures are formed by mode I cracks.
https://en.wikipedia.org/wiki/Fracture_mechanics#/media/File:Fracture_modes_v2.svg

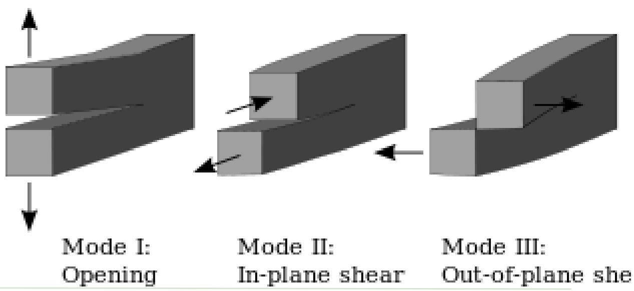

Needless to say, properties of the reservoir are of significant importance as they control the final geometry of the induced fractures. Reservoir permeability is not only of great importance for production of a reservoir, but also in the determination of the treatment schedule. It is generally well known or relatively easy to obtain. If the permeability is high, short wide fractures are required , whereas long thin fractures are needed for low permeability reservoirs.

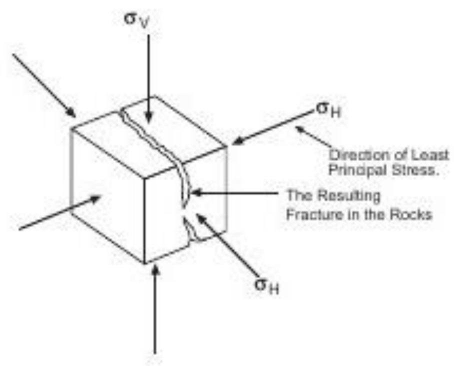

σ_v = Vertical stress
$\sigma_{h,min}$ = Minimum horizontal stress
$\sigma_{h,max}$ = Maximal horizontal stress

figure 3
Three dimensional representation of the principal stresses present in a reservoir and their relation to fracture formation.

From: *http://www.oilngasdrilling.com/category/formation-pressures*

Data on the current state of stress in the reservoir is also crucial, as the fracture initiation pressure depends (largely) on the value of the minimal principal stress. Also the orientation and magnitude of the three principal stresses control fracture dimensions as well as the direction to which it grows (Economides and Nolte, 2000). As is well known from rock mechanics, fractures (in an isotropic reservoir) will open perpendicular to the minimum horizontal stress (figure 3). In a normal stress regime, this implies vertical fractures propagating parallel to the maximum horizontal stress. The difference in magnitude between the maximum and minimum horizontal stress is called the differential horizontal stress. If this differential horizontal stress is high, the fracture will propagate in the general direction of the maximum horizontal stress. The direction will tend towards the azimuth of the maximum horizontal stress when the differential stress increases. Should the differential horizontal stress tend towards zero, then the fracture could theoretically propagate in any direction.

Vertical stress is usually the result of overburden pressure and as such is dependent on the density of the overlying strata. Magnitudes of the maximum horizontal stress can be determined (Zoback et al., 2003), although this does require specific logs to be run. Minimum horizontal stress can be calculated using Eaton's equation and the Poisson's ratio (Eaton, 1969). The Poisson's ratio is the ratio of the transverse strain to the axial strain when a certain amount of stress is applied.

For fracture dimensions, the Young´s modulus is an important factor. With thinner longer fractures developing for a higher value of E. It should be noted that the Young's modulus is part of the modulus of elasticity, which further consists of the Bulk and Shear modulus. As these moduli are elastic, they are only valid for elastic deformation up to failure. The three moduli are related to each other and the Poisson's ratio and as such that two of them can be determined when the other two are known, for more details regarding elastic moduli and their definition the reader is referred elsewhere (e.g. Jaeger et al., 2007).

Fracture toughness and tensile strength of a rock are measures of the amount of energy or pressure required to fracture it and are relevant for fracture initiation. The tensile strength is rather small in comparison with the compressional or frictional strength of rock. If the formation already contains fractures, the tensile strength can be assumed to be (close to) zero.

Shear fractures

As mentioned above, ´classic´ hydraulic stimulation is done in a reservoir where there is very little to no shear stress component present and involves mode I cracks and (usually) proppant. However the high price of these hydraulic frac jobs make them sometimes unattractive for reservoirs which do not produce enough economic revenue or require a high number of fractures (such as for instance an EGS project). In these cases stimulation by shear fractures becomes interesting.

Shear stimulation uses shear displacement on irregular fracture surfaces to create a self-propping fracture. The theory is that due to misalignment of the jagged fracture face, conductivity and permeability are improved. As it requires no proppant, this technique is significantly cheaper, although certain pre-requisites are required for it to work.

Due to the fact that, generally speaking, the tensile strength of most rocks is lower than their shear strength, shear stimulation usually requires some pre-existing fracture network that is favourably oriented (McClure, 2012; McClure and Horne, 2012). As the name suggests, shear fracs also require a (significant) shear stress component, which means that the principal differential stress must be high and anisotropic. The anisotropy is a requirement for slip to occur. Fracturing fluids are injected into the reservoir below the critical opening pressure (McClure and Horne, 2012), which is usually the magnitude of the minimum horizontal stress (equation 2.2). Subsequent fracture formation is controlled by the Mohr-Coulomb failure theory.

$$P_{ini} + P_{bfp} = \sigma_{Ten} + \sigma_{h,min} \qquad [2.2]$$

P_{ini} = Initial reservoir pressure [Pa]
P_{bfp} = Bottomhole flowing (applied) pressure [Pa]
σ_{Ten} = Tensile rock strength [Pa]
$\sigma_{h,min}$ = Minimal horizontal stress [Pa]

Should the pressure rise above this opening pressure, then both opening mode as well as shear mode stimulation will occur.

Quantifying the permeability and conductivity increase of a shear frac job is rather difficult as the rough fracture faces are of course unpredictable which leads to unpredictable results. However, it is rather well known that this type of stimulation works best in hard rock environments such as an EGS project, as slip-permeability coupling is much more common in these lithologies (Lee and Cho, 2002). Displaced fractures in a hard rock environment are also likely much more resilient to fracture healing and diagenetic processes such as dissolution precipitations, pressure solution and dislocation/ diffusion creep.

2.2 THERMAL STIMULATION

A frequently used technique in geothermal reservoirs and wells, thermal stimulation uses thermal shock to initiate fractures in the surrounding rock and thus improve the permeability and conductivity of the near-well strata and often also the reservoir. Thermal shock is produced by injection of cold fluids into a (hot) well/ reservoir, the resulting thermo-elastic stress change results in contraction of the rock leading to the initiation of fractures.

Use of this technique is rather widespread in the geothermal industry, it is one of the standard methods in Iceland (Axelsson et al., 2006) and it has been utilized successfully in i.a. New Zealand, Indonesia, Mexico and Japan (Siratovich et al., 2011). Its application in the hydrocarbon industry is, however, not as widespread. Thermal fracturing is an often undesired side effect of water flooding during conventional hydrocarbon production and as such work has been done to prevent this (de Koning, 1988). It should be noted, however, that its application in unconventional gas shale's shows promise (i.a. Enayatpour and Patzek, 2013).

The limited use of thermal stimulation techniques in the hydrocarbon industry, besides the risk of undesired fracturing leading to loss of hydrocarbons, could be due to the relative low reservoir temperatures. Hydrocarbon reservoir temperature is generally not very high, from a thermal stimulation standpoint, low reservoir temperatures mean less temperature difference between the reservoir and the injected fluid. This translates into less thermo-elastic stress change, meaning thermal stimulation is (significantly) less effective in these lower temperature environments. Conversely based on these principles, (high temperature) geothermal systems are suitable candidates for thermal stimulation as the thermal shock from cold fluid injection is much higher.

Thermal stimulation is considered a low injection pressure technique (Siratovich et al., 2011), as its goal is not to hydraulically fracture the formation, but to exploit thermo-elastic stress changes due to thermal shock. Injection pressures for thermal stimulation generally range from 10-60 bars at the wellhead (Flores and Tovar, 2008; Kitao et al., 1995), whereas for hydraulic fracturing operations injection pressures can exceed 400 bars (Legarth et al., 2005). This large difference in injection pressures is due to temperature effects. Due to thermal shock effective stress in the reservoir rock will decrease, lowering the fracture initiation pressure.

Temperature of injection fluids range from 20 °C up to ~ 150 °C and are mainly controlled by what is locally available (fresh/ sea water or separated geothermal brine/ condensate) (Bjornsson, 2004; Pasikki et al., 2010). When sea water is used, scaling agents have to be added in order to prevent scaling and precipitation inside the wellbore (e.g. Tulinius et al., 2000).

There is no current preferred methodology or standard operating procedure for execution of a thermal stimulation job. Details regarding design and implementation are usually controlled by available surface infrastructure, well completion details and the type and volume injection fluids available. However, despite these variables, most stimulation procedures described in literature are either cyclic in nature or long term sustained injection.

The latter is, as the name suggests, involves the sustained injection of cold fluid into the well for a variable period up to months. It is most often done on injection wells, and has shown to result in significant improvement of the injectivity index (Siega et al., 2009).

Cyclic injection of cold fluids into the wellbore is often done on production wells and has also demonstrated its effectiveness as a stimulation technique on multiple occasions (Axelsson et al., 2006). Here the cold fluid is injected into the wellbore for a certain period after which the well is allowed to heat up, timescales of injection and recalibration vary significantly. Subsequent repeating of this cycle and thus repeating of thermal shocks leads to stimulation (Siratovich et al., 2011).

2.3 CHEMICAL STIMULATION ("ACIDIZING")

Widely used in the hydrocarbon industry, chemical stimulation, or acidizing, involves the injection of reactive acids into the wellbore to enhance permeability and conductivity and lower the skin. The technique is generally used for near wellbore stimulation and wellbore cleanup as the reactive nature of the acid generally prevents stimulation far into the reservoir.

There are two general types of chemical stimulation (Portier et al., 2007): matrix acidizing and fracture acidizing.

- In matrix acidizing the reactive fluid is injected below fracturing pressure and is mainly used for wellbore clean-up and near wellbore permeability and conductivity enhancement. Although technically not reservoir stimulation, this (near) wellbore technique is very widely used in the event of wellbore damage or clogging of the well.
- In fracture acidizing pressures are above the fracturing pressure and is therefore technically a combination of hydraulic fracturing and acidizing (figure 4). The formed fractures are etched by the solvent making the use of proppant unnecessary.

In both matrix and fracture acidizing so called 'wormholes' can develop. These are acid-etched channels which preferentially consume the acid resulting in long 'corridors' in a runaway reaction that stops when the acid is spent. For matrix acidizing these are desirable, as the wormholes bypass damage. However, in fracture acidizing wormholes are detrimental as they divert live acid away from the fracture network resulting in a reduced etched fracture length.

Generally, there are two types of acid that are used; HCl and HF. These generally are mixed into the injection fluid at concentrations varying from 5 - ~15% (Economides and Nolte, 2000). The HCl is used when it concerns a carbonate reservoir whereas the HF is used when it concerns a sandstone reservoir, as the latter acid is more adept at dissolving sillica's, clays and feldspar. Some organic acids are sometimes used for more specific acid jobs (Economides and Nolte, 2000; Portier et al., 2007). As most geothermal reservoirs are in volcanic reservoirs, the main fluid used in geothermal systems is an HF solution.

Being one of the most widespread techniques in the oil and gas industry, many service companies have developed a large selection of commercial acidizing fluids.

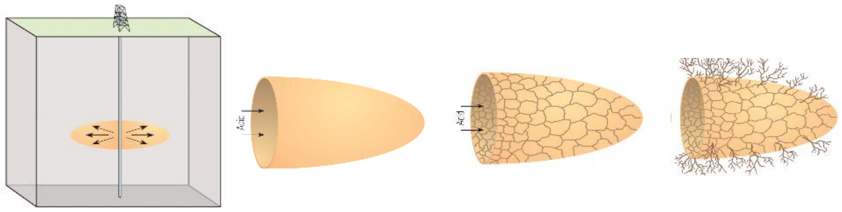

figure 4

Overview of acid fracturing principles. From left to right: rock is hydraulically fractured, acid is pumped into the fracture acid etches the fracture, and acid creating conductive wormholes. (Al-Anzi et al., 2003).

An acid stimulation operation generally consists of three phases, a pre-flush, main flush and over-flush. The aim of the pre-flush is to establish an injection rate and displace brine present in the wellbore, this is generally done with an HCl solution. Damage removal and/or stimulation is then carried out by the main flush. Liquids are often a mixture of HCl and HF at varying concentrations. The over-flush, usually done with fresh water or a (weak) acidic solution, is done to remove any still active acid and any reaction products from the wellbore (Schulte, 2008).

Although effectively applied at several geothermal fields (Akin, 2015; Jamies-Maldonado and Sánchez-Velasco, 2003; Pasikki et al., 2010; Pasikki and Gilmore, 2006), the high temperatures typically encountered in these fields pose several potential problems.

Many standard HCl acid inhibitors are only effective up to ~150 °C, whereas many of these fields have much higher reservoir temperatures, which also means that reaction rates of the acid are speeded up and live acid is spent earlier (Flores-Armenta et al., 2005). To counter this problem, several studies report that the wellbore was first cooled off to a lower temperature before the acid was injected (Akin, 2015; Pasikki and Gilmore, 2006). This might result in some unplanned thermal stimulation as well.

2.4 Unconventional methods

Besides the techniques outlined in section 2.3, there are several other methods which have been used for reservoir or wellbore stimulation. Uses of these methods are not or where not widespread due to a variety of reasons. Some of the newer technique's are still in a developing phase whereas some of the older techniques where not effective.

Explosive stimulation

The use of explosives as a means to enhance permeability in a reservoir was done mainly in the 1970's and 1980's. It has been applied at the Geysers field in California (Hanold, 1980), where a decrease in skin was observed. However, the permeability-thickness was reduced by 35% (Entingh, 2000). The main problem with this type of stimulation was that the energy was released so fast that it really only resulted in near wellbore damage, experiments were conducted using high energy gas fracturing (HEGF). In this technique slower burning propellant was used so the expanding gasses had time to form fractures (Aqui and Zarrouk, 2011; Entingh, 2000).

HEGF has also been tested in Iceland (Sigurdsson, 2015), where it was successful in (slightly) increasing the near well transmissivity. The authors had hoped for a larger increase based on initial testing, but also noted that the current observed boost could be due to other factors such as high injection rates during post stimulation circulation and low temperatures of injectate.

Jet stream stimulation

By using a high pressure water jet, jet stream stimulation can form fractures or tunnels in the reservoir. Further fracture propagation can then continue at the tips of these fractures. It should be noted that this technique is likely at its most effective in relatively soft reservoirs.

In addition, the high velocity water could possibly remove scaling and other types of wellbore damage, making it a good candidate for wellbore cleaning. Application of this technique is not widespread, but some studies have reported its use (Hernandez et al., 2013).

Electric stimulation

The use of electricity as a means of reservoir stimulation is still in its infancy. However, as a potential tool for wellbore cleaning it has already shown great promise (Nitters *pers. communication*, 2015). By releasing up a significant charge between two electrodes, very short powerful pressure waves can be generated (Baterbaev and Bulavin, 2002; Chen et al., 2012), making it technically a form of acoustic stimulation. Smaller charges can also be generated, possibly by using the metal casing of a wellbore, to induce electric shocks that increase the stress on both the casing and the reservoir, leading to cleaning of scaling and possibly fracture initiation. However, the complications of this technique when used in a fluid rich geothermal reservoir are unknown.

Acoustic stimulation

Use of acoustic methods for cleaning of everyday applications such as water filters or in dental equipment shows that this method has potential as a reservoir stimulation tool. The technique has a high and low power frequency variant (Cidoncha and Ignacio, 2007). High power frequency waves are mainly used for wellbore stimulation and cleanup as the high frequency (~20 kHz) results in high acoustic adsorption and the effect is thus confined close to the source.

Low power frequency waves (~40 Hz) are effective over larger distances, and thus are better suited for reservoir stimulation. They are often applied using surface vibrators (Cidoncha and Ignacio, 2007).

2.5 SUMMARY OF STIMULATION TECHNIQUES

table 1 gives an overview of all the stimulation techniques treated in sections 2.1-2.4 along with various advantages and disadvantages of each technique. A column with possible applications is also included. It is stressed that table 1 is in no way a complete table and it should not be solely relied on for site selection criteria. It is merely a summary of pro's and cons of the techniques described above.

The four techniques described in section 2.4 are included, but the pro's and cons are somewhat limited in scope and possible applications should be tentatively interpreted. This is due to the limited data and experience available for these techniques. They are merely there to indicate that innovation and development in this field is ongoing.

Stimulation technique	Pro	Con	Possible applications
Hydraulic	Effective in tight formations Good modelling software available	Proppant problems under high P&T conditions. High water usage	Low permeability formations with moderate temperatures.
Thermal	Low costs Low environmental risk, Easy to use Low risk of formation damage	Relative long treatment times Limited experience Production wells uncertain	High reservoir temperatures In combo with other techniques to lower frac pressure.
Chemical	Low costs Easily available Low operating pressures	Limited fracture penetration Risk of corrosion and precipitation at high T	Near wellbore formation damage Clogged matrix
Explosive	No fluids and chemicals required Low costs Multiple fractures in single treatement	Limited fracture penetration. Relies on self propping fractures. Gas back flow can clog well	Chemically inert reservoirs (e.g. basalt) Limited fluid availability
Jet stream	Larger control on fracture initiation	Limited fracture penetration Limted experience	When precise fracture initiation is required
Electric	No fluids and chemicals required	Limited fracture penetration Limited experience	Limited fluid availability
Acoustic	No fluids and chemicals required	Very limited experience	Limited fluid availability Removal of clogging material

table 1

Overview of the pro's and con's of the different stimulation techniques and when could be utilised.

Note that this is not a definitive table for site selection, but only an indication of pro's and con's of each technique.

2.6 RISKS AND UNCERTAINTIES

Predictions for stimulation jobs always contain uncertainties and the implementation of the technique itself carries risks, economical, environmental and also, to some extent, for the local populations. This is inherent to any geological venture, scientific or commercial, whether it concerns geological mapping of an area, earthquake 'predictions' or exploitation of resources present in the Earth. Nevertheless, it is important to gain as much insight as possible into these risks and strive to minimize their impact on safety and operations.

Induced seismicity

One of the major risks to any stimulation job is induced seismicity. It is seismic activity that results from manipulation of stresses and strains in the Earth´s surface as a result of human activity. Although induced seismicity due to stimulation often has no negative effects on operations or surrounding communities, public perception of the number and magnitude of events and their safety is nevertheless very important. Seismic activity is a risk when the surface acceleration resulting from a seismic event is sufficient to damage population or infrastructure (Majer et al., 2007). This generally means that events with a magnitude $M_w < 1$ are not noticeable, however exceptions to this rule of thumb are possible.

Seismic activity, natural or induced, occurs when the stresses acting on a fault plane, fracture or rock volume are larger than the strength of such a feature. It has long been known that the creation of new faults requires significantly more stress than the reactivation of pre-existing ones.

Pore fluid pressure has a significant effect on fracturing, as pore fluids are generally incompressible. This means that it cancels some of the rock strength and lowers the failure stress. In fracturing operations this is of course the aim, as rock failure creates new fractures enhancing permeability and conductivity. However, if a pre-existing fracture is nearby or a system is in a critical stress state, the increase in pore fluid pressure can lead to failure and a (significant) seismic event. It is therefore paramount that during the design of any fracturing operation the regional stress field is characterised, faults are observed and rock mechanical information is gathered as this all will provide information concerning the risk of induced seismic activity.

All fracturing operations are accompanied by some sort of (micro)seismic activity, most of which is not noticeable ($M_w < 1$) (Ellsworth, 2013). For a significant seismic event (M_w > 4-5) to be felt on the surface, large amounts of slip must take place (in the order of kilometres)

(Majer et al., 2007). This is usually only the case when a pre-existing fault plane is reactivated. Geothermal reservoirs are often in tectonically active areas, meaning that the risk of tectonic activity (induced or natural) is significantly higher as stress levels are higher and the density of faults is also large.

Environmental risks

Many geothermal reservoirs are located in or near natural parks, as the surface manifestations of geothermal potential are often protected. Drilling and stimulation fluids almost always contain additives, which can vary from gels, breakers, acid and/or iron inhibitors, clays and many more. These fluids can result in significant groundwater pollution should they leach out of the wellbore into the groundwater or surface water table. As such these fluids pose a possible risk to the ecosystem. High temperature and pressure resistant proppants are often coated. Weathering of these coatings can result in pollution of production fluids or steam. Many wellbore's have a cemented steel casing, at least in the upper parts of the well, significantly reducing the risk of these leaching of these harmful substances into the local ecosystem. However, not all nations have legislation requiring cemented casings, making it sometimes attractive from an economic standpoint not to cement the casings in the wellbore.

Stress on the local environment and population as a result of 'normal' operations is also something that might have to be considered, as excessive noise due to steam production, increased (freight) traffic, generator and pumping noise can all impact the direct enviorment of the well.

Operational risks and uncertainties

Besides the seismic and environmental concerns, economic and operating risks are very important for the economic viability and the safety of onsite personnel. The high pressures required for fracturing operations pose risk inherent to the technique. Use of acids also presents dangers, as especially HF acid is one of the most dangerous acids currently used. The acid is usually mixed on site in large tanks, requiring well trained personnel with adequate equipment.

As mentioned before, the uncertainties that come with working in the subsurface are quite substantial and are never completely obviated. Low and uneconomic injectivity or production of a well can persist even after stimulation.

Precipitation and fine problems

Chemical reactions can cause precipitates which can clog the wellbore. This is especially the case for acid mixtures used in acidizing. Especially reactions of HF acids with sandstones or volcanic rocks can lead to precipitation of insoluble reaction products. The main reactions result in calcium fluoride (CaF_2), colloidal silica ($Si(OH)_4$), ferric hydroxide ($Fe(OH)_3$) and asphaltene sludges (Economides and Nolte, 2000). Additionally fines (small particles originating in the reservoir), scales (precipitation due to changing chemical conditions as a result of production) and swelling clays can also lead to an increased skin either by precipitation or flocculation.

Proppant problems

The high pressures encountered in the subsurface can lead to several problems with long term conductivity of proppant or self-propping fractures.

Proppant crushing mainly happens inside the reservoir due to high closure pressures, although damage at other stadia can also occur. Poor distribution can lead to higher stresses on the proppant grains and enhance crushing (Legarth et al., 2005). Composition plays an important role in this, as higher strength proppant retains higher conductivities longer (Weaver et al., 2007). The embedding of proppant into the fractured rock, embedment, is a function of the ratio of the proppant and rock strength and closure pressure in the reservoir (Legarth et al., 2005).

Diagenetic processes are also a factor leading to decreased permeability and conductivity. Rates depend on proppant size, reservoir temperature and closure pressure (Yasuhara et al., 2006). Reducing the reaction rate can be achieved by coating both the proppant and the fracture face with a dielectric, hydrophobic filming material, which reduces the geochemical reactions (Weaver et al., 2007).

Fracture healing is mainly relevant for self-propping fractures such as shear fracs. The rough fracture walls are of course in contact with each other. Pressure due to the closure stress on these contact points results in deformation and movement of material away from the stressed locations. This usually achieved by processes as dissolution and precipitation of minerals, pressure solution and, at high (> 300 °C) temperatures, dislocation or diffusion creep.

3 HIGH ENTHALPY GEOTHERMAL ENERGY – THE INDONESIAN SITUATION

3.1 GEOLOGICAL SETTING OF INDONESIA

In order to be able to adequately present and interpret data and details regarding geothermal fields in Indonesia, a general overview of the geological and tectonic setting will be presented below.

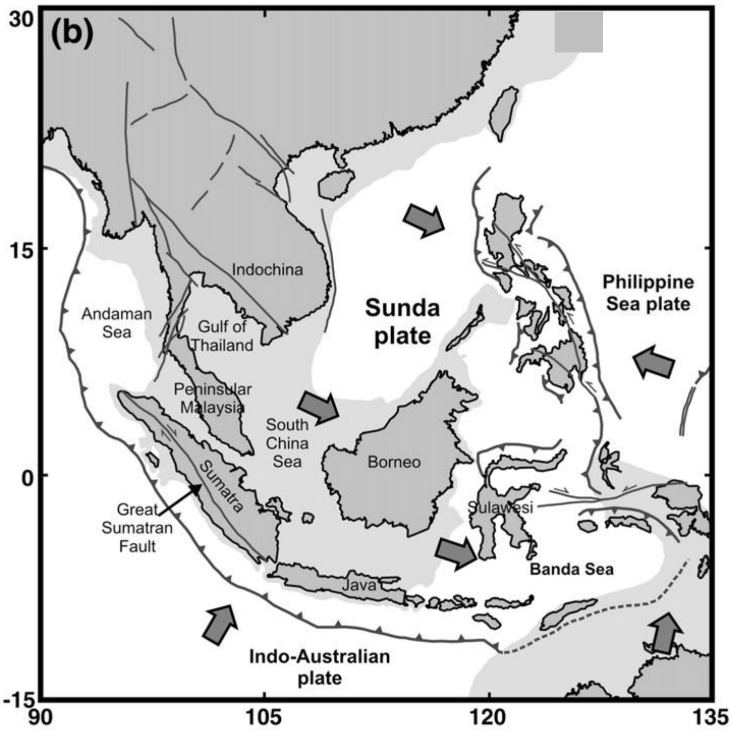

Located in south east Asia,

figure 5
Tectonic setting and geometry of the Sunda plate. Large arrow indicate absolute plate motions. Note the change in obliquity of subduction when going south from Sumatra to Java. From: *Hall and Morely (2004).*

Indonesia is part of the Sunda plate, which is one of the two major continental plates with the other being the Indo-Australian plate. A third region, which is part of the western Pacific plate, is comprised of a mosaic of microplates which are mainly oceanic in nature (figure 5). However, close to the margins of Australia, Sunda and Asia, the Pacific plate fragments have a continental character(Hall, 2002). The exact geometry of the plates in the region is still the source of some controversy (Tingay et al., 2010 *and references therein*). Absolute movement of the Indo-Australian and Pacific plates are NE and WNW respectively.

The absolute movement direction towards the ESE (figure 5). The core of the Sunda plate consists of Paleozoic and Mesozoic igneous, sedimentary and metamorphic rocks accreted as a result of closure of the Paleo and Mesotethyan oceans (Hall, 2002).

Situated in the south of the Sunda plate, the Sumatra arc is a classic example of an subduction zone morphology (Hall, 2002). This subduction zone is responsible for some of the largest seimic events in recent history (9.1 M_w 2004; 8.5 M_w 2007). Subduction along this zone has been going on since, at least, the late Paleozoic (McCourt et al., 1996), although some periods of inactivity are known . Movement in the northern part of the subduction zone is oblique and results in a movement orthogonal as well as parallel to the trench. The later results in strike slip movement along the Sumatra Fault system (e.g. (Fitch, 1972). For Java, the subduction becomes almost orthogonal to the trench (figure 1) and little to no trench parallel movement is observed (Hall, 2002). Subduction rate is estimated at around 6-7 cm/yr (Simandjuntak and Barber, 1996) and (re)startred, for Java, in the Middle Eocene (Hall, 2002).

Java

For Java, this subduction resulted in the formation of a Cenozoic volcanic arc. Volcanism in Western Java started on continental crust (Simandjuntak and Barber, 1996)(Setijadji, 2010). In Eastern Java, volcanism formed in pre-existing accreted arc crust. Paleogene structures where formed in an extensional and subsidence dominated tectonic setting. During Neogene times, the system was again placed under compression. During the Late Neogene Sunda orogeny, the volcanic arc was thrusted northwards over the older sediments with displacements for West Java estimated at roughly 50 km. Total displacement for East Java is uncertain although it seems it is much less than the movement in West Java (Clements et al., 2009). Central Java contains exposures of Cretaceous basement, the volcanic arc is not present. Clements et al. (2009) suggesting that the arc was thrusted northwards and subsequently removed by erosion.

Four main faults control the tectonic setting of Java, the E-W back-arc – thrust of Barabis-Kendeng, the NE-SW strike-slip fault of Cimandiri, the SE-NW Citandui fault in West Java and the NE-SW Central Java Fault (figure 6) (Hoffmann-Rothe et al., 2001).

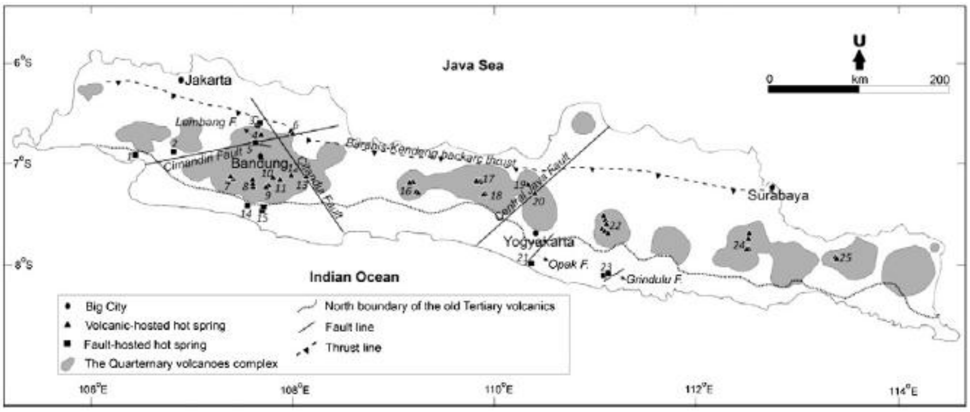

figure 6
Schematic structural map of Java. From: *Purnomo and Pichler (2014)*

The latter two faults are wrench faults and accommodated the northward movement of the volcanic arc in Central Java (Purnomo and Pichler, 2014).
The three regional segments of Java, west, central and east, each have a different geothermal potential. West Java has the highest potential and also by far the highest production. It is associated, on regional scale, with high crustal heatflow and crustal seismic activity (Setijadji, 2010). On smaller, district scale, it becomes clear that the majority of the big geothermal fields formed in and around volcano´s of Upper Pleistocene age. Further details regarding each field and their (Quaternary) geological setting will be presented further on.

Sumatra

Sumatra has a structural grain roughly parallel to its length and is underlain by a Carboniferous – Permian continental crust on which oceanic and continental terranes have since accreted (figure 7) (Pulunggono and Cameron, 1984; (McCourt and Cobbing, 1993); Simandjuntak and Barber, 1996). These terranes consist predominantly of basaltic to andesitic volcanic rocks and granites, associated volcaniclastic sediments and mostly marine sediments associated to the arc. Uplift of the Barisan mountains was the result of transpressive movements along the Sumatra Fault system during the Miocene and was accompanied by intrusions in the volcanic arc and subsidence and infill of the fore- and back-arc basins figure 7) (Simandjuntak and Barber, 1996).

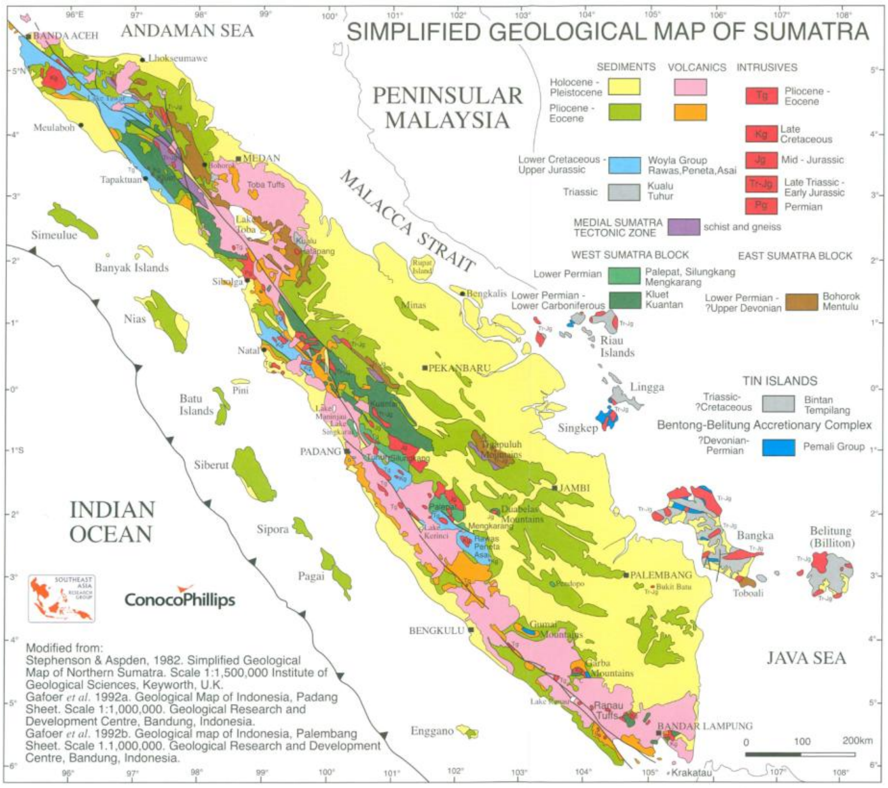

figure 7

Simplified geological map of Sumatra. Note the general orientation of the various units parallel to the length of the island and the structural layout of the island. The oldest, Upper Palaeozoic units in the centre of the Barisian mountains with younger units accreted against this core. From: *(Crow and Barber, 2005)*

3.2 GEOTHERMAL ENERGY IN INDONESIA

Indonesia currently has 7 locations where geothermal energy is being produced with a total production of around 1200 MW of electricity, as of 2011 (figure 8).The Directorate General of Geology and Mineral Resourses estimates the total potential of Indonesia to be 27.000 MW. As mentioned before, the most developed geothermal resources are on Java. With a production of approximately 1000 MW, it is the biggest producer of geothermal energy of all Indonesian islands. The most productive fields are located in Western Java and are located around Quaternary volcano's (Setijadji, 2010). As it has huge potential, Indonesia is often thought of as a sleeping giant in terms of geothermal energy production.

figure 8

Overview of the current producing geothermal plants in Indonesia.

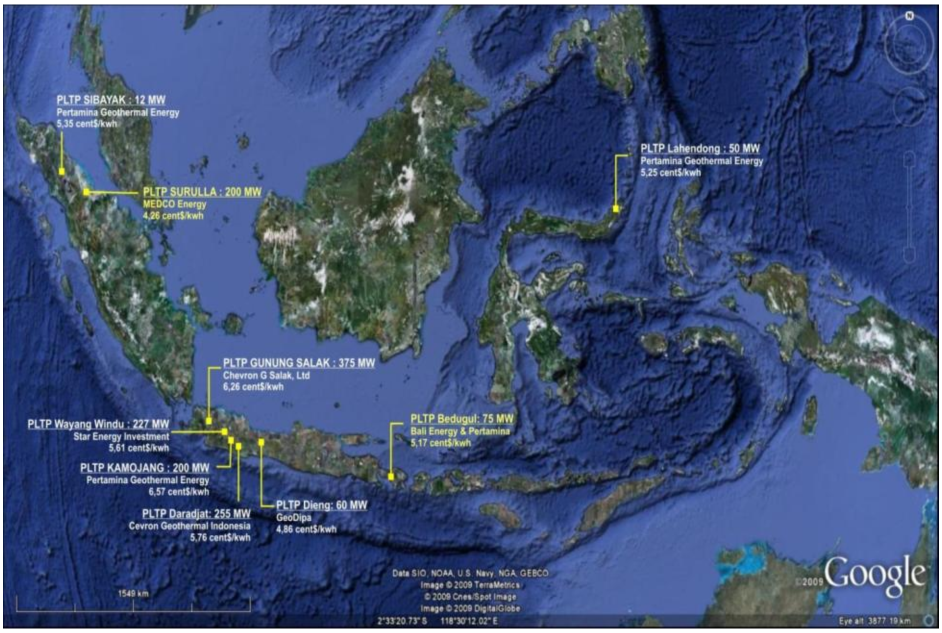

The 7 currently producing locations are, in descending order of productivity:

• Gunung Salak, Java	377 MWe production
• Darajat, Java	255 MWe production
• Wayang Windu, Java	227 MWe production
• Kamojang, Java	200 MWe production
• Dieng, Java	60 MWe production
• Lahendong, Sulawesi	60 MWe production
• Sibayak, Sumatra	12 MWe production

The Gunung Salak field is the largest geothermal field in Indonesia. It has also been extensively described in literature, both the field in general as well as details regarding different stimulation jobs. Whether the field is representative for other Indonesian fields is unknown at this time, however because the information on the Salak field is so readily available in literature, it is decided that the Gunung Salak field will be described in more detail.

3.3 OVERVIEW OF THE GUNUNG SALAK GEOTHERMAL FIELD

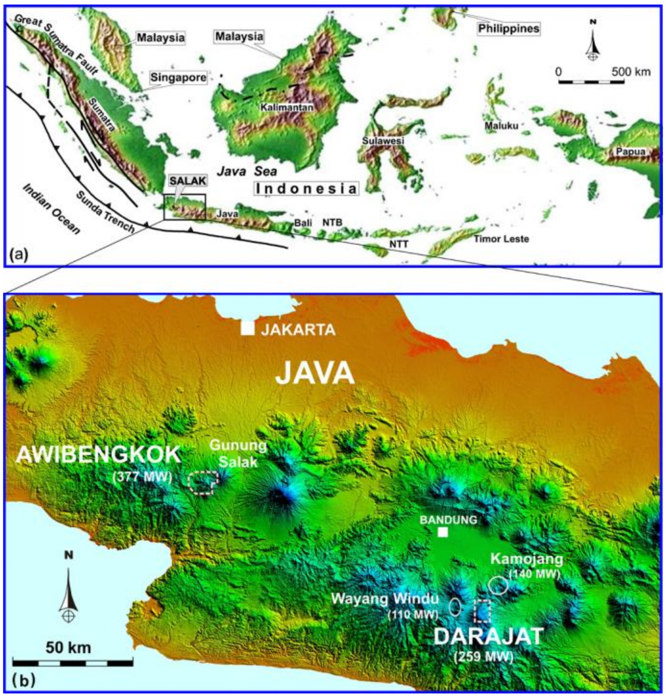

figure 9

Map showing the location of the Awibengkok/ Salak, Wayang Windu, Kamojang and Darajat goethermal fields in relation to major cities and volcanic centres (b) and their position in Indonesia (a). From: Stimac et al. (2008).

Located roughly 60 km south of Jakarta, the Salak geothermal field, sometimes also known as Awibengkok, lies known as Awibengkok, lies on the southwestern flank of the Gunung Salak volcano (

figure 9). It is the largest producer of geothermal power in Indonesia. The proven reservoir area for this field is 18 km^2 and it has an installed capacity of 377 MWe. It is currently managed by Chevron Geothermal Salak Ltd., which acquired the field in 2005. The field contains 81 wells, as of mid-2007. Of these 81 wells, 51 are used for production and 18 for injection (figure 11) (Stimac et al., 2008)

3.3.1 Geological setting and stratigraphy

The Salak geothermal system is bordered to the E, NW, SE and S sides by the inactive Gunung Salak, Gagak, Perbakti and Endut volcano's respectively. These peaks are the highest in the area and elevation ranges from 950 – 1500 m asl (above sea level). Towards the N and S, topography becomes more gentle with hills ranging in elevation from 600-950 m asl (figure 10). Further to the west, a collapsed stratovolcano, the Cianten Caldera, is present with a floor height of 850 – 950 asl. This Cianten Caldera is located west of the reservoir (figure 10) and was active from 1610 – 670 ka, based on unpublished K- Ar and $^{40}Ar/^{39}Ar$ dating done by Unocal/ Chevron on the ancestral andesitic cone (Stimac et al., 2008). From the same study (unpublished) it was determined that the Awibengkok area, which lies within the (exploited) reservoir (figure 10), was built up from 860 – 180 ka.

Inside the production area, the collapsed scars of the Kiaraberes cone have been partially filled by andesitic to rhyodatic tuffs and lavas deposited from 280 – 185 ka. These flowed downslope towards the west, southwest and north (figure 10). These tuffs and lavas are overlain by rhyolitic domes, lavas and related tephra sequences deposited from 120 – 40 ka (based on K- Ar and $^{40}Ar/^{39}Ar$ dating)(Stimac et al., 2008). Eruption of these sequences was mostly along a NNE – trending fault in the eastern part of the Salak field (figure 10). The NNE trend of this fault is similar to the inferred maximum horizontal stress as well as the dominant trend of major fractures from borehole image logs (Stimac et al., 2008). The 'Orange Tuff' tephra is the youngest silicic unit present in the area. It is dated to 40.000 and 8.400 years B.P. (before present) based on ^{14}C dating (Stimac et al., 2008) and is abundantly present in most of the exploitation area. Eruption is thought to have originated in a vent between Awi 1 & 14 drilling pads (figure 10) trending similar to the vent described above. However, overlying hydrothermal breccias prevent direct observation of this vent (figure 10 & figure 11). These breccias have a thickness varying from 10 – 4 m and are erupted close to the inferred Orange Tuff vent. Near Awi 14 (figure 10) hydrothermal breccias underlie the Orange Tuff, indicating that hydrothermal activity was taking place before the deposition of this unit (Stimac et al., 2008).

Dacite lavas thought to have erupted after the collapse of the Cianten Caldera suggest that its collapse occurred before 318 ± 14 ka. Combining this with the previously mentioned ages of the andesitic lavas forming the eroded caldera rim (1610 – 670 ka) indicate that the collapse occurred somewhere between 670 and 318 ± 14 ka (Stimac et al., 2008). Subsequent deposition of volcanic, sedimentary rocks overlain by lahars at the top filled the caldera. These lahars are dated, using ^{14}C dating, at 37 – 40 ka and are overlain by Tuffs from the Lower Brown and Orange Tuff sequence also present at Awibengkok (figure 10) (Stimac et al., 2008).

Stratigraphy of the reservoir is dominated mainly by andesitic and lesser basaltic lavas, breccias, tuff and lahar (Hulen et al., 2000; Stimac and Sugiaman, 2000).

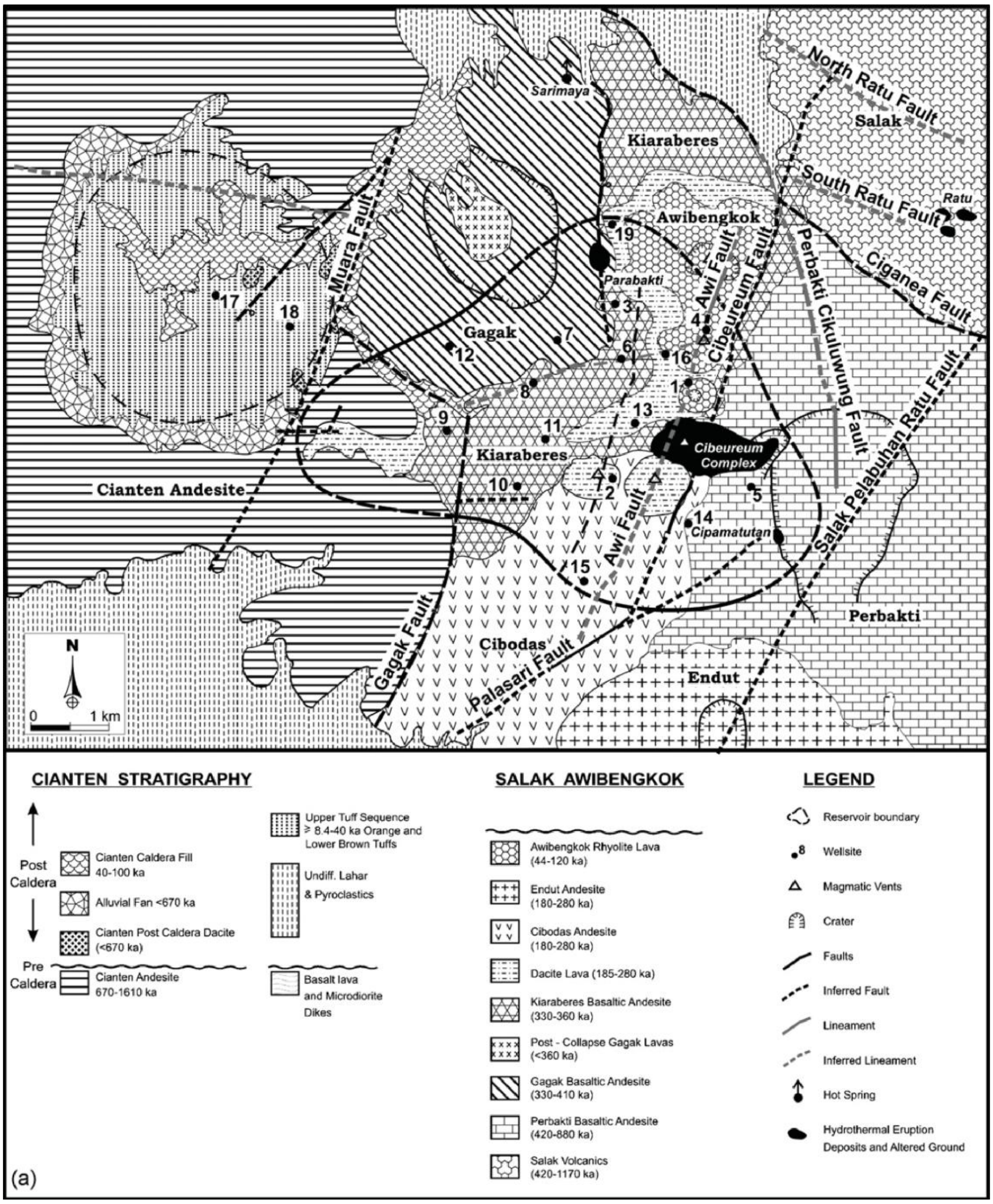

figure 10

Geological map of the Salak/ Awibengkok area showing major rock types, prominent faults and altered ground. Reservoir boundary, well locations and hot springs are shown for reference. Ages are in thousands of years (ka). From: Stimac et al. (2008).

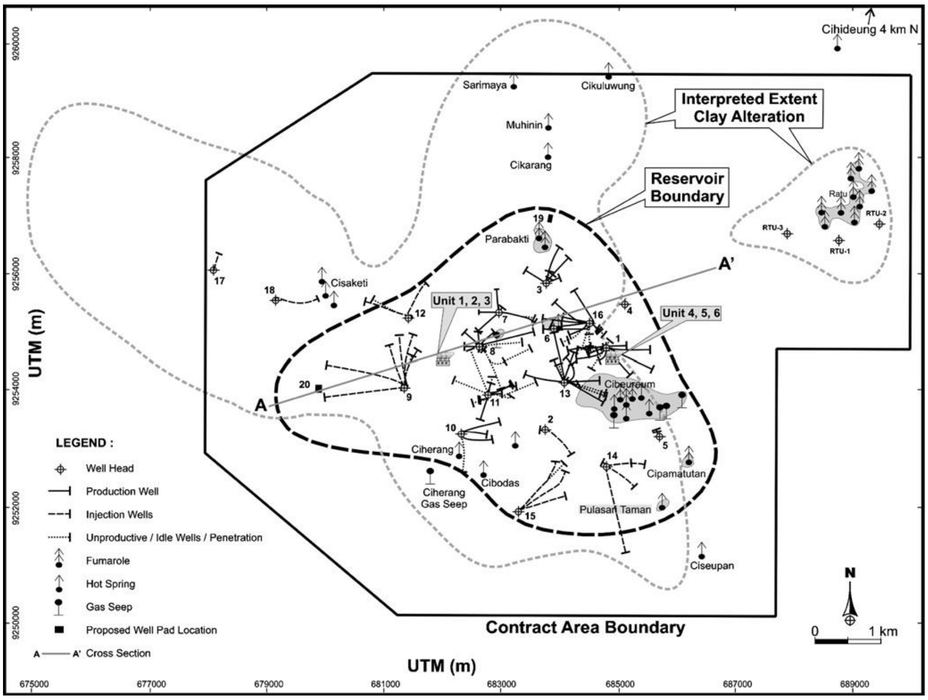

figure 11
Map of the Gunung Salak contract area (solid black line) with the commercial reservoir boundary (dashed black line) as well as thermal features. Wells are numbered based on the sequence of drill sites established. The clay alteration outlines possible areas for increasing the commecial reservoir. From Stimac et al. (2008).

Four major units can be identified in the stratigraphy (figure 12), it is thought that each of these units represents a discrete volcanic episode in the evolution of the Sunda Arc in west Java. Each unit can be subdivided into an lower andesitic part and an overlying rhyolitic or dactic part. These rhyolitic or dactic sections are likely the result of partially overlapping to separate, more silicic, volcanic events (Stimac et al., 2008).

The oldest rocks are shallow-marine carbonates and epiclastic sediments containing volcanic ash and lithic debris (figure 12). Cuttings from Awi 17-1 show that these basement rocks have been metamorphosed, by contact metamorphism, at depths of roughly 1-3 km as a result of intrusions in the Cianten Calera and western Awibengkok.

Consisting of andesitic to basaltic volcanics, the lower volcanic formation is interbedded with the Miocene sedimentary section (figure 12). It is thought that this episode marks the transition from marine to subaerial conditions (Stimac et al., 2008). This is overlain by the Rhyodactice Marker. This is the second widespread sequence present in the Awibengkok reservoir and consists of three thick rhyolitic to rhyodactic units that are separated by thinner beds of dactic and andesitic tuffs (figure 12). These units comprise the bulk of the western Awibengkok reservoir (Stimac et al., 2008).

The middle volcanic formation consists of a sequence of andesitic to dactic lavas, tuffs, lahars and debris flow (figure 12) formed by the lifecycle of stratovolcanos and lave and dome complexes (Stimac et al., 2008). It is the dominant lithological unit present in the eastern part of the field. The stratigraphy of the shallow part of the eastern reservoir is well observed in a continuous core from Awi 1-2 (Hulen and Anderson, 1998) and comprised the uppermost stratigraphic unit. It is composed of two parts; andesitic lavas, tuffs (lower part) and lahars (upper part) overlain by coarse epiclastic sediments and dactic lavas, domes and related breccias, tuffs and lahars also overlain by coarse epiclastic sediments. The presence of these sediments suggest a decline in volcanism as well as erosion of edifices or fault uplift of adjacent areas. Identified in a lot of wells (e.g. Awi 1, 2, 4, 9, 12, 17, 18), silicic to intermediate intrusive rocks are present at the Cianten Caldera (shallow) and along the eastern caldera wall.

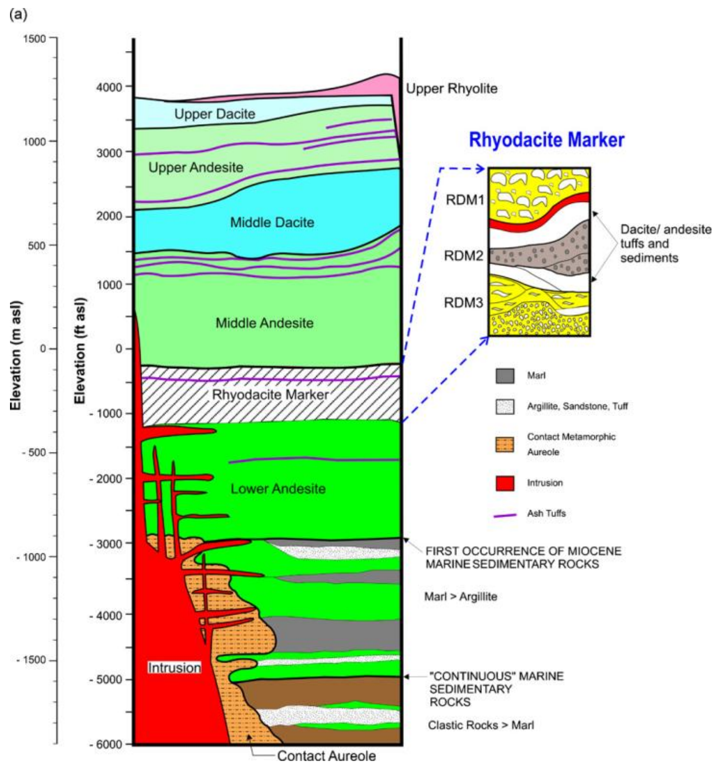

figure 12

Schematic stratigraphic column for the Awibengkkok reservoir. From: Stimac et al. (2008).

3.3.2 Reservoir and rock properties

Permeability at Awibengkok is, for the most part, controlled by the presence of a highly interconnected network of open/ partial sealed fractures. Porosity measurements where done on 87 core samples from wells throughout the field, but the main bulk of data was obtained from the Awi 1-2 continuous core (Hulen and Anderson, 1998).

These samples showed an average porosity of roughly 10,6%. Although it is a function of rock type, dense crystalline rock (lava flow and domes) has average value of 8.6% and breccias, tuffs and lahars have an average porosity of 13.1%.Trends in the obtained data show a declining porosity with depth (figure 13), it is likely explained by the compaction induced declining porosity of fragmental rocks with depth.

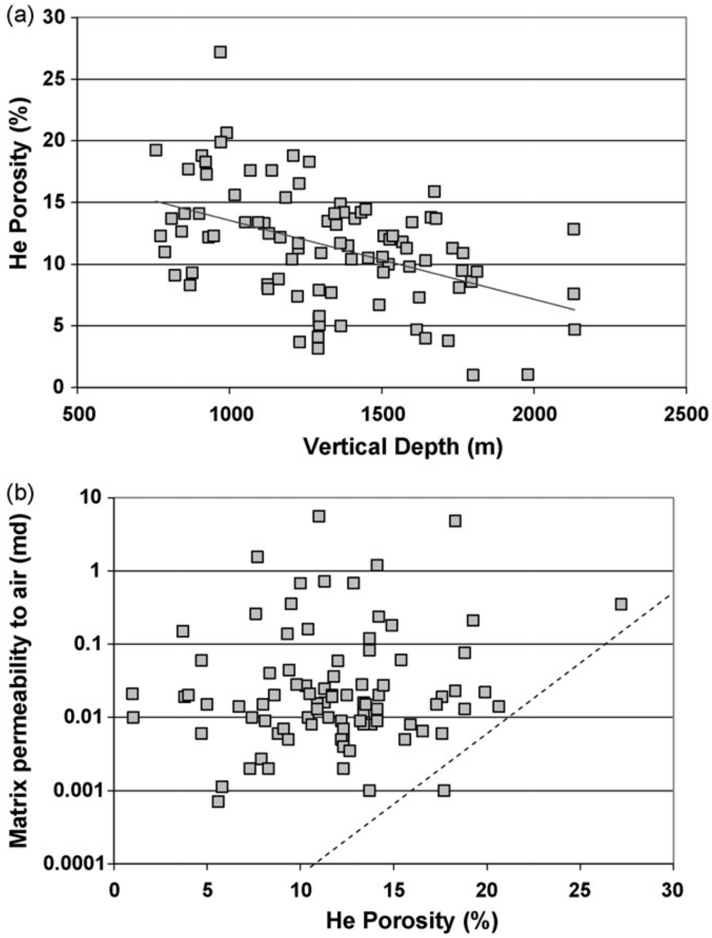

figure 13

Matrix porosity and permeability trends in the Awibengkok reservoir. (a) Matrix porosity to helium gas versus vertical depth. Not the declining porosity with depth. (b) Matrix permeability to air versus matrix porosity to helium gas. The dashed line represents the minimum matrix permeability as a function of increasing porosity. From: Stimac et al. (2008).

Twenty six samples from Awi 1-2 where analyzed with mercury injection capillary porosimetry (MICP). This technique averages roughly 1 porosity unit lower than conventional core porosity. Average pore size was 0.0338 µm ranging from 0.005 - 0.1 µmm.

Permeability was also determined at 0,0038 md using the MICP technique. Matrix permeability to air varied from <0,001 – 5.6 md with an geometric mean of 0.026 md. Both measurements where done on the same samples. Stimac et al. (2008) point out that one of the possible reasons for the lower MICP permeability is that the MICP technique does not measure permeability associated with partially sealed fractures, vugs, microchannels and hairline fractures when filled at low pressure. Poor correlation between porosity and permeability, however with increasing porosity the permeability also increases. Reason for this is the high pore volume geometrically requires connectivity and permeability (figure 13). The low matrix permeability and pore throat aperture of these samples imply that the matrix is likely to produce steam instead of water with declining pressures (Stimac et al., 2008).

3.3.3 Temperature distribution

The Salak geothermal field can be subdivided into four separate sectors, based on (subtle) variations in fluid (subtle) variations in fluid chemistry (Stimac et al., 2008)*. These sectors, or cells, are likely bounded by NNE bounded by NNE trending faults and are termed Western, Central, Eastern and Far Eastern cells (table 2*
Overview of the temperatures of the different cells and production/ injection wells present within that cell.

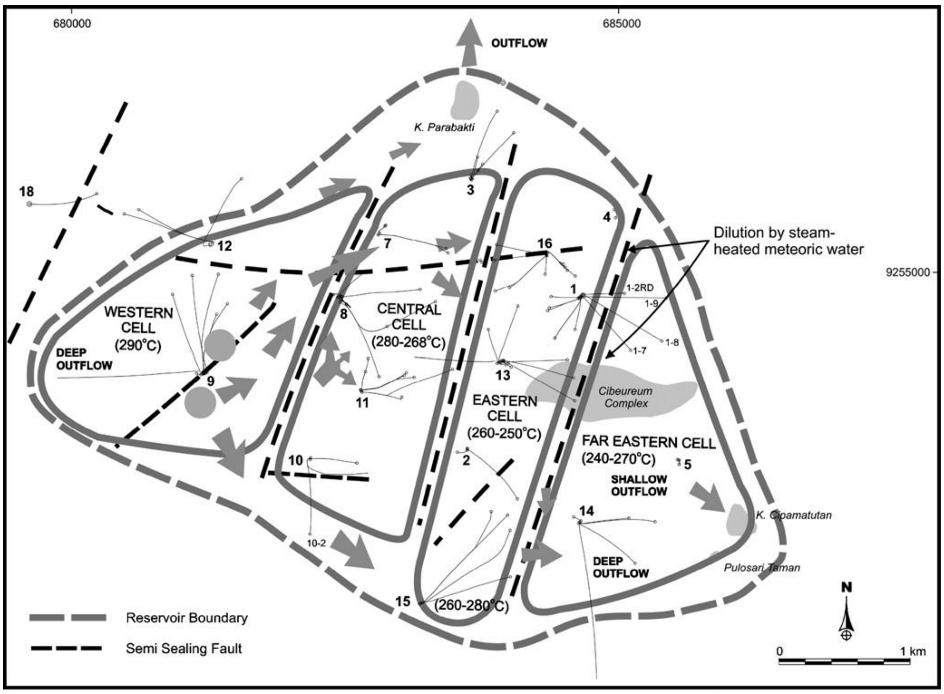

figure 14, table 2).

The western cell had the highest (initial) temperatures, which indicate it is a 'locus of deep fluid upflow' (Stimac et al., 2008). Chemical composition of the fluid and the results from modelling studies indicate that the central cell experienced gass loss resulting from long-term fumarolic emissions.

As the shallowest part of the Awibengkok reservoir, the eastern cell has higher temperatures in the south at Awi – temperatures in the south at Awi – 15. Dilution patterns from Awi – 16 to Awi – 13 suggests that meteoric or that meteoric or steam-heated water is descending along the structural zone that localized the most recent the most recent volcanic activity trending NNE (Stimac et al., 2008). *The Far Eastern cell is drilled by legs of drilled by legs of several different wells that cross the Awi and Cibeureum faults (table 2*

Overview of the temperatures of the different cells and production/ injection wells present within that cell.

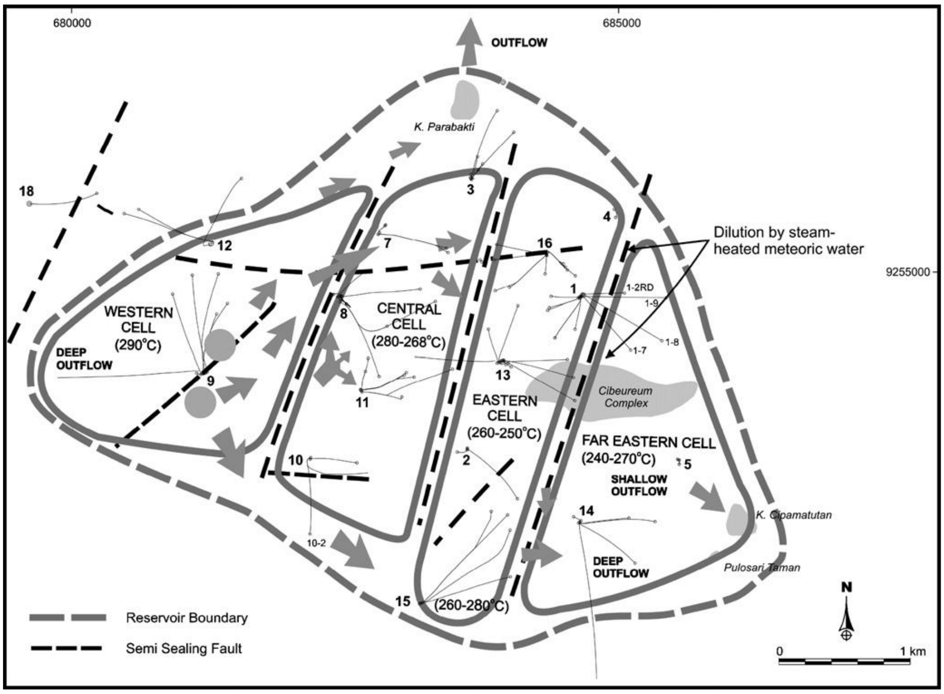

figure 14). As shown in table 2, it has a higher temperature then the adjacent Eastern cell.

	Western cell	Central cell	Eastern cell	Far E. cell

Wells in cell	Awi - 9	Awi - 7,8,10,11	Awi - 1,2,13,15*,16	Awi - 1-2RD, 1-7, 1-8, 1-9, 5, 14
Initial temperature	290 - 312 °C	270 - 280 °C	250 - 260 °C - 277 °C*	270 °C
NaKCa geothermometer	316 °C	260 °C	x	x
Quartz geothermometer	280 °C	280 °C	x	x

table 2

Overview of the temperatures of the different cells and production/ injection wells present within that cell.

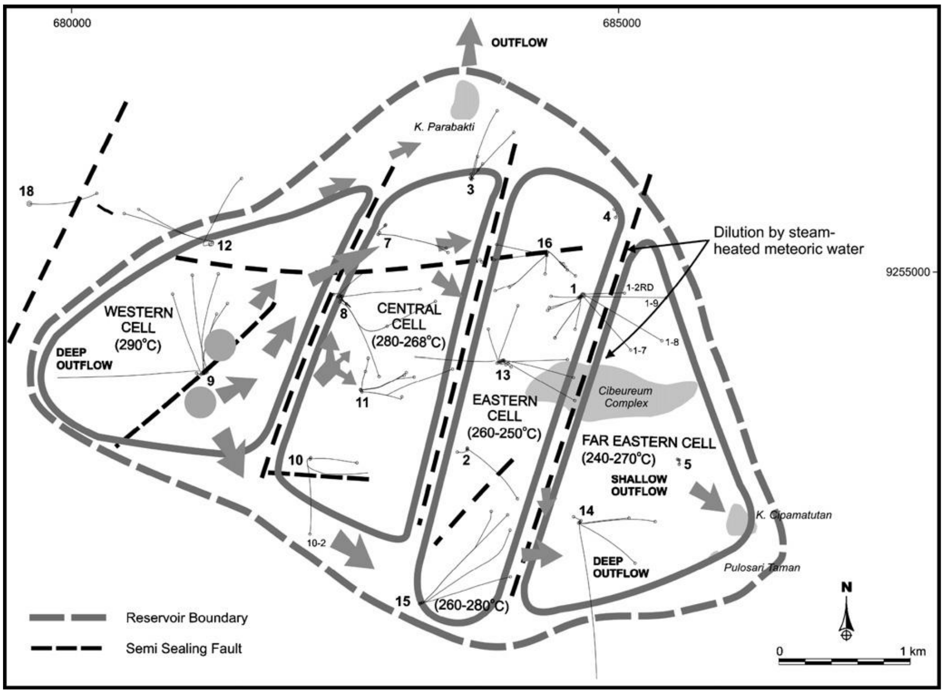

figure 14

Map of the Salak geothermal reservoir showing the four separate sectors. Each sector has distinctive temperature and fluid chemical signatures. Faults seem to play a major role as sector boundaries. Arrows indicate natural fluid flow direction, prior to production. From: Stimac et al. (2008).

3.3.4 State of stress in the reservoir

Based on photolineaments on satellite images and aerial photographs and orientation of faults observed in the field, structures in the Awibenkok area trend N-to-NE, NW and E-W (figure 15). Slip on these faults varies from normal dip-slip to strike-slip along N-to-NE trending structures (Stimac et al., 2008). Results from well leak-off tests, downhole image and density logs and apparent active fault offsets indicate a vertical principal stress and a maximal horizontal stress oriented NNE (roughly parallel to the convergence of the tectonic plates) (Sugiaman, 2003 *via* (Stimac et al., 2008). The ratio of min – max horizontal stress is 2:1 and thus anisotropic.

Focal mechanisms of microseismic activity also indicate an extensional stress state, which is consistent with the orientation of the structures and the other results mentioned above as well as the abundance of open fractures in the reservoir. The local stress state is slightly different from the regional interpretation. The regional state of stress has the maximal horizontal stress towards the N (Shemeta 1994 *via* (Stimac et al., 2008), whereas the local stress state indicates a maximal horizontal stress towards N20°E (Sugiaman 2003 *via* Stimac et al., 2008).

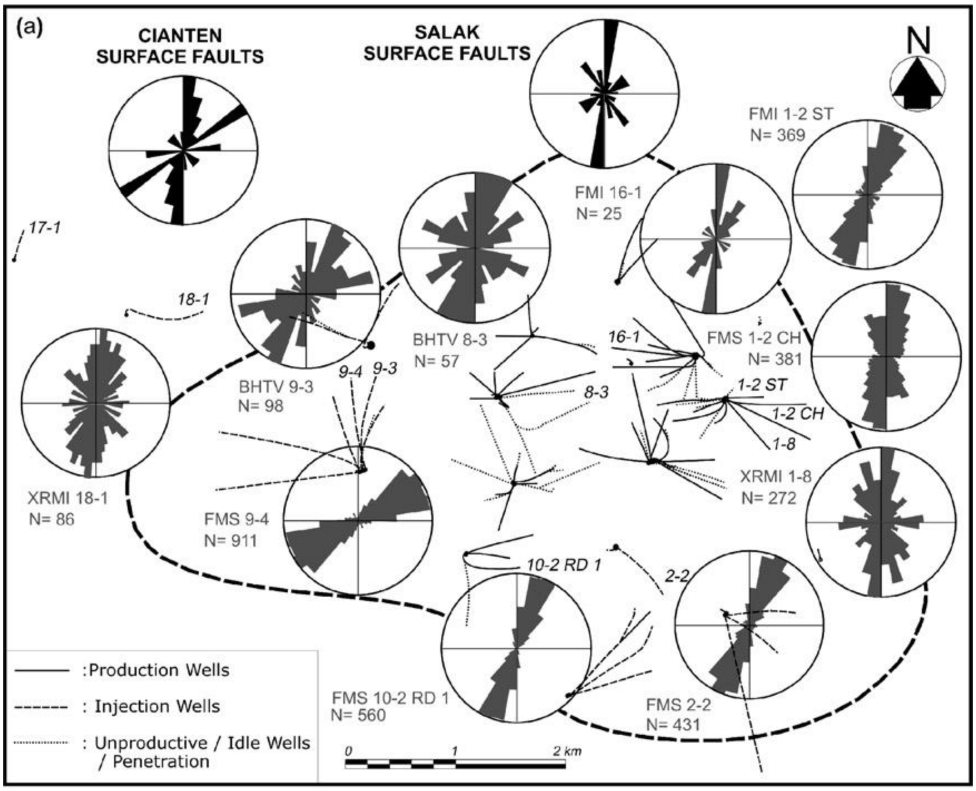

figure 15

Rose diagrams of surface fault strike mapped (black strike) and open fracture orientations interpreted from downhole image logs (dark gray). N refers to the no. of open fractures mapped. The well numbers and reservoir boundary are shown as reference. From: Stimac et al. (2008)

3.3.5 Production details

figure 10, figure 11, table 2

Overview of the temperatures of the different cells and production/ injection wells present within that cell.

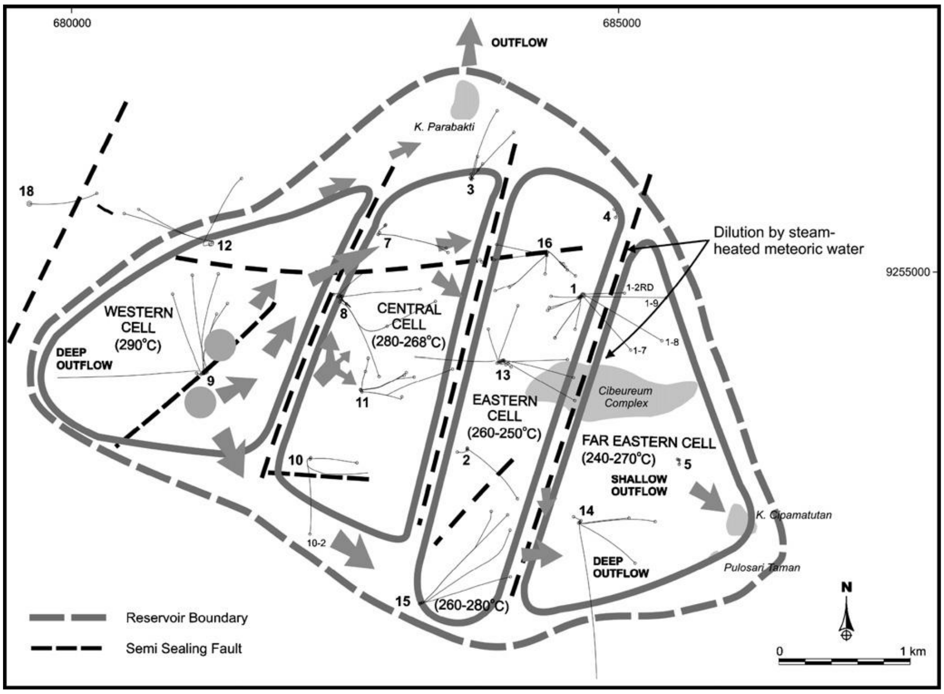

figure 14 figure 15 all display the locations of the various wells of the Salak geothermal field. The wells are numbered by the sequence they were drilled. Discovered in the early 80's by Unocal, production of the Salak geothermal field started in 1994 with the production 110 MWe (Murray et al., 1995) from 7 production wells on well pads Awi 7, 8 & 11 with injection being done at 7 injection wells on pads Awi 9 & 10 (Acuña et al., 2008). Awi 11-1 & 11-2 experienced rapid chemical breakthrough in early production stages due to 250 kg/s brine injection at Awi 10-1.

Expansion of the commercial reservoir towards the east in 1997 increased the nominal capacity of the field to 330 MWe (Soeparjadi et al., 1998). This was done by drilling 24 production wells and 12 injection wells. Three well pads (Awi 1, 13 & 16) where upgraded to handle additional steam capacity. Two new well pads (Awi 14 & 15) where developed as well as Awi 2, 3 & 4 on the field edge where used to accommodate the increased injection.

Further increase of production in late 2002 resulted in a target production of 377 MWe (Acuña et al., 2008). This was accomplished by an extensive make-up drilling program active for several years as well as numerous technical drilling and reservoir innovations taking place worldwide. For example, since Awi 10-1, all wells have been drilled using $13^3/_8$ in. pipes instead of $9^5/_8$ in. as well as 16 in. tiebacks. Some wells have been drilled on low-angle trajectories through the steam cap in order to encounter as many fractures as possible. Awi 16-7 reached 60° and produced more than 40 kg/s of steam (Acuña et al., 2008).

This steam cap developed in the shallow, eastern part of the reservoir. Starting from the initial production in 1994, the steam-water interface has dropped from 560 masl to 0 masl. The descent rate increased after the 1997 expansion. It not includes well-feed zones from Awi 3, 7, 7, 10 & 11 (Acuña et al., 2008). A total of 3 wells exclusively produce dry steam, whereas many other wells produce enthalpies intermediate between liquid and steam. It is likely that these wells produce steam from shallow feed zones and liquid from deeper feed zones (Acuña et al., 2008).

During initial production years (< 1997), low steam flash required large volumes of brine injection in order to be sufficiently productive. Brine production rate during these initial year was around 1000 kg/s. Brine production peaked at 3000 kg/s in 1997, upon expansion to 330 MWe, but declined to 2000 kg/s. Due to the growth of the steam cap, injection requirements have decreased. As a result of this, managing of thermal breakthrough has been successful.

Both during the initial years of production as well as after the 330 MWe expansion, chemical breakthrough was observed at various wells. Tracer analysis was used to determine the origin of these contaminations and several injectors where shut in and injection was shifted elsewhere.

As mentioned above, as of late 2007, 81 wells have been drilled in the Salak field so far, of these 81 wells, 51 are producing, 18 are used for injection and 12 are currently idle (Stimac et al., 2008).

3.3.6 Stimulation history of the Salak geothermal field

Numerous wells in the Salak field have been subjected to different types of stimulation, an overview is presented stimulation, an overview is presented in

Table 3. The average production/ injection improvement was 168%, with a relatively good spread with two slight outliers (

figure 16).

A total of 16 wells have been stimulated, of which 11 were successful and 4 were partly successful (

Table 3). The main stimulation technique used is chemical stimulation, with 12 wells of which 10 were successful.

Well Awi 8-7 is a 1900 m deep well with a temperature of 260 °C located in the central cell of the Salak field (table 2

Overview of the temperatures of the different cells and production/ injection wells present within that cell.

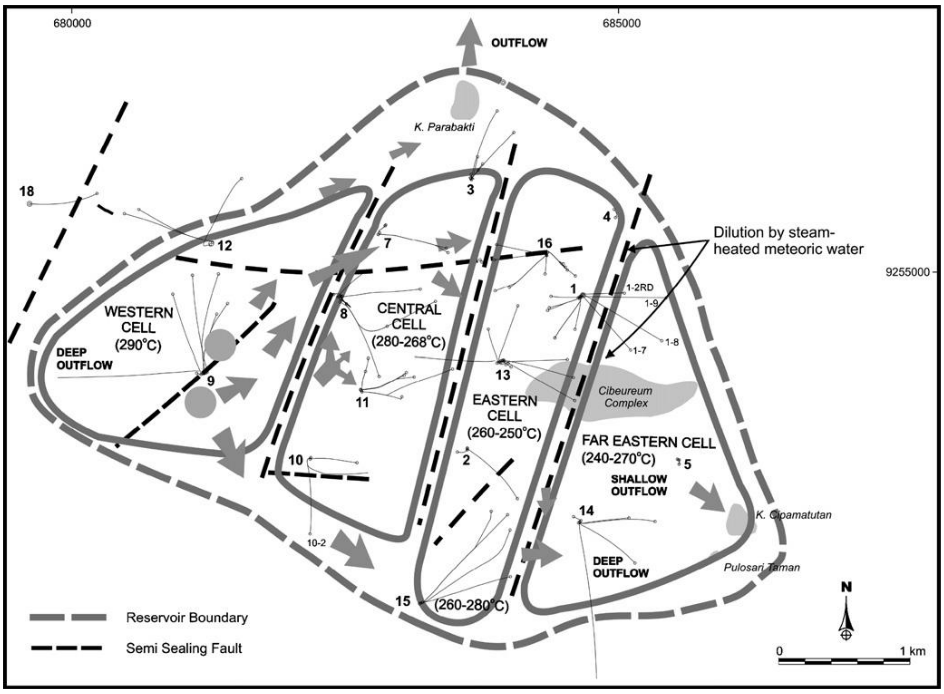

figure 14). It had a low initial injectivity index (4.68 kg/s/bar). It was successfully stimulated using coiled tubing acid stimulation (Pasikki and Gilmore, 2006), the skin decreased from +2.2 to -1.2 and the injectivity index increased to 12.06 kg/s/bar. Due to the fact that corrosion inhibitors for the acid are only effective up to 150 °C, the well was cooled to roughly 100 °C using fresh water (Pasikki and Gilmore, 2006). Well Awi 8-7 was thus also partly stimulated in a thermal manner.

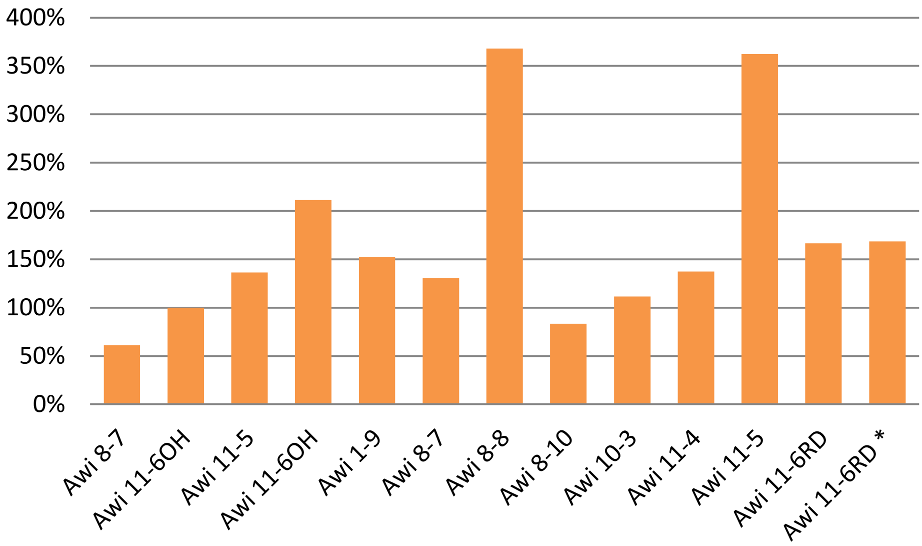

figure 16
Improvement percentages of stimulated wells in the Salak Geothermal field.

Pasikki et al.

(2010) presented results from numerous stimulation jobs preformed in the Salak field. After drilling, wells Awi 11-6OH and Awi 11-5 (table 2

Overview of the temperatures of the different cells and production/ injection wells present within that cell.

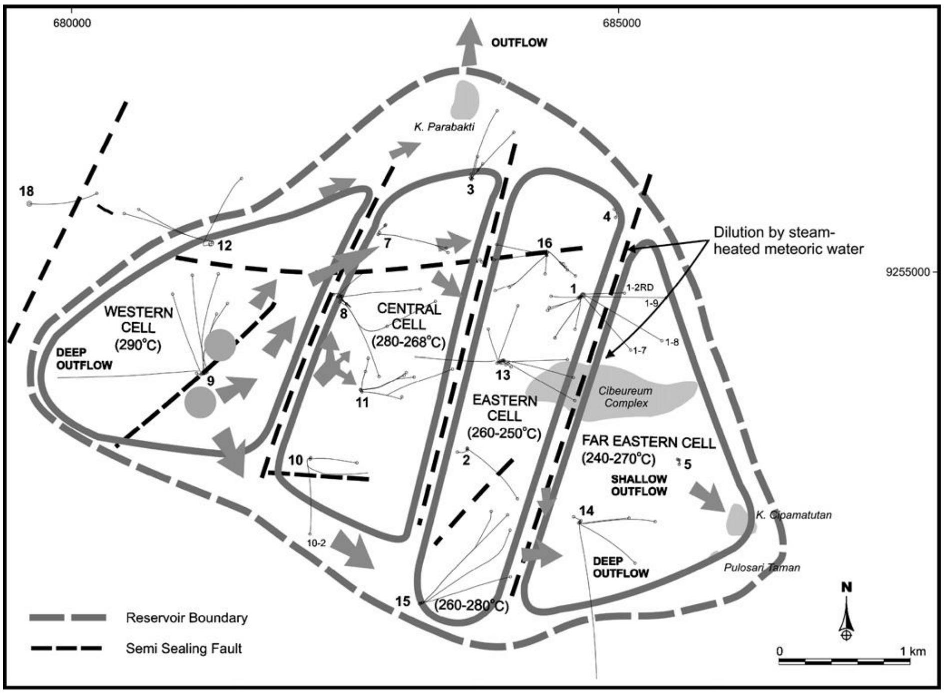

figure 14) both suffered from very low permeability due to poor connectivity to the main fracture network in the central cell of the Salak geothermal reservoir. They where therefore thermally stimulated by alternating injection of 166 °C brine and 38 °C condensate water over periods of 1-4 weeks. Injectivity indexes did increase initially (

Table 3), however the improvement did not grow during subsequent injection cycles. The thermal stimulation was halted due to cooling of the surrounding wells (Pasikki et al., 2010). Awi 11-5 showed a larger increase then Awi 11-6OH (

Table 3), which Passiki et al. (2010) attributed to the higher temperature of well Awi 11-5 resulting in a larger thermal shock.

As the injectivity of Awi 11-6OH no longer improved as a result of thermal stimulation, the treatment was modified by including inhibited HCl acid (Pasikki et al., 2010). Initial bullhead treatments (pumping everything directly into the well without an packers or coiled tubing) with a 27 °C fluid containing15 wt% HCl caused complications as the wellbore and pumps where corroded. Modification of the fluid to 177 °C water with 1 wt% HCl was then attempted, however the wellhead continued to corrode due to failure of the corrosion inhibitor (Pasikki et al., 2010). The slow acid stimulation did not result in further increase of the injectivity index and two months after the stimulation ended, the well was still not able to produce steam at commercial wellhead pressures. The authors speculated that the initial bullheading may have caused problems as the fluids may have flowed into undesired parts of the formation.

In order to prevent similar problems, Pasikki et al., (2010) used HF acid and coiled tubing to stimulate 9 more tubing to stimulate 9 more wells (

Table 3). By using coiled tubing, the feedzones could be targeted more directly. All wells where quenched with 30 bpm of fresh water for 48 hours in order to prevent acid inhibitor failure. Thus, as in Awi 8-7, all wells were also partly thermally stimulated. Wells where located in the western, central and eastern cells (

Table 3; table 2

Overview of the temperatures of the different cells and production/ injection wells present within that cell.

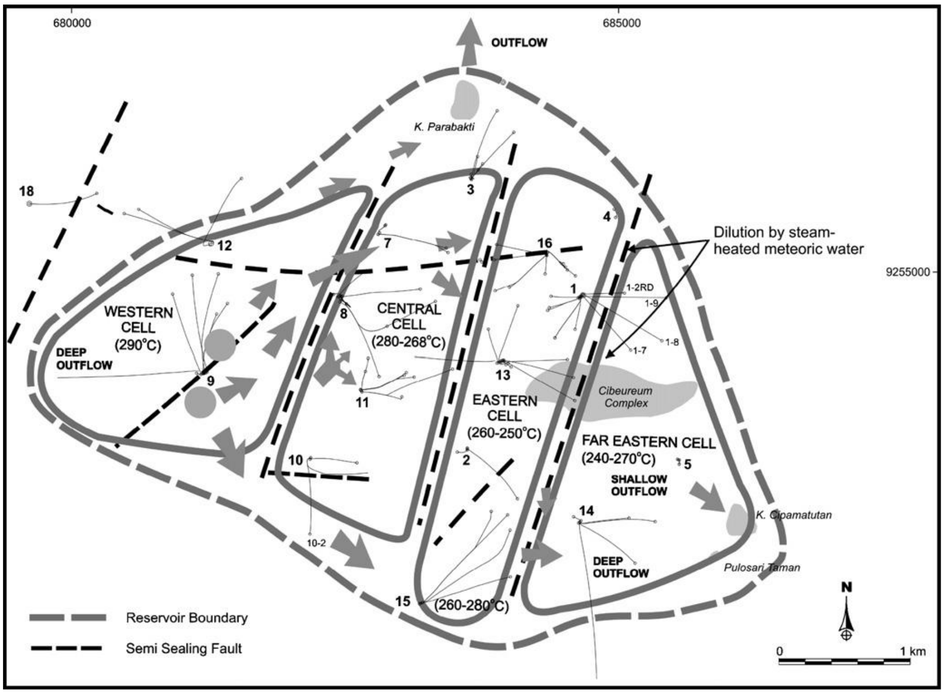

figure 14). The coiled tubing acid stimulation achieved a 100% success rate (Pasikki et al., 2010), as all wells showed production improvements (

Table 3). Well Awi 11-6RD was stimulated twice in order to investigate whether increasing of acid concentrations or volume loads would further increase the productivity. This was not the case and the second stimulation of Awi 11-6RD was unsuccessful.

Wells Awi 18-1 and 20-1 where drilled in the western Cianten Caldera to delineate reservoir extension towards reservoir extension towards the west (figure 10, table 2

Overview of the temperatures of the different cells and production/ injection wells present within that cell.

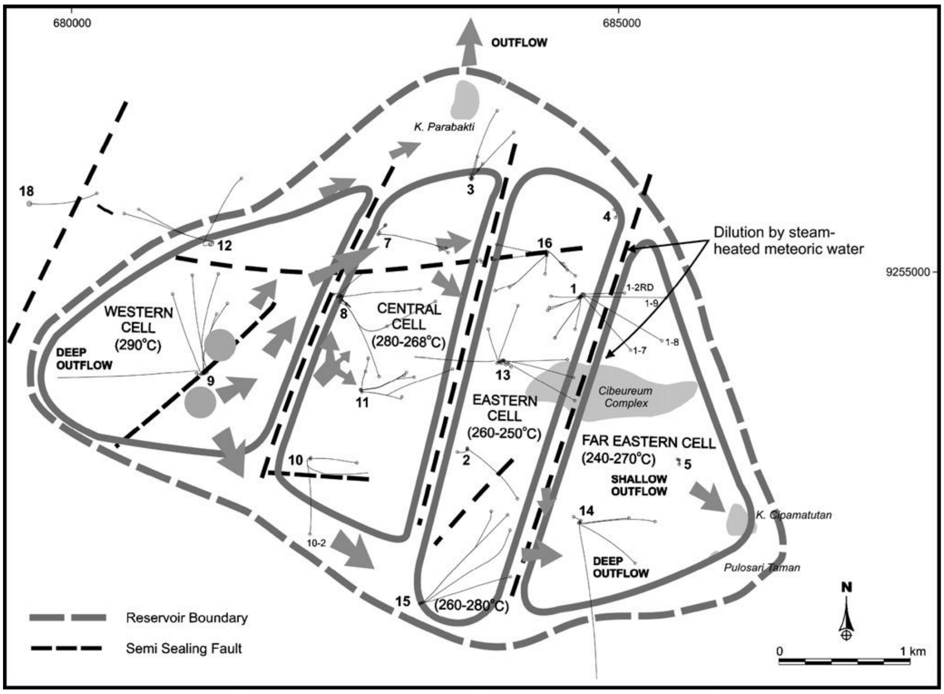

figure 14). Both wells suffered from low, non-commercial permeability (Pasikki et al., 2010). In order to enhance the permeability to commercial levels, both wells where stimulated using combination of hydraulic and thermal stimulation. Awi 18-1 was stimulated in two phases, the first phase consisted of a continuous injection of fluid injection of fluid (unspecified temperature). Based on conceptual modelling (Yoshioka et al., 2009), it was 2009), it was decided to use cycling pressures to improve injectivity. The injectate was condensate water with a condensate water with a temperature of 35 °C. Stimulation was successful and resulted in an improvement of the an improvement of the injectivity index with169% (

Table 3). Injection capacity improved tenfold which was attributed to a connection with a low pressure system (Pasikki et al., 2010).

Stimulation of Awi 20-1 followed the same procedure as Awi 18-1. The injectivity index did not improve after stimulation, however the injection performance did increase with a 26 bar drop in wellhead pressure (Pasikki et al., 2010). It was concluded that the stimulation resulted in a connection between Awi 20-1 and a lower pressure fracture network, not a permeability improvement of the existing fracture network (Pasikki et al., 2010).

During the drilling campaign in 2012-2013, zonal isolation hydraulic stimulation was proposed as a new more effective method of hydraulic stimulation (Yoshioka et al., 2015). Results from modelling indicate that the method is superior to bullhead stimulation. The method forces stimulation in parts with intrinsic lower permeability's. This results in isolated stimulation of the zone with a lower permeability. With no zonal isolation, pressure would focus on the parts with high intrinsic permeability, as this is ´easier´.

Although hard data is lacking, Yoshioka et al. (2015), indicated that zonal hydraulic stimulation was successful for Awi 18-3 based on Hall plots. For more details the reader is referred to Yoshioka et al. (2015).

Successful	**CT**: Coiled Tubing
Un-successful	**SAS**: Slow Acid Stimulation
Partly succesful	*) Stimulated twice

Well	T (°C)	P (Mpa)	Initial II/PI (kg/s/bar)	Post stim II/PI (kg/s/bar)	Increase (%)	Hydraulic	Thermal	Acid
Awi 8-7	260	10	4,68	12,06	61%			CT
Awi 11-6OH	235	n.a.	2,00	4,00	100%			
Awi 11-5	280	n.a.	1,10	2,60	136%			
Awi 11-6OH	235	n.a.	2,60	2,60	0%			SAS
Awi 1-9	> 230	n.a.	1,64	5,12	211%			CT
Awi 8-7	> 230	n.a.	3,84	9,69	152%			CT
Awi 8-8	250	n.a.	4,20	9,69	130%			CT
Awi 8-10	> 230	n.a.	4,57	21,38	368%			CT
Awi 10-3	> 230	n.a.	4,39	8,04	83%			CT
Awi 11-4	> 230	n.a.	6,40	13,52	111%			CT
Awi 11-5	> 230	n.a.	2,92	6,94	138%			CT
Awi 11-6RD	> 230	n.a.	1,46	6,76	363%			CT
Awi 11-6RD *	> 230	n.a.	6,76	6,76	0%			CT
Awi 19-2	> 230	n.a.	1,10	2,92	167%			CT
Awi 18-1	~ 250	n.a.	0,82	2,21	169%			
Awi 20-1	~ 200	n.a.	1,44	1,29	-11%			

Table 3

Overview of stimulated wells in the Salak field. The lightly tinted cells represent secondary, non intentional, stimulation due to cooling of the wellbore. More details are presented in appendix A.

4 High enthalpy geothermal energy - worldwide

4.1 Setup of literature evaluation

Although Indonesia is a large country in terms of produced geothermal energy and literature concerning reservoir stimulation is available. Although stimulation in the Salak field has been extensively reported and geological information is readily available from literature, literature on stimulation of other fields is limited and insufficient to answer the outstanding questions.

Geothermal energy from high enthalpy systems is being produced worldwide in a variety of settings and the experience and knowledge gained there is very relevant for this rapport. Therefore it is decide to evaluate literature concerning stimulation of high enthalpy producing fields all over the world.

The evaluation will be focused on existing high enthalpy (energy) producing fields which are or have been stimulated. All stimulation techniques will be included, although a focus will be on hydraulic and thermal stimulation as well as acidizing. As the project concerns enhancement of already existing reservoirs, enhanced geothermal systems (EGS) or hot dry rock (HDR) systems will not be included. Also, the main focus will be on reservoir stimulation and not on wellbore cleaning or scale removal.

Keywords and phrases used to search for literature include:

- High temperature
- High enthalphy
- Thermal stimulation
- Hydraulic stimulation
- Shear fracturing
- Shear stimulation
- Chemical stimulation
- Acidizing
- Acid stimulation

When searching in a generic scientific database, the keywords ‘geothermal’ or ‘geothermal reservoir’ are often added to narrow down the results to potentially relevant literature.

High enthalpy geothermal systems require very high temperatures close to the surface of the Earth. As such, these systems are formed at or near places where (significant) volcanic activity is present. Therefore, the most high enthalpy geothermal systems are located near spreading ridges, continental rift zones, hot spots and convergent plate boundaries (figure 17). A focus is therefore placed on stimulation literature from countries around the 'Pacific Ring of Fire' and Iceland. Many of these countries posses well developed geothermal plays, which enhances the probability that literature on stimulation jobs carried out in that country was published.

figure 17

Global overview of (potential) regions containing high enthalphy geothermal plays.

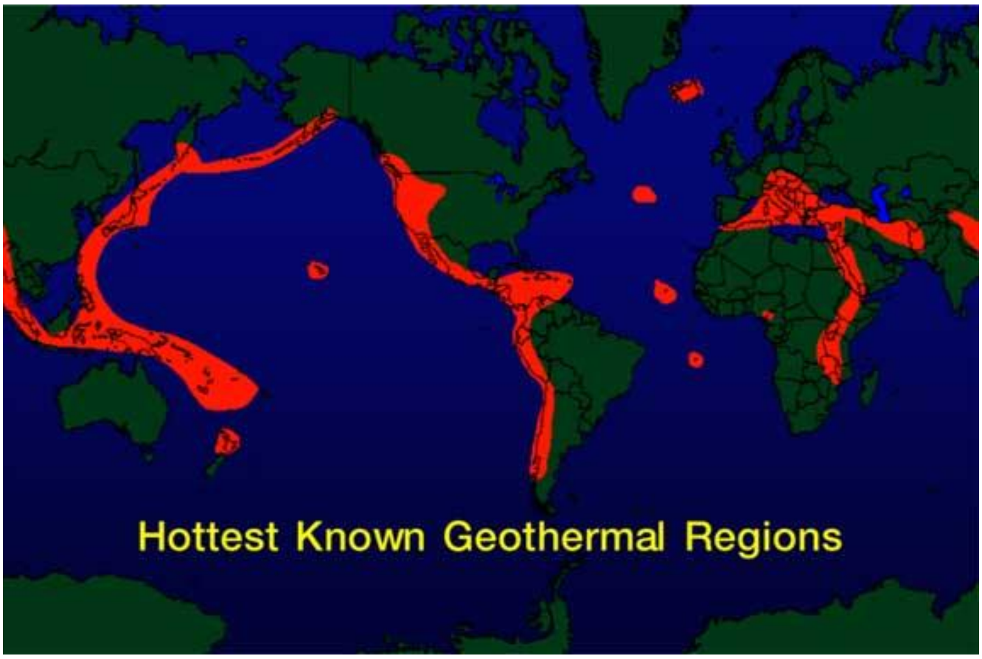

From:http://geothermaleducation.org/GEOpresentation/sld015.htm

4.2 UNDEVELOPED LOCATIONS

The most developed high enthalpy geothermal plays are located at various locations around the 'Pacific Ring of Fire' and in Iceland. However, not all countries along this 'Ring of Fire' have developed high enthalpy geothermal (power) plants.

For instance, Canada has no high enthalpy geothermal production despite the potential resources in British Columbia and the Yukon (Thompson, 2010). It should be noted that there are plans to construct EGS systems. Alaska also has seen limited development, despite its potential (Lund et al., 2010). South America as a whole has no (high enthalpy) geothermal energy production, despite its potential (Cardoso et al., 2010). The Himalayas are also a region with high potential and although some of it is being produced (eg. Tibet; Zheng and Wang, 2012), some other regions, most notably India, are still underdeveloped (Craig et al., 2013). Hot spot islands (Canary islands, Azoures, Cook island) and islands in an island arc (Caribbean) are also good candidates for geothermal energy production from high enthalpy fields, but most of them still do produce only limited amounts geothermal energy. A region with some of the highest heat flow values in the world, the East African Rift has significant geothermal potential. And although Kenya is producing around 200 MWe of geothermal power (Omenda, 2012), the rest of the region lags behind somewhat.

There are numerous reasons responsible for underdevelopment of (obvious) potential high enthalpy geothermal fields.

Many of these underdeveloped fields are located in remote regions with a small local population. The potential plays in Canada or on the small islands in the Atlantic or Pacific ocean are located in such sparsely populated regions that projects struggle to be economically feasible. Islands such as the Canaries, the Azores and Tuvalu are good candidates for geothermal energy, especially as it could bring independence from imported energy. However the cost of a geothermal power plant is often uneconomical when considering drilling and exploitation costs vs consumers. Also, drilling equipment and personnel would have to be imported, which would also be a significant cost.

Other reasons for underdevelopment could be political or legislative in nature, or the (local) government has little to no knowledge of geothermal energy and its potential.

4.3 OVERVIEW OF STIMULATED HIGH ENTHALPY GEOTHERMAL SYSTEMS

Literature that has been found concerning stimulated high enthalpy geothermal systems is summarized in Appendix B, attached at the back of this report. In this overview, the following data, when available, is included.

- Country
- Field
- Reservoir lithology
- General stress state
- Steam or liquid producing/ injection well

(*) *PI: Production index*
II: Injectivity index

- Depth of feedzones
- Downhole Pressure
- Downhole temperature
- PI/II(*) increase (%)
- Type of stimulation
- Literature references

If the literature does not give the reservoir pressures of the wells, then it is assumed that the reservoir is under that the reservoir is under hydrostatic pressure which is then calculated accordingly. Not all papers provide all papers provide all this data, so if the cell is left blank it is due to an absence of information. As this all results in a As this all results in a very large table (Appendix B), the main results are summarized in table 4. Results are characterised in three categories, successful, unsuccessful and partly successful. If stimulation was partly successful, permeability or transmissivity has been improved, but the well failed to be commercially viable.

Successful
Unsuccessful
Partly successful

table 4

Summarized overview of the results of the literature evaluation. Results are ordered by country and geothermal field. The numbers in the cells indicate the amount of wells that had that specific outcome (successful/ unseccussfull etc.)

For more details the reader is referred to Appendix B.

Successful

Unsuccessful

Partly successful

Country	Field	Wells	Hydraulic	Thermal	Acid	Reference
New Zealand	**Rotokowa**	**2**		2		(Davidson et al., 2012; Sherburn et al., 2015; Siega et al., 2009; Siratovich et al., 2011)
	Ngatamariki	**3**		3		(Clearwater et al., 2015)
	Tauhara	**1**			1	
	Kawerau	**4**		2		(Lim et al., 2011; Milicich et al., 2015; Siega et al., 2009))
					2	(Lim et al., 2011)
Iceland	**Krafla(**)**	**1**		1		(Axelsson et al., 2006; Siratovich et al., 2011)
	Hellisheidi	**1**		1		(Bjornsson, 2004; Gunnarsson, 2011)
	Reykanes (+)	**7**		5		(Axelsson and Thórhallsson, 2009)
				2		
Japan	**Sumikawa**	**7**		3		(Ariki et al., 2000; Kitao et al., 1995)
				1		
	Matsukawa	**1**	1			(Hyodo et al., 1995)
	Mori	**?**				(Fukuda et al., 2010; Nitsuma et al., 1985)
	Kakkonda	**5**	4			(Kato et al., 2000; Kizaki and Sato, 1996)
			1			

Krafla field

(**) Most of the wells in the Krafla field have been stimulated. Only one reported.

Reykanes field:

(+) Thirtheen wells where stimulated, but only 7 had both before and after Injectivity indexes.

Guadeloupe	**Bouillante**	**1**		1		(Sanjuan and Brach, 2000; Tulinius et al., 2000)
Costa Rica	**Borinquen**	**1**		1		(Castro-Zùñiga, 2015)
	Las Pailas	**1**		1		
Philippines	**Palinpion 1**	**4**			3 1	(Amisoto et al., 2005)
	Mt. Apo	**2**		1	1	(Esberto et al., 1998; Malibiran et al., 2013) (Malate et al., 2000)
	Leyte	**11**			9 2	(Malate et al., 1997; Yglopaz et al., 1998) (Caranto et al., 2010)
Italy	**Larderello**	**3**			3	(Scali et al., 2013)
	Latera	**2**			2	(Barelli et al., 1985)
USA	**Geysers**	**1**				(Entingh, 2000; Hanold and Morris, 1982)
	Bacca	**2**				(Entingh, 2000)
	Beowawe	1				(C. W. Morris and A. R. Sinclair, 1984; Entingh, 2000)
Mexico	**Los Humeros**	**5**		5		(Sánchez Luviano et al., 2015)
	Las Tres Virgines	**6**			1 5	(Flores and Ramírez, 2010) (Gutiérrez-Negrín, 2015)
	Los Azufres	**13**			12 1	(Flores and Ramírez, 2010)

Based on the literature evaluation, a total of 92 stimulation jobs have been carried out worldwide (

worldwide (

table 4 & *table 5*). The total number of wells stimulated is 84, which is less than the total number of stimulation jobs. This is due to the fact that some of these wells have been stimulated with multiple techniques (Appendix B). For instance, wells in the Latera field (Italy) have been stimulated using all three main techniques (Barelli et al., 1985) and a well in the Kawerau field (New Zealand) has undergone both thermal and chemical stimulation (Lim et al., 2011; Siega et al., 2009).

Successful
Unsuccessful
Partly successful

Stimulation is deemed successful when the treated well is producing or injection at commercial rates and is thus economically viable. If stimulation resulted in an increase in injectivity or productivity index or injected or produced volumes, but the well was not commercially viable, the treatment is deemed partly successful. If no improvement is observed the stimulation is deemed unsuccessful. An overview of number of stimulated wells per technique are presented in *table 5* and figure 18 and success rates in *table 5*and figure 19. Results indicate that 74% of all stimulation jobs is successful, although publication bias has to be considered. And the drawing of conclusions thus has to be done with care.

Worldwide	**Total no. of wells**	**92**
	Successful	68
	Partly successful	10
	Unsuccessful	14
Chemical	**Total no. of wells**	**47**
	Successful	34
	Partly successful	4
	Unsuccessful	9
Thermal	**Total no. of wells**	**34**
	Successful	29
	Partly successful	2
	Unsuccessful	3
Hydraulic	Total no. of wells	11
	Successful	5
	Partly successfll	4
	Unsuccessful	2

figure 18

Distribution of applied stimulation techniques as found in literature (table 5).

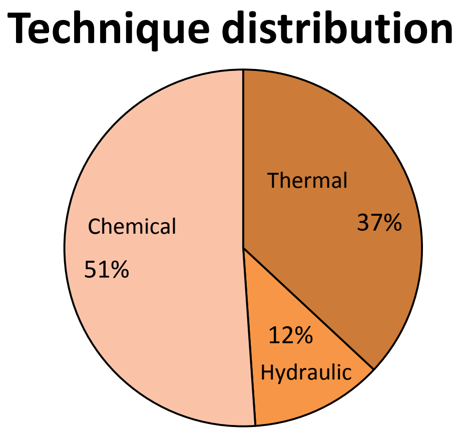

figure 19

results fron

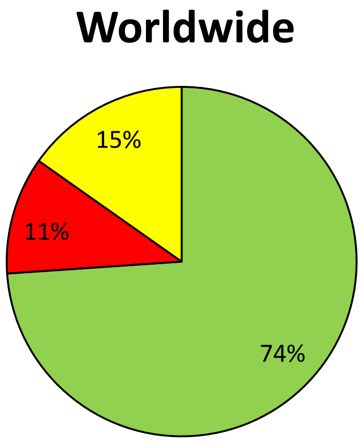

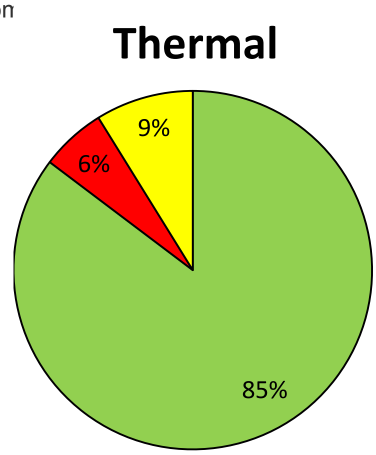

table

of all

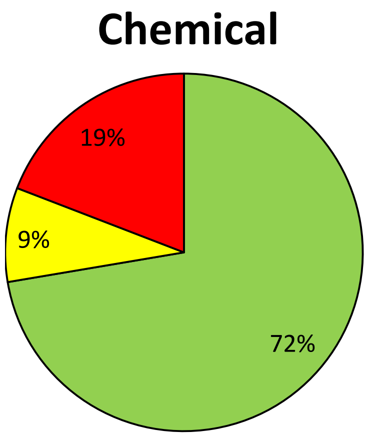

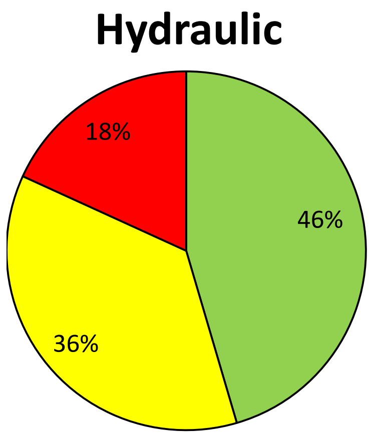

5

Summary of the success rate

stimulation jobs based on

table 4

Successful
Unsuccessful
Partly successful

Chemical stimulation

It is clear that chemical stimulation is the most popular technique (figure 18, 51%), this is most likely due to the ease of operation and the fact that most service companies can complete the job in a short time span and for relatively low costs. They also actively market specific acidizing fluids. This all leads to a relatively large percentage of acidizing jobs. However, not all geothermal reservoirs are suitable for acidizing. For instance, reservoirs in Iceland are composed of basaltic rocks, making acidizing rather difficult. Thus acidizing is not very common in Iceland (Axelsson et al., 2006). Acidizing is also limited to the wellbore and near wellbore region as it can be quickly spent. Inhibitors can delay the reaction with some time, but it is still a near wellbore technique. Reaction rates are especially relevant in high enthalpy geothermal reservoirs as these rates tend to increase with increasing temperatures. High reservoir temperatures (> 150 °C) also reduce the effectiveness of corrosion inhibitors present in the acidizing fluid. Several cases have been found where precipitation and corrosion problems have limited the success of the stimulation (Flores and Ramírez, 2010; Pasikki et al., 2010; Pasikki and Gilmore, 2006).

Acidizing has been applied, with varying success (figure 18), in Mexico, the Philippines, New Zealand, Japan and the US (Appendix B). Almost all acidizing jobs have been conducted in Andesitic reservoirs and have used hydrofluoric acid (HF).

Thermal stimulation

Thermal stimulation has also been utilised at multiple fields around the world and makes up 37% of the total stimulated fields found (figure 18). In Iceland, the technique is almost standard procedure (Axelsson and Thórhallsson, 2009) and not all results are reported as the technique is used so often. New Zealand has also utilised thermal stimulation on numerous occasions (Siega et al., 2009; Siratovich et al., 2011). Costa Rica used thermal stimulation to increase the permeability in the Borinquen and las Pailas fields (Castro-Zùñiga, 2015).

The technique is very interesting for high enthalpy fields due to the large thermo-elastic stress shock that can be induced as a result of the large temperature differential and the relatively low costs, making it economically attractive as well (Flores-Armenta et al., 2005). As mentioned in section 2.2, thermal stimulation has no real standard procedure, but most effective treatments used a cyclic schedule where the reservoir was subjected to several cycles of cooling and heating. By using this cyclic nature, the reservoir is repeatedly exposed to thermal shocks and fractures are formed more effectively. Also, by repeating it multiple times, the fractures can remain open for a longer time even when the reservoir has heated up again. Success rates in literature are quite high (figure 19), although some publication bias is likely partly responsible.

Hydraulic stimulation

Hydraulic stimulation is not used very often in high enthalpy geothermal systems and its implementation is also not very recent (most recent papers are from 2000; Ariki et al., 2000; Kato et al., 2000). Literature overview of high enthalpy geothermal systems stimulated by hydraulic stimulation alone yielded only 11 wells (12%; figure 18), so any interpretations made concerning (propped) hydraulic fracture treatments should be carefully reviewed. The technique has seen use in Japan, the US and Italy, mainly in the 1980's and 1990's. It should be noted that hydraulic stimulation is much more common in EGS systems, however these have been left out as mentioned above.

Results from these propped fracture treatments have been mixed (figure 19). One of the main problems with this technique is long term increase in conductivity and permeability. Especially when using proppant, the long term result could be less satisfying due to diagenetic effects (see section 2.5). Thermal degradation of fracturing fluids due to high reservoir temperatures mean that stability of drilling fluids is also a concern (Flores-Armenta et al., 2005). This problem also presents itself with chemical stimulation fluids.

It is speculated that hydraulic fracture treatments that do not explicitly mention the use proppant (e.g. some wells in the Kakkonda field; Kizaki and Sato, 1996) are possibly self propping due to a shear displacement on the fracture face. However, this is not directly mentioned in the publication.

4.4 Discussion of literature evaluation and tentative conclusions

During the course of this literature study, a total of 92 stimulation job reports have been found. The real number of stimulated systems is likely to be much higher, as published results are subject to publication bias and not all stimulation jobs are reported. Nevertheless, some tentative concluding remarks can be made as well as recommendations for further research.

All literature reviewed pertained to high temperature geothermal reservoirs. It is therefore important to realise that many of these stimulation jobs have a component of thermal stimulation as well. It is very likely that, regardless of fluid composition, the injected fluids have almost always a lower temperature than the reservoir temperature they are injected in. Therefore, it is possible that part of the increase due to stimulation is due to an (unintentional) thermal stimulation component.

Conclusions concerning the effectiveness of hydraulic stimulation cannot be readily drawn as there are only 11 hydraulic fracturing treatments found in literature and data regarding the improvement of the injectivity/ productivity index is not provided. With regard to its potential, problems with fluid stability and proppants, as mentioned above, give rise to scepticism about the effectiveness of the technique in high enthalpy geothermal reservoirs. At this point, several authors feel that more research is required to test whether (propped) hydraulic fracturing treatments yield sufficient economic improvements at high temperature reservoir conditions (Flores and Ramírez, 2010). However, hydraulic stimulation has been utilised effectively in combination with thermal stimulation in the Salak geothermal field in Indonesia (see section 3.3.6) (Pasikki et al., 2010), and as such hydraulic fracturing does show potential.

As mentioned above, chemical stimulation is by far the most widely used technique, as 51% of all treatments found are chemical in nature (figure 18, table 6). It does seem that thermal stimulation is slightly more successful than chemical stimulation with 85% versus 72% success respectively (table 6).

Type	Application distribution	Successful outcome	Average improvement
Chemical	47 (51 %)	72%	167% (190%)
Thermal	34 (37%)	85%	155%
Hydraulic	11 (23%)	46%	

Successful
Unsuccessful
Partly successful

table 6. Summary of outcomes of the literature evaluation (table 4, table 5, *figure 18* & *figure 19*). Improvement percentage between brackets is the percentage including abnormal high improvements (Appendix B; *figure 20*).

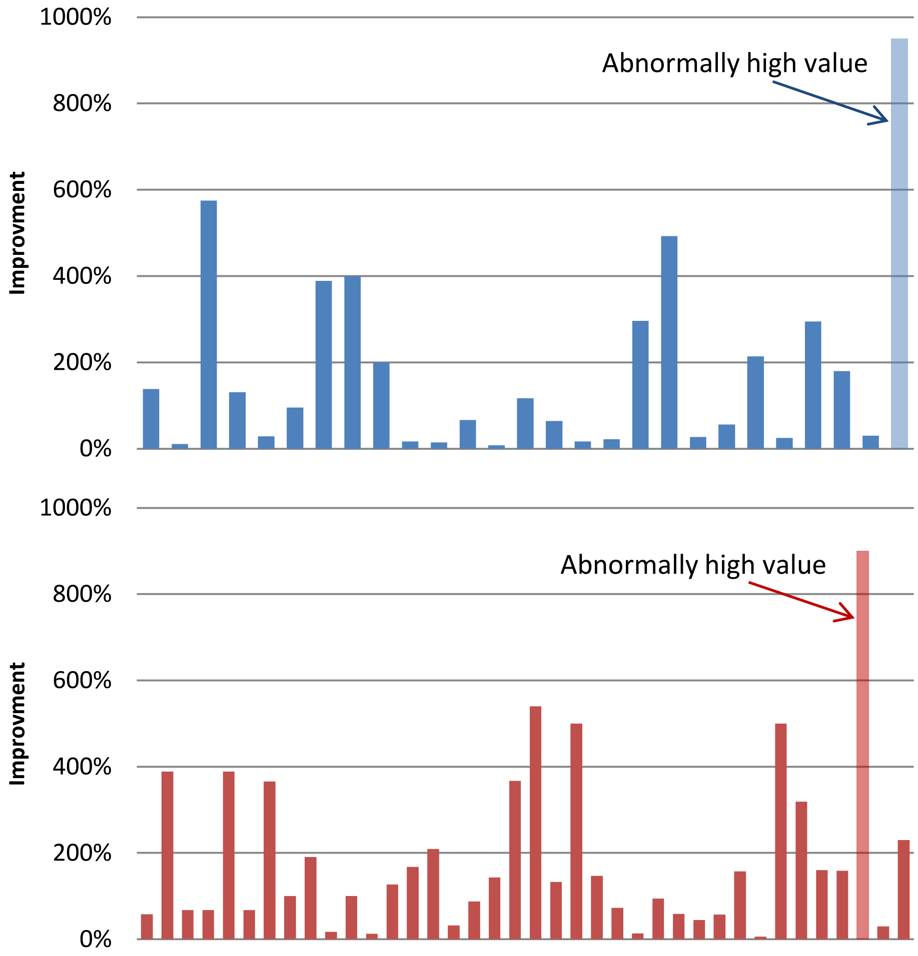

figure 20

Improvement percentages of the individual wells for both thermal (top) and chemical (bottom) stimulation. Note the large spread.

Improvement of individual wells varies significantly for both chemical and thermal stimulation (figure 20). But it stimulation (figure 20). But it seems that most wells which have improved by 10-200%. The average improvement for chemical stimulation is 167% and the average improvement for thermal stimulation is 155% (table 6). Results from the Salak field show an average improvement of 168% (section 3.3.6). Variation in well improvement of the individual wells in the Salak field is less than the variation in well improvement from the literature review (

figure 16 vs figure 20). Also, the stimulation results from the Salak field do not contain questionably high improvement values. This first observation is not unexpected as it seems likely that stimulated wells in the Salak field show similar results due to the fact that the reservoir conditions are similar. The fact that there are no abnormally high improvement values could be due to the relatively low number of stimulated wells (16). With more stimulated well, the statistical change of a very successful stimulation treatment would increase.

The average improvement values for chemical and thermal stimulation treatments worldwide is determined without results from an abnormally high improvement values from a well in the Philippines (950%) and a well in Italy (900%) (figure 20; Appendix B).

If we were to include the two very high improvement values, the average improvement would become 186% for thermal stimulation and 190% for chemical stimulation (table 6). This influence is very significant and these values are therefore deemed outliers.

Based on the data gathered in the literature evaluation, chemical stimulation yields a slightly higher average improvement depending on whether the very high improvement values are taken into account, 12% (not including high values) to 4% (including high values) difference. But thermal stimulation has a higher success rate, with 85% of the thermal treatments being successful versus 72 % of chemical treatments having a successful outcome (figure 19).

The majority of the thermal stimulation treatments have been performed in countries with a relatively long history in geothermal development (New Zealand, Iceland, Japan). It seems that many other countries with high potential (e.g. Mexico, Philippines, Indonesia) mostly rely on chemical stimulation. Provided the conditions are right and sufficient research into the local reservoir has been done, it is the opinion of this author that (significant) improvements can be made to producing geothermal fields by implementing thermal stimulation where chemical or hydraulic stimulation is difficult.

Recommendations for further research

A significant amount of literature has been reviewed. But there are some issues that can be potentially interesting enough to warrant further research.

This study excluded any enhanced geothermal system (EGS), however results from stimulation in these fields could be interesting. Especially since hydraulic stimulation is one of the most used techniques in EGS reservoir development. It could thus provide more data on the effectiveness of hydraulic stimulation in high temperature environments.

Also, there are some papers on stimulation treatments preformed in EGS projects where self propped fractures are created using shear stimulation (Chabora et al., 2012; McClure, 2012). These self propping fractures are very interesting and it is felt that they merit some further investigation. However, for self propping shear fractures to be effective, mechanically strong reservoirs are required. Otherwise the offset fracture faces would quickly close due to crushing as a result of stress or diagenetic reactions. For high enthalpy geothermal systems, reservoir consisting of fractured granite or another high competence reservoir rock would be potential candidates for shear stimulation. Shear stimulation of volcanic tuffs and other weaker lithologies is unlikely to be successful.

As mentioned at the beginning of chapter 3, not a lot of literature has been found and reviewed on stimulation treatments in other Indonesian fields. Although some details regarding stimulation of other fields have been found (Mulyadi, 2010) the actual amount of information is not very much. Therefore, more information regarding stimulation in Indonesia would enhance the understanding of the effectiveness of various stimulation techniques. Results would be relevant for worldwide efforts in geothermal reservoir stimulation but also specifically for the Indonesian situation itself.

5 MODELLING OF THERMAL STIMULATION

As concluded in the previous chapter, thermal stimulation can be a very effective stimulation method to increase production of a (high enthalpy) geothermal field. Therefore this chapter, as outline in the introduction, provides a detailed outline of an analytical model for thermal stimulation. It aims to simulate the first order effects of cold fluid injection into a hot reservoir. Using the results, operators and planners can use this model as a quick scan tool to investigate if thermal stimulation could be a viable stimulation technique for a certain site.

The model has to be easy and quick in use and easy to edit, should that be necessary. Therefore, a simple analytical model is to be constructed. The aim is also not to use this model to design an entire stimulation treatment, but rather to assess the potential gains (production or injection) of such a treatment and thus act as a site selection tool.

Although not really used in the oil and gas industry, thermal stimulation has been successfully applied at several geothermal sites throughout the world, as shown in the literature overview presented above. The reasons to decide to construct a model for thermal stimulation are manifold.

Commercial software for 'conventional' propped hydraulic fracturing treatments is available from several companies (e.a. MFrac) and modelling would therefore be rather superfluous. Predicting the exact effects of an acid treatment is very complex as it depends on the composition of the acid, which is often confidential, as well as the geochemistry of the rock and geothermal fluid and the well and reservoir history.

Thermal stimulation is also a relatively easy method in its implementation and it has high potential when used in high temperature geothermal systems, as the high temperature difference results in high amounts of thermo-elastic stress change or thermal shock. From an economical standpoint, thermal stimulation is also relatively cheap.

5.1 DERIVATION AND CONSTRUCTION OF ANALYTICAL MODEL

Model construction is based on work from Perkins and Gonzalez, (1985), de Koning, (1988) and Detienne et al. (1998). All these papers deal which deal with preventing excessive fracture growth due to waterflooding. Although thus not directly related to thermal stimulation, the thermal aspect is adequately treated to function as a basis for this work.

In thermal stimulation, the temperature of the injectate is cooler than the temperature of the reservoir. This results in a growing cooled region around the wellbore, which leads to contraction of the rock matrix. This contraction results in a decrease in the stress around the wellbore. The continued injection of fluid also leads to an increase in pore pressure, resulting in fracture formation. Due to the cooling effect, this fracture initiation pressure is lower than the initiation pressure of conventional hydraulic fracturing treatments. This is the basic concept of thermal stimulation. Sign convention in this model is that compressive stresses are positive and tensile stresses are negative.

General assumptions

The dissertation of de Koning (1988) was used as a starting point for model construction. He assumed a radially symmetric reservoir of infinite extent (figure 21). His other assumptions where:

- Reservoir rocks have some form of consolidation, otherwise linear elastic theory is not valid.
- Stress changes are relatively small with respect to tectonic stresses. In this manner non-linear behaviour of material properties can be disregarded.
- The reservoir is an infinite radial symmetric disc with finite height. Its axis coincids with the wellbore and the rock is linearly elastic , isotropic, homogeneous and permeable.
- It is over and underlain by an impermeable, linearly elastic, isotropic, homogeneous cap and base rock with the same mechanical properties as the bulk rock. These cap and base rocks have infinite thickness.
- Neglectable coupling between fluid and heat flow and elastic behaviour.

figure 21

Geometry of wellbore in the reservoir.

The cap and base rock are assumed to have infinite thickness. Reservoir is of infinite radial extent.

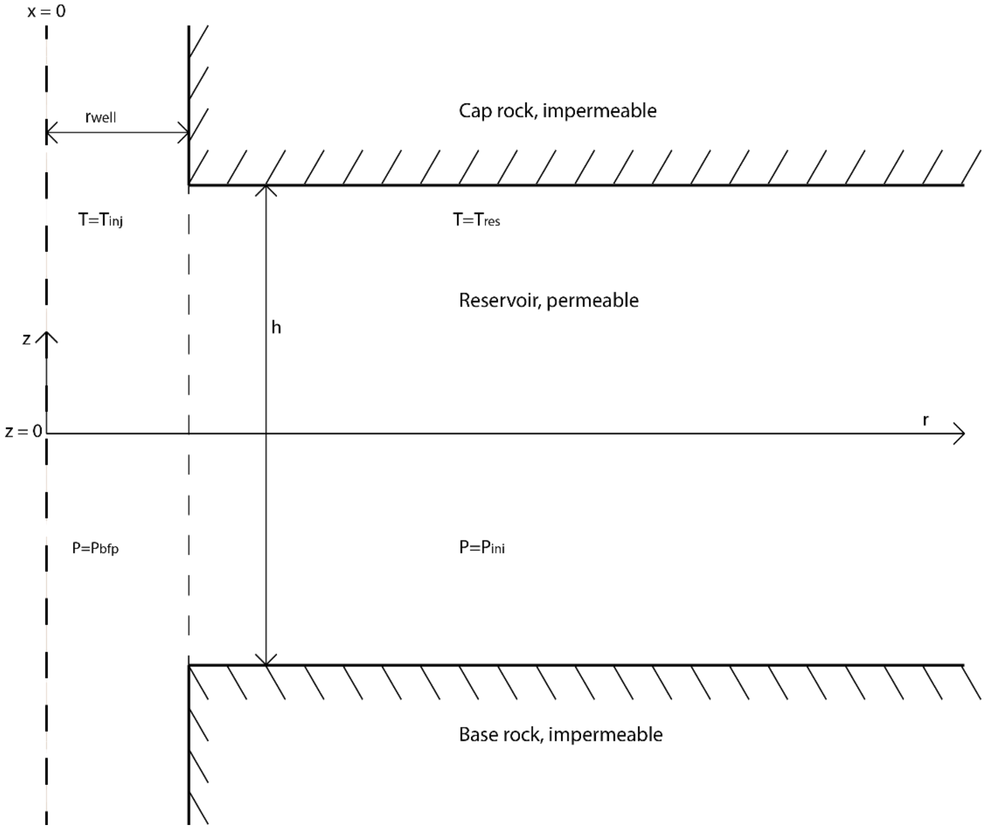

Temperature distribution around the wellbore

The temperature field is given by Lauwerier's solution in cylindrical coordinates (Boyadjiev et al., 2005; de Koning, 1988) which applies to constant rate injection of an incompressible fluid. Horizontal heat conduction is neglected, but vertical heat conduction in underlying and overlying strata is taken into account. The bottomhole temperature is assumed to be equal to the temperature of the injected fluid and temperature in the reservoir is assumed constant in the vertical direction (de Koning, 1988).

Lauwerier's solution can then be written as follows:

$$T_D = \operatorname{erfc}\left\{\sqrt{\tau_D}\frac{{R_D}^2}{2\left(1-{R_D}^2\right)}\right\} \quad R_D < 1;\ |z| \le \frac{h}{2}$$

$$T_D = \operatorname{erfc}\left\{\frac{{R_D}^2\tau_D+\Delta z_D}{2\sqrt{\left(\tau_D\left(1-{R_D}^2\right)\right)}}\right\} \qquad R_D < 1;\ |z| > \frac{h}{2} \quad [5.1]$$

$$T_D = 0 \qquad R_D \ge 1;\ -\infty < z < \infty$$

With the terms being defined as follows:

$$T_D = \frac{T - T_{res}}{T_{inj} - T_{res}} \qquad [5.2]$$

$$\tau_D = \frac{4\alpha_s t\, M_s^2}{h^2 M_r^2}$$

$$R_D = \frac{r}{R_C}$$

$$R_c = \left\{\frac{M_w}{M_r}\frac{qt}{h\pi}\right\}^{\frac{1}{2}}$$

$$\Delta z_D = \frac{M_s}{M_r}\left(\frac{2z}{h} - 1\right)$$

With the symbols being:

T_{res} = Initial reservoir temperature [°C]
T_{inj} = Injection temperature [°C]
t = Injection time [s]
h = Reservoir height [m]
α_s = Thermal diffusivity of cap and base rock [m^2/s]
M_s = Heat capacity ofcap and base rock [J/m^3 °C]
M_r = Heat capacity offluid filled reservoir rock [J/m^3 °C]
M_w = Heat capacity of injection fluid [J/m^3 °C]
q = Injection rate [m^3/s]

The subscript D means the terms is dimensionless. R_c is the radius of the temperature front and follows the convective heat balance of heat absorbed by injection fluid is heat given off by the reservoir (de Koning, 1988):

$$qt\, M_W\, \Delta T = \pi\, R_c^2\, h\, M_r\, \Delta T \qquad [5.3]$$

When $r \rightarrow R_c$, the temperature difference tends to zero (equation 5.1).
Horizontal heat conduction can be neglected when the radial velocity of the temperature front is much greater than the temperature transients in the over and underlying rocks. This means that, with isotropic thermal conductivities and approximately equal thermal properties of the reservoir and cap and base rock, horizontal heat conduction can be neglected (de Koning, 1988). It is justified if the Peclet number is much larger then 1 (equation 5.4).

$$Pe = \frac{M_r\, R_c^2}{M_s\, \alpha_s\, t} \gg 1 \qquad [5.4]$$

Inserting the expression for R_c from equation 5.2 into 5.4 gives:

$$\frac{M_w\, q}{M_s\, \pi\, h\, \alpha_s} \gg 1 \qquad [5.5]$$

Equation 5.5 is satisfied for most field conditions. The assumption that the temperature distribution approximates a step profile is dependent on the value of τ_D as is evident from equation 5.2. figure 22 shows the (dimensionless) temperature distribution inside a reservoir with varying values for τ_D. It is apparent from the plot that the approximation of the temperature distribution as a step function is valid for $\tau_D < 0.05$. If the value where higher, the amount of heat given off by the over and underlying rock would be higher than the amount given off by the reservoir (de Koning, 1988).

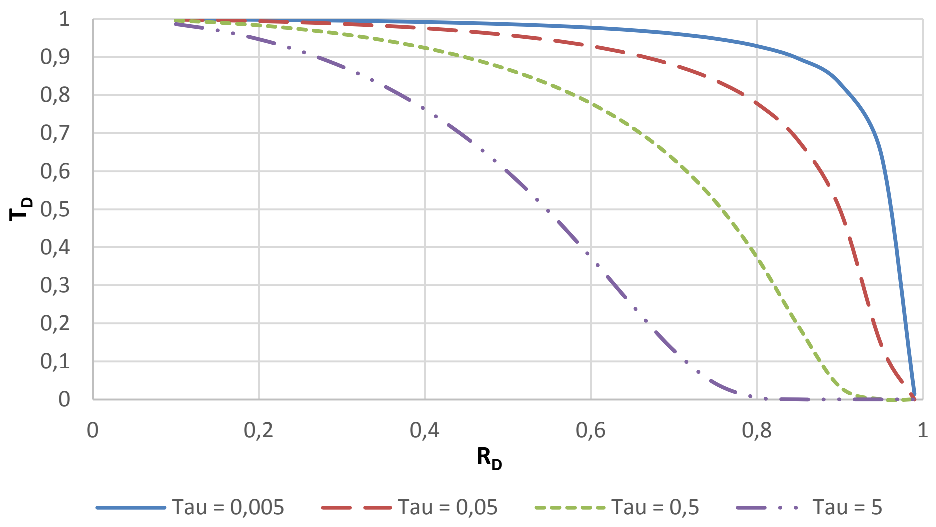

figure 22
Plot of dimensionless reservoir temperature (Lauweriers temperature distribution) versus dimensionless radiuses.

Pressure distribution around the wellbore

The pressure distribution is determined from the Theis well function. This function solves non stationary flow to complete drainage in a confined reservoir (Theis, 1935). It is usually used to determine hydrological properties in a given reservoir, but can also be used to determine the drawdown and thus the pressure distribution. It is defined by Kruseman and de Ridder (1994) and is often dubbed an exponential integral:

$$s = \frac{q}{4\pi\, Tr} \int_u^{\infty} \frac{e^{-y}}{y}\, dy \qquad [5.4]$$

$$u = \frac{r^2 S}{4\, Tr\, t} \qquad [5.5]$$

$$S = \rho_{inj} g h (c_t + \phi c_{inj})$$

$$Tr = k * \frac{\rho_{inj}\, g}{\mu}$$

Where:

$q = \text{Injection rate } \left[\frac{m^3}{d}\right]$
$r = \text{Radial distance from the well } [m]$
$s = \text{Drawdown } [m]$
$t = \text{Injection time } [m]$
$Tr = \text{Transmissivity } \left[\frac{m^2}{d}\right]$
$k = \text{Permeability } [D]$
$\mu = \text{Viscosity } [Pa * s]$
$S = \text{Storativity } [-]$

$$\rho_{inj} = \text{Density of injection fluid } [kg/m^3]$$

Srivastava and Guzman-Guzman (1998) constructed very accurate approximate expressions for the integral of equation 5.4 which is simple enough to be utilized in a spreadsheet.

$$\int_u^\infty \frac{e^{-y}}{y}\, dy = \ln\left(\frac{e^{-\lambda}}{u}\right) + 0.9653\, u - 0.1690\, u^2 \qquad u \le 1 \quad [5.6]$$

$$\int_u^\infty \frac{e^{-y}}{y}\, dy = \frac{1}{u\, e^u} \frac{u + 0.3575}{u + 1.2800} \qquad u \ge 1$$

$\lambda = 0.5772156649$ (Euler – Macheroni constant, used these decimals)

The drawdown is then converted to pressure change (equation 5.7).

$$\Delta P = \rho_{inj}\, g\, s \qquad [5.7]$$

With:

$\Delta P = \text{Pressure change as a result of injection} [Pa]$

Thermo-elastic stress change

As the reservoir rock cools and contracts due to the cold water injection, thermo-elastic stress changes are induced leading to a reduction of the minimal horizontal stress.

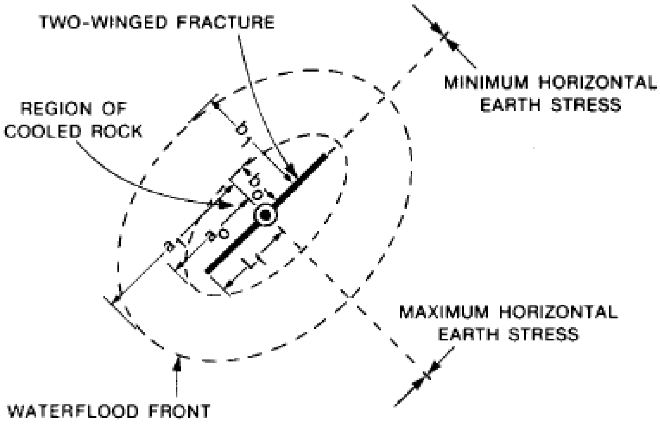

figure 23

Schematic plan view of the wellbore and nearby reservoir during injection. Geometric variables used in calculations are shown in relation to each other and the wellbore. From *(Perkins and Gonzalez, 1985)*.

Perkins and Gonzalez (1985) provided an expression for the thermo-elastic stress change (equation 5.10 – 5.11) by numerically approximating them for regions of elliptical cross section and finite thickness (Perkins and Gonzalez, 1985; Appendix B).

During the initial phase of injection, before the fracturing criterion is met, the cooled region expands radially outward. The major and minor semi axis of the ellipsoid are thus equal. If and when the fracturing pressure is achieved, fractures will develop and the cooled region will become elliptical. The semi axis of the cooled region are determined using a procedure from Perkins and Gonzalez (1985 appendix B) (equations 5.8 - 5.9).

$$a_c = L_f(F_1^{1/2} + F_1^{-1/2})/2 \qquad [5.8]$$

$$b_c = L_f(F_1^{1/2} - F_1^{-1/2})/2$$

$$F_1 = \frac{2V_c}{\pi L_f^2 h} + \frac{1}{2}\sqrt{\left(\frac{4V_c}{\pi L_f^2 h}\right)^2 + 4} \qquad [5.9]$$

$$V_c = \frac{M_w}{M_r} qt$$

Where

a_c = Major semi axis of the elliptical cooled region [m]
b_c = Minor semi axis of the elliptical cooled region [m]
V_c = Volume of cooled region [m^3]

The procedure requires the input of a fracture half length. This is set equal to the well radius, as the model assumes an infinitely thin well this simulates the small distance between the centre of the injection point and the outer edge of the wellbore. Although fracturing has not yet occurred and thus use of a fracture half length is, on first glance, questionable, sensitivity analysis has shown that such a small fracture length has little to no influence on the results and the results show a radial symmetric cooled region.

Thermo-elastic stress changes in the cooled region are related to the semi axis of the cooled region, so they will be radial symmetric when calculated for a radial symmetric volume:

$$\mathrm{Co_{H1}} = \frac{e_c}{1+e_c} + \left[\frac{1}{1+e_c}\right] * \left(1/\left\{1 + 0.5\left[1.45\left(\frac{h}{2b_0}\right)^{0.9} + 0.35\left(\frac{h}{2b_0}\right)^{2}\right] * \left[1 + e_c^{0.774}\right]\right\}\right)$$

$$\Delta\sigma_{yT} = \frac{E\beta\Delta T}{1-\upsilon} * \mathrm{Co_{H1}} \qquad [5.10]$$

$$\mathrm{Co_{H2}} = \frac{1}{1+e_c} + \left[\frac{e_c}{1+e_c}\right] * \left(1/\left\{1 + \left[1.45\left(\frac{h}{2b_0}\right)^{0.9} = 0.35\left(\frac{h}{2b_0}\right)^{2}\right] * \left[1 + (1 - e_c^{1.36}\right]\right\}\right)$$

$$\Delta\sigma_{xT} = \frac{E\beta\Delta T}{1-\upsilon} * \mathrm{Co_{H2}} \qquad [5.11]$$

Where

$$e_c = \frac{b_c}{a_c}\,(\text{Ratio of the semiaxes})\ [-]$$

$$\Delta\sigma_{yT} = \text{Thermo} - \text{elastic stress change perpendicular to } \sigma_{h,min}\ [\text{Pa}]$$

$$\Delta\sigma_{xT} = \text{Thermo} - \text{elastic stress change parallel to } \sigma_{h,min}[\text{Pa}]$$

Poro-elastic stress change

The injection of fluids into the reservoir also results in pore pressure changes, which leads to poro-elastic stress change. This stress change can be calculated in a similar manner as the thermo-elastic stress change, provided that the porosity and permeability can be assumed to be independent of the state of stress (Lubinski, 1954 via Perkins and Gonzalez, 1985). The relationship between stress and pore pressure is given by the linear poro-elastic expansion coefficient (equation 5.12).

$$J = \frac{1-2\upsilon}{E} * \mathrm{bi} \qquad [5.12]$$

$\mathrm{bi} = \text{Biot's constant(usually 1 for fluid filled reservoir rocks Biot, (1941)}$

The (elliptical) semi axis of the flooded region are calculated in the same manner as for the cooled region. However, pressure changes are present in the entire flooded region, therefore the flooded volume instead of the cooled volume is used (equation 5.13 -5.14).

$$a_{fl} = L_f(F_2^{1/2} + F_2^{-1/2})/2 \qquad [5.13]$$

$$b_{fl} = L_f(F_2^{1/2} - F_2^{-1/2})/2$$

$$F_2 = \frac{2V_{fl}}{\pi L_f^2 h} + \frac{1}{2}\sqrt{\left(\frac{4V_{fl}}{\pi L_f^2 h}\right)^2 + 4} \qquad [5.14]$$

$$V_{fl} = \frac{qt}{\phi}$$

With

$$a_{fl} = \text{Major semi axis of the flooded region } [-]$$

Poro-elastic stress changes are then calculated using equations 5.15 – 5.16 and will be radial symmetric, just as the thermo-elastic stress changes. The $Co_{H1,2}$ coefficients are the same as in equations 5.10 & 5.11 with e_c being replaced by $e_{fl} = b_{fl}/a_{fl}$.

$$\Delta\sigma_{yP} = \frac{EJ\Delta P}{1-\upsilon} * Co_{H1} \qquad [5.15]$$

$$\Delta\sigma_{xP} = \frac{EJ\Delta P}{1-\upsilon} * Co_{H2} \qquad [5.16]$$

Where

$\Delta\sigma_{yP} =$ Poro − elastic stress change perpendicular to $\sigma_{h,min}$ [Pa]

$\Delta\sigma_{xP} =$ Poro − elastic stress change parallel to $\sigma_{h,min}$ [Pa]

Fracturing criterion

As the aim of a thermal stimulation job is to form fractures so as to increase the connectivity and permeability of a reservoir, it is necessary to evaluate the reduction in thermo and poro-elastic stress changes induced by the injection of cold injectate. The change in the pressure and stress field has to satisfy the fracturing criterion (equation 5.17) in order for fractures to form.

The fracturing criterion, which includes the pressure and stress changes due to cold fluid injection, has the following form:

$$(P_{ini} + \Delta P_{tot}) - (\sigma_{Ten} + \sigma_{h,min} + \Delta\sigma_{inj}) > 0 \qquad [5.17]$$

Where:

$$\Delta\sigma_{inj} = \Delta\sigma_T + \Delta\sigma_{P,cold} + \Delta\sigma_{P,fl} \qquad [5.18]$$

With:

$$\sigma_{Ten} = \text{Tensile rock strength [Pa]}$$
$$\Delta\sigma_{P,cold} = \text{Poro} - \text{elastic stress change in cooled region [Pa]}$$
$$\Delta\sigma_{P,fl} = \text{Poro} - \text{elastic stress change in flooded region [Pa]}$$

Tensile rock strength is assumed to be 0 Pa, as the tensile strength of an already fractured reservoir rock is generally assumed to be negligible.

The poro-elastic effects of the stress change have been divided into two parts: a part affecting the cooled region and a part affecting the entire flooded region. This approach is chosen due to the different evolution of average reservoir pressure versus pressure changes near the well (Detienne et al., 1998) (figure 24 & figure 26).

Using the pressure and temperature distribution (figure 24), the cooled region was defined as the radius where the temperature is equal to half the temperature difference at the wellbore (equation 5.19). The radius of the flooded region was determined by the use algebra and the assumptions regarding the reservoir and injected region (equation 5.20).

$$r_{cold} = r\left(\frac{\Delta T(r_{well})}{2}\right) \qquad [5.19]$$

$$r_{fl} = \sqrt{\frac{V_{fl}}{\pi h}} \qquad [5.20]$$

Rearranging the stress changes from equation 5.18:

$$\Delta\sigma_{P,cold} = \Delta\sigma(r_{well}) - \Delta\sigma(r_{fl})$$

The stress change in the cooled region was then determined by taking the stress change for r_{cold} from figure 26. Stress change in the flooded region was determined in the same manner, but with r_{fl} (equation 5.20) instead of r_{cold}.

Only the initial reservoir pressure and the initial minimum horizontal stress are unknown at this point but play a crucial role in the evaluation of the fracturing criterion. The tensile rock strength for already fractured or jointed rock is zero, or very small for intact rock. Assuming a hydrostatic gradient and pressure, the initial reservoir pressure is a function of depth and rock density (equation 5.21).

$$P_{ini} = \rho_{inj}\, g\, d \qquad [5.21]$$

With:

$$\rho_{inj} = \text{Injectate density } [\mathrm{kg/m^3}]$$
$$g = \text{Gravitational acceleration constant } [9.8\ \mathrm{m/s^2}]$$

The initial minimum horizontal stress is calculated using Eaton's equation (equation 5.22). Starting with the vertical stress which, assuming a lithostatic gradient, is related to the rock density (ρ_{res}) (equation 5.23).

$$\sigma_{hmin} = \left(\frac{\upsilon}{1-\upsilon}\right) * (\sigma_v - P_{ini}) + P_{ini} \qquad [5.22]$$

$$\sigma_v = \rho_{res}\, g\, d \qquad [5.23]$$

With:

$$P_{ini} = \text{Initial reservoir pressure } [\mathrm{Pa}]$$
$$\upsilon = \text{Poisson'sratio } [-]$$
$$\sigma_{hmin} = \text{Minimum horizontal principle stress } [\mathrm{Pa}]$$
$$\sigma_v = \text{Vertical principal stress } [\mathrm{Pa}]$$

5.2 PRELIMINARY RESULTS AND CALIBRATION

All modelling thus far has been done using a simple spreadsheet. It has been tested and calibrated using input and calibrated using input parameters and results from de Koning, (1988) and Perkins and Gonzalez (1985) Gonzalez (1985) (table 7 &

table 8). The test case concerns a relatively high permeability reservoir and a temperature difference of 70 °C.

Injection properties		
Parameter	**Input unit**	**Value**
Injection rate	m^3/d	8000
Injection time	D	730
Temperature difference	°C	-70
Density of injection fluid (H2O)	kg/m^3	1000
Viscosity of injectate	Pa*s	$1,0*10-^{3}$
Heat capacity of injectate	J/m^3 °C	$4,20*10^6$
Compressibility of injectate	1/Pa	$4,40*10^{-10}$

table 7

Properties of the injectate used as input for initial tests and calibration of the temperature and pressure distribution and the stress changes.

Pressure and temperature distribution

Pressure and temperature change where calculated for a radius of 200 m and a time of two years (figure 24). two years (figure 24). Pressure is increased with 39 bars and radially decreases according to the natural logarithm (equation 5.6). As the reservoir has relatively high permeability (250 mD,

table 8), the pressure change would increase when permeability would be lower.

The results for the temperature change show a typical Lauwerier's solution, the reservoir remains unaffected at $r = 176$ m, which is equal to R_c (equation 5.2). It shows that, due to the long injection time, a relatively large volume of reservoir rock has been cooled. Using the results presented in figure 24 as input for equations 5.10-5.11 and 5.15-5.16, the resulting poro and thermo-elastic stress changes can be calculated at any radial distance from the wellbore.

table 8

Overview of the reservoir properties used as input for testing and calibration of the pressure and temperature distribution and the poro and thermo-elastic stress changes.

Reservoir properties		
Parameter	**Input unit**	**Value**
Height of reservoir	m	120
Depth of reservoir	m	2000
Position relative to centre of reservoir	m	0
Radius of the wellbore	m	0,11
Radial distance from the wellbore	m	0,11 – 240
Permeability	m2	$2{,}50*10^{-13}$
Porosity	-	0,24
Density of reservoir rock	kg/m^3	2500
Formation compressibility	1/Pa	$8{,}60*10^{-5}$
Heat capacity of formation	J/m^3 °C	$2{,}10*10^{6}$
Heat capacity of cap and base rock	J/m^3 °C	$2{,}10*10^{6}$
Linear thermal expansion coefficient	mm/mmK	$1{,}00*10^{-6}$
Biot's constant	-	1
Initial fracture half length (equal to r_{well})	m	0,11
Young's modulus	Pa	$4{,}50*10^{10}$
Poisson's ratio	-	0,15
Thermal diffusivity of cap and base rock	m^2/s	$1{,}00*10^{-6}$
Thermo-elastic constant	Pa/°C	$1{,}00*10^{5}$
Poro-elastic constant	Pa/Pa	0,5

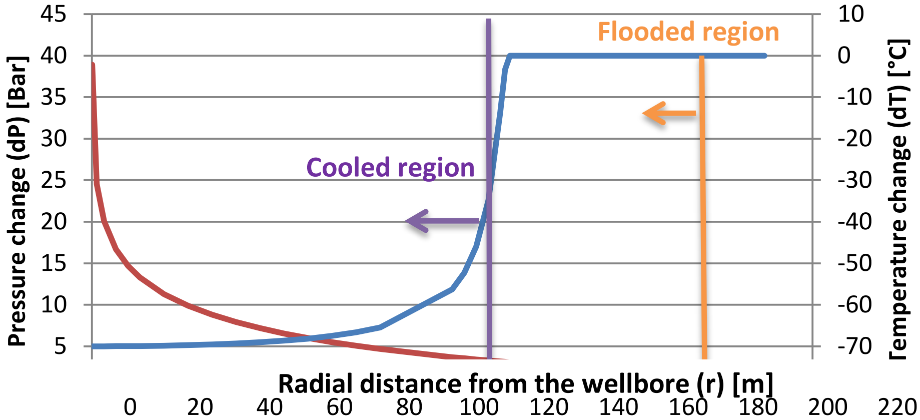

figure 24

Radial pressure ar ı

de Koning (1988).

Note the left axis c T).

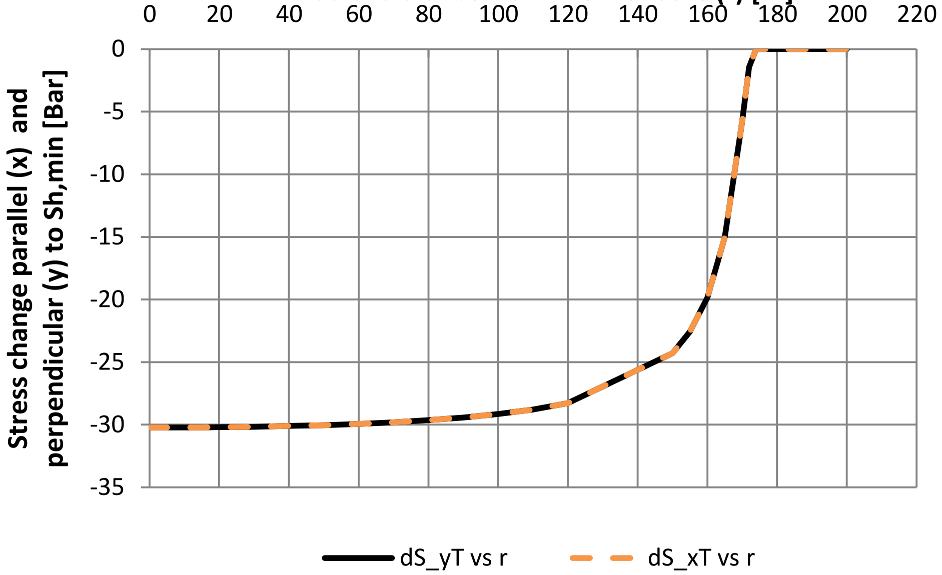

figure 25

Thermo-elastic stress change as a result of dT. Both the stress variation in parallel (x) and perpendicular (y) to the direction of Sh, min are plotted.

As can be seen in equations 5.10-5.11, the thermo-elastic stress is strongly dependant on the temperature distribution. Therefore the thermo-elastic stress change is analogous to Lauwerier's temperature solution (figure 25). The 70℃ temperature difference between the reservoir and the injectate results in a negative stress change of 57 bar. It is negative as the thermal shock decreases the effective reservoir rock strength. For high enthalpy geothermal systems, the change in stress would increase linearly with the temperature difference (equation 5.10-5.11). figure 25 displays the stress change perpendicular (x) and parallel (y) to the minimal horizontal stress direction. The two curves overlap completely, indicating a radial symmetric zone of stress change, which is in accordance with the model setup. Should fractures develop, the region would grow elliptical and the stress changes with respect to the direction of the minimum horizontal stress would not be overlapping.

Poro-elastic stress change

As is predictable, based on equations 5.15-5.16, the pressure induced poro-elastic stress change is also dependant on the pressure distribution from figure 24 and thus equations 5.6. The injection results in a positive stress change of 17 bars, which is linearly dependant on the injection rate and also non – linearly on time (equation 5.24).

$$\Delta\sigma_{dP} \propto \frac{q}{t}\ln(t) = q\ln\left(t^{1/t}\right) \qquad [5.24]$$

As was the case with the thermo-elastic stress change, the curves for the pressure induced stress variation overlap as the affected region is circular. The curve displays a steep gradient, equivalent to the shape of the logarithm (equation 5.15). Its steep behaviour is due to the ratio of $e^{-\gamma}/u$, with $u \propto r^2$. Meaning that when r increases, $\ln(u)$ decreases significantly. This results in relatively significant stress variations near the wellbore which rapidly decrease outward (figure 26).

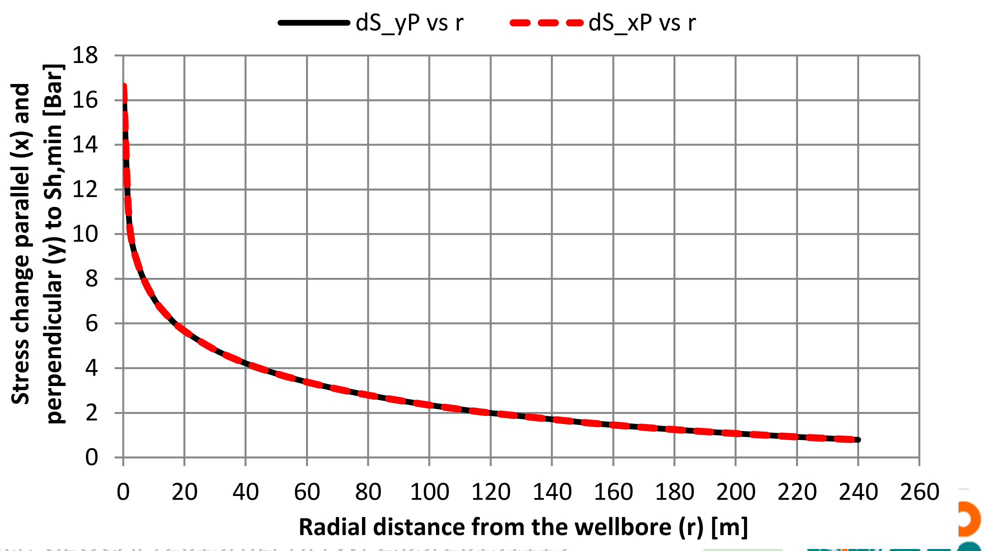

Fracturing criterion

Using the input data from table 7 &

table 8, the fracturing criterion of equation 5.17 is evaluated, and results are presented in

table 9. Model results indicate that there is no fracture in initiation under the currently assumed conditions.

Fracturing Criterion		
P_{ini}	Bar	245
σ_v	Bar	490
σ_{hmin}	Bar	288
ΔP_{tot}	Bar	37
$\Delta\sigma_P(r_{cold})$	Bar	26
$\Delta\sigma_P(r_{fl})$	Bar	1.1
$\Delta\sigma_T$	Bar	-15
$P_{bfp}(r_{well})$	Bar	**282**
$\sigma_{tot}(r_{well})$	Bar	**300**
$P_{bfp}(r_{well}) - \sigma_{tot}(r_{well})$	Bar	**-18**
		No frac

figure 26

Poro-elastic stress change as a result of dP. Stress variations are plotted parallel (x) and perpendicular (y) to the direction of Sh, min.

table 9

Overview of the bottomhole flowing pressure and total stress in the reservoir using the parameters defined in table *7*

table 8.

5.3 Discussion of preliminary results

Based on these initial results, some comments can be made regarding the changed stress state of the reservoir and the fracturing criterion.

First of all, the it is apparent that the thermo-elastic stress reduction *at the well* is dominant over the poro-elastic term with |30| vs |17| bars respectively (figure 25 & figure 26). The thermo-elastic stress change is also significant over a larger radius, whereas the poro-elastic component is only really significant very close to the wellbore.

Evaluation of the fracture criterion using the input from table 7

table 8 show there are no fractures formed (

table 9). However, the deficit until the critical state is reached is only 18 bar. As is clear from the derivation in section 5.2, there are numerous factors that influence the results of the fracturing criterion. Decreasing the reservoir depth and permeability will increase the net pressure, creating more favourable conditions for fracturing to occur.

A larger temperature difference will naturally increase the thermo-elastic stress change, optimizing the reservoir change, optimizing the reservoir conditions for fracture initiation. The temperature difference assumed in table 7 assumed in table 7 &

table 8 is relatively low for high enthalpy geothermal systems (70 °C). If we assume a temperature difference of 200 °C, $P_{bfp}(r_{well}) - \sigma_{tot}(r_{well}) = 10$ bar. Thus with a more realistic temperature difference for high temperature geothermal reservoirs fracturing would occur.

Sensitivity analysis shows that the thermo-elastic stress change is very sensitive to variation of the thermo-elastic expansion coefficient (β), as it is linearly related to the thermo-elastic stress change. A single order of magnitude change thus has the same effect on the thermo-elastic stress change, which can lead to unrealistic results. It is possible that this is the result of some error in the derivation or interpretation from previous work (de Koning, 1988; Detienne et al., 1998; Perkins and Gonzalez, 1985). However, evaluation of the derivation has yielded any errors. Thus when varying the thermo-elastic expansion coefficient, great care has to be taken not to create unrealistic input values or results.

Several other assumptions are a point of discussion. All previous work on which the derivation was based assumed that the viscosity of the injectate and the reservoir fluid is similar and use a single value (de Koning, 1988; Detienne et al., 1998; Perkins and Gonzalez, 1985). However, these works concern waterflooding and thermal induced fracturing (TIF) in hydrocarbon reservoirs, where temperatures are never so high as in high enthalpy geothermal systems. The total dissolved solids (TDS) content is also not taken into account. As these properties are related to each other and the pressure and temperature, a possible solution is to use an algorithm that calculates the viscosity of the injectate based on these parameters.

The assumption used here and by Detienne et al. (1998) and Perkins and Gonzalez (1985) concerning pressure behaviour in the cooled and flooded zones is disputable. It is assumed that the pressure and temperature changes are uniform in an elliptical (or in this case circular) area. For the temperature distribution this is quite realistic (figure 24) and it is considered valid. However, as can be clearly seen in the pressure distribution, this assumption is not really realistic. It has been partly corrected by dividing the affected region into zones for which the poro-elastic stress changes have been separately determined. However, it is still a point where the model could be improved. It should be noted that de Koning (1988) was pointed this out and used a different approach. However, attempts to use this methodology have been unsuccessful, it is rather complicated and results were unrealistic.

As has been mentioned at the start of this chapter, the model is a first order approximation of reality. As such there are several assumptions used that may be invalid under certain circumstances. Any model is a theoretical approximation of reality and as such some complexities are not or cannot be considered in this model. For instance, the model assumes a radially infinite symmetric reservoir. This is likely unrealistic in the complex geological environment of a volcanic reservoir. Incorporating the unknown 3D structure and geometry of a reservoir is however, outside the scope and aim of this study. The effect of structures (geometrical or fault related) can also be minimised by positioning the well as far away from such structures as possible, as stimulation is at its most effective near the wellbore. Therefore it is concluded that the model can be utilised as an indicative tool for stimulation treatment planning, but care should be taken where in the reservoir the well is positioned.

Also, more complex problems exist, for instance the manner in which pore fluid pressure increase acts on the reservoir. It is generally assumed that these pressures translate directly. But it is unclear if this assumption is valid and this is a current topic of scientific research. Or the fact that the bottom hole flowing pressure is generally assumed to be equal to the reservoir pressure, as it is unclear what effect of skin is the translation of these pressures.

Outstanding issues

The model is not yet finished, although the current results are a good start. Poro and thermo-elastic stress changes due to injection are calculated and a fracturing criterion has been developed. If there is fracture initiation, fractures will continue to grow as long as the net pressure remains larger than 0. Subsequent injection will no longer be radial as the developing fractures will have to be taken into account.

When using the following assumptions (de Koning, 1988), the evolution of fracture propagation can be calculated.

- Fractures are elliptical in plan view and rectangular in cross-section (figure 27).
- Fracture height is equal to the reservoir height.
- The fracture has infinite conductivity, there is no pressure drop along the fracture.
- The leak of rate into the reservoir is equal to the injection rate.
- Injection fluid has the same mobility and compressibility as the reservoir fluid.
- The fracture propagates with a constant pressure inside (P_{frac} is equal to P_{bfp}).

figure 27
Assumed 3D geometry of a fracture. Note that 'L' in the figure is equal to 'Lf´. From: *de Koning (1988)*.

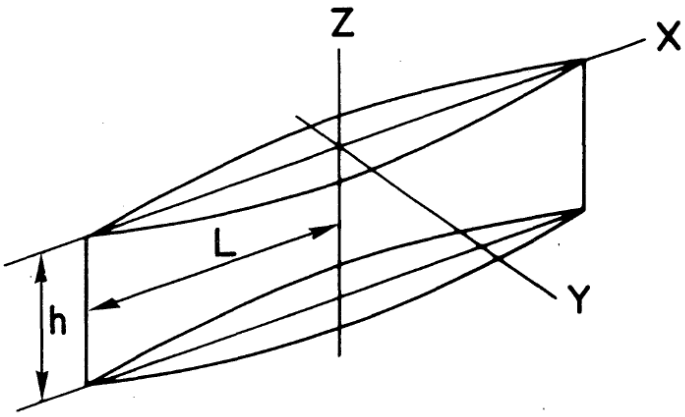

Thermo-elastic tress at the fracture tip is determined using Lauwerier´s solution (equation 5.1; figure 24), but the temperature at the well is replaced with the temperature at the fracture tip (T_{L_f}).

For determination of the fracture length equations 5.8-5.11 and 5.13-5.16 are reiterated for different fracture lengths (L_f) until the bottomhole flowing pressure is equal the stress at the tip of the fracture: $\mathrm{P}_{\mathrm{bfp}}(\mathrm{r_{well}}) = \sigma_{\mathrm{frac.tip}}$ (Detienne et al., 1998). Using the final fracture length, a skin factor resulting from the stimulation treatment can be determined using equation 5.25.

$$\mathrm{s_f} = \mathrm{G} - \ln\left(1 + \frac{\mathrm{L_f}}{\mathrm{r_{well}}}\right) \qquad [5.25]$$

Where:

$\mathrm{G} = \mathrm{Conductivity} = 0.69$

The conductivity G has an asymptotic value of 0.69 for relative conductivities larger then 30 (Detienne et al., 1998), which is valid as it is assumed that the fracture has infinite conductivity.

Recommendations

The procedure stated above requires iteration to determine the fracture length. All the modelling up to this point has been done using a spreadsheet, therefore the fracture length and corresponding skin factor could not be determined. Due to time constraints on the project, an iterative model could not be finalised. But a start was made and initial results seem promising. Using this iterative procedure, it is possible to model time steps instead of a final situation and thus the evolution of the fracture development and growth. A function relating the viscosity of the fluid to the TDS (total dissolved solids) concentration, pressure and temperature has also been inserted. However, this iterative model is not yet finalized and therefore not presented.

By further implementation of the procedure stated above it should not be difficult to finalize this model using some sort of numerical modelling software (e.g. Matlab). If possible, it would be desirable to use an approach to the poro-elastic stress change that does not assume a step profile.

Testing and validation of the model using real data is the highest recommendation made as without this, the purpose of constructing this model is mute. In order to properly test the final model it would be desirable to have the following data from a successful thermal stimulation treatment in a (volcanic) high enthalpy geothermal reservoir.

- Raw data of drilling activities, well tests and data during production:
- Well logs (depth, reservoir pressures, temperatures), drilling mud data
- Borehole breakout data (calliper-four-arm method)
- Stress magnitudes (horizontal/vertical)
- Pressure curves during drilling and during well test/production
- Flow rates, volumes, temperatures produced/injected
- Volume and Temperature of injected water during (fracture)tests or injection of waste water.
- (micro)seismic activity data
- Historical data about the well
- Rock properties (Young’s modulus, Poisson’s ratio)
- Injection fluid properties
- Reservoir fluid and gas properties

6 CONCLUSIONS

The main goal of GEOCAP WP 2.05 is the enhancement of geothermal reservoir productivity by application of stimulation techniques, this study covered a part of this main goal. Evaluation of available literature on stimulated high enthalpy geothermal wells has produced an overview of available techniques and their success rates. Literature evaluated focussed on situations worldwide with similarities to the Indonesian situation as the available literature on stimulation of geothermal wells in Indonesia was insufficient.

Modelling – conclusions and recommendations for further research

A start was made with a model for thermal stimulation. The model is designed to be used for quick initial evaluations in order to assist in selection of the best stimulation technique. It incorporates thermo and poro-elastic stress changes resulting from cold fluid injection. Initial results indicate that cooling of the reservoir is an effective way to decrease the effective stress in the reservoir and thus lowering the fracture initiation pressure. Higher temperature differences between the injectate and the reservoir result in larger decrease of effective stress, making thermal stimulation a very interesting technique for high temperature reservoirs. The model is not yet finished, construction of an iterative model is required to model the evaluation of the evolution of fracture initiation and propagation. A promising start has been made and it should be relatively easy to finish this using numerical modelling software (e.g. Matlab).

When finalized, it is important that the model be adequately tested and evaluated by running a test case with data from a successful thermal stimulation treatment.

Literature – conclusions and recommendations for further research

The literature evaluation produced data on a total of 92 stimulation treatments worldwide. Literature on Literature on stimulation of 16 wells in the Salak field was also found. Overall results of these treatments are treatments are positive with a 74% success rate overall. Stimulation in the Salak field in Indonesia was performed Indonesia was performed on 16 wells, most of which have been subjected to chemical stimulation with a thermal stimulation with a thermal component (Appendix A,

Table 3). Success rate was 68% with an average improvement of 168%.

Conclusions regarding hydraulic stimulation are problematic due to insufficient data, only 11 treatments where found in literature.

Based on 47 wells, chemical stimulation was successful in 74% of the time (figure 19). Wells showed an average improvement of 167% (*table 5* & table 6). Thermal stimulation was, based on 34 wells, successful 85% of the time (figure 19) with an average improvement of 155% (*table 5* & table 6). figure 20 displays improvement data from both techniques and it is observed that the spread of the improvement data is quite large.

Looking at these numbers, it is concluded that chemical stimulation has a slightly higher average improvement rate but the success rate of thermal stimulation is slightly higher. It should be noted that the large differences in the improvement of individual wells indicate that exact predictions of the improvement of an individual well is impossible.

From Appendix B it can be observed that most thermal stimulation treatments are performed in countries with relatively long geothermal development histories (e.g. New Zealand, Iceland). Therefore, when designing stimulation treatments, it is recommended that the designers considers thermal stimulation as an option. Based on the results presented in this report, thermal stimulation can be a powerful stimulation technique.

Although a significant amount of literature has been evaluated, some recommendations for future research are:

This study did not include stimulation in enhanced geothermal systems (EGS). However hydraulic stimulation is the most applied stimulation technique in EGS systems. Therefore, evaluation of literature pertaining to (hydraulic) stimulation EGS systems could provide valuable insights into the effectiveness of hydraulic stimulation. Shear stimulation has also been applied to EGS systems can could be especially interesting for high competence geothermal reservoirs with suitable conditions.

Finally, although literature on stimulation treatments performed in Indonesia is scarce, it is recommended that further investigation in the future be conducted. Results could enhance the understanding of the effectiveness of various stimulation techniques in the Indonesian situation.

7 List of symbols

$$P_{bfp} = \text{ Bottomhole flowing (applied)pressure [Pa]}$$
$$\Delta P = \text{Pressure change as a result of injection[Pa]}$$
$$\sigma_{Ten} = \text{Tensile rock strength [Pa]}$$
$$\Delta T = T_{inj} - T_{ini} \text{ [°C]}$$
$$r_{well} = \text{Well radius [m]}$$
$$S = \text{Storativity [−]}$$
$$d = \text{Reservoir depth [m]}$$

8 REFERENCES

Acuña, J.A., Stimac, J., Sirad-Azwar, L., Pasikki, R.G., 2008. Reservoir management at Awibengkok geothermal field, West Java, Indonesia. Geothermics, Indonesian geothermal prospects and developments 37, 332–346. doi:10.1016/j.geothermics.2008.02.005

Akin, S., 2015. Coiled Tubing Acid Stimulation of Alaşehir Geothermal Field, Turkey, in: Proceedings World Geothermal Congress 2015. Melbourne, Australia.

Amisoto, A.E., Aqui, A.R., Yglopaz, D.M., Malate, R.C.M., 2005. Sustaining steam supply in Palinpinon 1 production field, Southern Negros Geothermal project, Philippines, in: Proceedings. Presented at the World Geothermal Congress, Antalya, Turkey, p. 5.

Aqui, A.R., Zarrouk, S., 2011. Permeability Enhancement of Conventional Geothermal Wells, in: Proceedings. Presented at the New Zealand Geothermal Workshop, Auckland, New Zealand.

Ariki, K., Kato, H., Ueda, A., Bamba, M., 2000. Characteristics and management of the Sumikawa geothermal reservoir, northeastern Japan. Geothermics 29, 171–189. doi:10.1016/S0375-6505(99)00056-5

Axelsson, G., Thórhallsson, S., 2009. Reviw of well stimulation operations in Iceland. GRC Trans. 33, 6.

Axelsson, G., Thórhallsson, S., Björnsson, G., 2006. Stimulation of geothermal wells in basaltic rock in Iceland. Engine 1–9.

Barelli, A., Cappetti, G., Manetti, G., Peano, A., 1985. Well stimulation in Latera field. Geotherm. Resour. Counc. Trans. 9, 8.

Baterbaev, M.D., Bulavin, V.D., 2002. Application of Technology of electroinfluence for intensification of an oil recovery in Russia and abroad. Neft. Khozyaistvo - Oil Ind. 11, 92–95.

Biot, M.A., 1941. General Theory of Three-Dimensional Consolidation. J. Applies Phys. 12, 155–164.

Bjornsson, G., 2004. Reservoir conditions at 3-6 km depth in the Hellisheide geothermal field, SW-Iceland, estimanted by deep drilling, cold water injection and seismic monitoring., in: Proceedings. Presented at the Twenty-Ninth Workshop on Geothermal Reservoir Engineering, Stanford University, Stanford, California, p. 8.

Boyadjiev, L., Kamenov, O., Kalla, S., 2005. On the Lauwerier formulation of the temperature field problem in oil strata. Int. J. Math. Math. Sci. 2005, 1577–1588. doi:10.1155/IJMMS.2005.1577

Caranto, J.A., Bayrante, L.F., Lagmay, A.M.F.A., 2010. Configuration of the Geothermal prospects in the Leyte Geothermal Reservation (Philippines) and implications of a volcano-tectonic framework in exploration, in: Proceedings. Presented at the World Geothermal Congress, Bali, Indonesia, p. 5.

Cardoso, R.R., Hamza, V.M., Alfaro, C., 2010. Geothermal resource base for South America: A continental perspective, in: Proceedings. Presented at the World Geothermal Congress, Bali, Indonesia, p. 6.

Castro-Zùñiga, S., 2015. Increasing permeability in deep geothermal wells through water injection for the Las Pailas and Borinquen geothermal fields, Costa Rica, in: Proceedings. Presented at the World Geothermal Congress, Melbourne, Australia, p. 9.

Chabora, E., Zemach, E., Spielman, P., P Drakos, Hickman, S., Lutz, S., Boyle, K., Falconer, A., Robertson-Tait, A., Davatzes, N.C., Rose, P., Majer, E., Jarpe, S., 2012. Hydraulic stimulation of well 27-15, Deser Peak Geothermal Field, Nevada, USA, in: Proceedings. Presented at the Thirty-Seventh Workshop on Geothermal Reservoir Engineering, Stanford University, Stanford, California.

Chen, W., Maurel, O., Reess, T., De Ferron, A.S., La Borderie, C., Pijaudier-Cabot, G., Rey-Bethbeder, F., Jacques, A., 2012. Experimental study on an alternative oil stimulation technique for tight gas reservoirs based on dynamic shock waves generated by Pulsed Arc Electrohydraulic Discharges. J. Pet. Sci. Eng., Unconventional hydrocarbons exploration and production Challenges 88–89, 67–74. doi:10.1016/j.petrol.2012.01.009

Cidoncha, G., Ignacio, J., 2007. Application of Acoustic Waves for Reservoir Stimulation. Society of Petroleum Engineers. doi:10.2118/108643-MS

Clearwater, J., Azwar, L., Barnes, M., Wallis, I., Holt, R., 2015. Changes in injection well capacity during testing and plant start-up at Ngatamariki., in: Proceedings. Presented at the World Geothermal Congress, Melbourne, Australia, p. 11.

Clements, B., Hall, R., Smyth, H.R., Cottam, M., 2009. Thrusting of a volcanic arc: a new structural model for Java. Pet. Geosci.

15, 159–174. doi:10.1144/1354-079309-831

Craig, J., Absar, A., Bhat, G., Cadel, G., Hafiz, M., Hakhoo, N., Kashkari, R., Moore, J., Ricchiuto, T.E., Thurow, J., Thusu, B., 2013. Hot springs and the geothermal energy potential of Jammu & Kashmir State, N.W. Himalaya, India. Earth-Sci. Rev. 126, 156–177. doi:10.1016/j.earscirev.2013.05.004

Crow, M.J., Barber, A.J., 2005. Simplified geological map of Sumatra.

C. W. Morris, A. R. Sinclair, 1984. Evaluation of bottomhole treatment pressure for geothermal well hydraulic fracture stimulation. J. Pet. Technol. 36, 829–836.

Davidson, J., Siratovich, P., Wallis, I., Gravley, D., McNamara, D., 2012. Quantifying the Stress Distribution at the Rotokawa Geothermal Field, New Zealand, in: Proceedings. Presented at the New Zealand Geothermal Workshop, Auckland, New Zealand, p. 8.

de Koning, E.J.L., 1988. Waterflooding under fracturing conditions (Phd Thesis). Technische Universiteit Delft, Delft.

Detienne, J.-L., Creusot, M., Kessler, N., Sahuquet, B., Bergerot, J.-L., 1998. Thermally Induced Fractures: A Field-Proven Analytical Model. SPE Reserv. Eval. Eng. 1, 30–35. doi:10.2118/30777-PA

Eaton, B.A., 1969. Fracture Gradient Prediction and Its Application in Oilfield Operations. SPE-2163-PA. doi:10.2118/2163-PA

Economides, M.J., Martin, T., 2007. Modern Fracturing; enhancing natural gas production. ET Publishing, Houston, Texas.

Economides, M.J., Nolte, K.G., 2000. Reservoir stimulation, Third. ed. John Wiley & Sons.

Ellsworth, W.L., 2013. Injection-Induced Earthquakes. Science 341, 1225942. doi:10.1126/science.1225942

Enayatpour, S., Patzek, T., 2013. Thermal Shock in Reservoir Rock Enhances the Hydraulic Fracturing of Gas Shales, in: Unconventional Resources Technology Conference, Denver, Colorado, 12-14 August 2013, SEG Global Meeting Abstracts. Society of Exploration Geophysicists, American Association of Petroleum Geologists, Society of Petroleum Engineers, pp. 1500–1510.

Entingh, D.J., 2000. Geothermal well stimulation experiments in the United States, Proceedings World Geothermal Congress. Kyushu - Tohoku, Japan, May 28 - June 10, 2000.

Esberto, M.B., Nogara, J.B., Daza, M.V., Sarmiento, Z.F., 1998. Initial response to exploitation of the Mt. Apo geothermal resrvoir, Cotabato, Philippines, in: PROCEEDINGS,. Presented at the Twenty-Third Workshop on Geothermal Reservoir Engineering, Standford University, Stanford, California, p. 8.

Fitch, T.J., 1972. Plate convergence, transcurrent faults and internal deformation adjacent to southeast Asia and the Western Pacific. J. Geophys. Res. 77, 4432–4462.

Flores-Armenta, M., Davies, D., Couples, G., Palsson, B., 2005. Stimulation of geothermal wells, can we afford it?, in: Proceedings. Presented at the World Geothermal Congress, Antalya, Turkey, p. 8.

Flores, M., Ramírez, M., 2010. Evaluation of acid treatments in Mexican geothermal fields. Geotherm. Resour. Counc. Trans. 34, 7.

Flores, M., Tovar, R., 2008. Thermal fracturing of well H-40, Los Humeros Geothermal Field. GRC Trans. 32, 5.

Fukuda, D., Watanabe, M., Arai, F., Sasaki, S., Sako, O., Matsumoto, Y., Yamazaki, S., 2010. Removal of anhydrite and Mg-silicate scales from production wells using chemical agents at the mori geothermal field in Hokkaido, Japan: an application of chemical well stimulation., in: Proceedings. Presented at the World Geothermal Congress, Bali, Indonesia, p. 5.

Guillermo, J., Sánchez-Velasco, R., 2003. Acid stimulation of production wells in Las Tres Vírgenes geothermal field, BCS, México. Geotherm. Resour. Counc. Trans. 27, 8.

Gunnarsson, G., 2011. Mastering reinjection in the Hellisheide field, SW-Iceland: a story of successes and failures., in: Proceedings. Presented at the Thirty-Sixth Workshop on Geothermal Reservoir Engineering, Stanford University, Stanford, California, p. 8.

Gutiérrez-Negrín, L.C.A., 2015. Mexican Geothermal Plays, in: Proceedings. Presented at the World Geothermal Congress, Melbourne, Australia, p. 9.

Hall, R., 2002. Cenozoic geological and plate tectonic evolution of SE Asia and the SW Pacific: computer-based reconstructions, model and animation. J. Asian Earth Sci. 20, 353–431.

Hanold, R.J., 1980. Explosive stimulation of geothermal well at the Geysers., in: Proceedings. Presented at the Geothermal Reservoir Well Stimulation Symposium, U.S. Department of Energy, Santa Fe Springs, California, pp. 215–221.

Hanold, R.J., Morris, C.W., 1982. Induced fractures - Well stimulation through fracturing. Geotherm. Resour. Counc., Fractures in Geothermal Reservoirs: A workshop 1–10.

Hernandez, I., Del Valle, J., Espindola, S., 2013. Geothermal Well stimulation using water jet cutting in Mexico. GRC Trans. 37, 4.

Hoffmann-Rothe, A., Ritter, O., Haak, V., 2001. Magnetotelluric and geomagnetic modelling reveals zones of very high electrical conductivity in the upper crust of Central Java. Phys. Earth Planet. Inter. 124, 131–151.

Hulen, J.B., Anderson, T.D., 1998. The Awibengkok, Indonesia, geothermal research project, in: Proceedings. Presented at the Twenty-third workshop on Geothermal Reservoir Engineering, Stanford University, Stanford, California, p. 8.

Hulen, J.B., Stimac, J.A., Sugiaman, F., 2000. The Awibengkok core research program, pt. II - Stratigraphy, Volcanic Facies and Hydrothermal Alteration., in: Proceedings. Presented at the World Geothermal Congress 2000, Kyushu-Tohoku, Japan, p. 6.

Hyodo, M., Shinohara, N., Takasugi, S., Wright, C.A., Green, A.S.P., 1995. Hydraulic fracturing test and pressure behaviour analysis for fracture evaluation., in: Proceedings. Presented at the World Geothermal Congress, Florence, Italy, pp. 2591 – 2596.

Jaeger, J.C., Cook, G.W., Zimmerman, R.W., 2007. Fundamentals of rock mechanics, 4th ed. Blackwell Publishing, Oxford, UK.

Kato, O., Okabe, T., Shigehara, S., Doi, N., Tosha, T., Koide, K., 2000. Permeable fractures and in-situ stress at the Kakkonda geothermal field, Japan, in: Proceedings. Presented at the World Geothermal Congress, Kyushu-Tohoku, Japan, p. 6.

KeH, 2012. Kennisdocument hydraulic fracturing.

Kitao, K., Ariki, K., Watanabe, H., Wakita, K., 1995. Cold-water well stimulation experiments in the Sumikawa geothermal field, Japan. Geotherm. Resour. Counc. Bull. 10.

Kizaki, Y., Sato, K., 1996. Increase in steam prodocutivity by hydraulic fracturing stimulation in the Kakkonda geothermal field, Japan. Geotherm. Resour. Counc. Bull. 11.

Kruseman, G.P., de Ridder, N.A., 1994. Analysis and evaluation of pumping test data, 2nd ed, ILRI publication. ILRI.

Lee, H.S., Cho, T.F., 2002. Hydraulic Characteristics of Rough Fractures in Linear Flow under Normal and Shear Load. Rock Mech. Rock Eng. 35, 299–318. doi:10.1007/s00603-002-0028-y

Legarth, B.J., E. Huenges, G. Zimmermann, 2005. Hydraulic fracturing in a sedimentary geothermal reservoir: results and implications. Int. J. Rock Mech. Min. Sci. 42, 1028–1041.

Lim, Y.W., Grant, M., Brown, K., Siega, C., Siega, F., 2011. Acidising case study - Kawerau injection wells, in: Proceedings. Presented at the Thirty-Sixth Workshop on Geothermal Reservoir Engineering, Stanford University, Stanford, California, p. 6.

Lubinski, A., 1954. Theory of elasticity for porous bodies displaying a strong pore structure., in: Proceedings. Presented at the 2nd US National Congress of Applied Mechanics, University of Michigan, Ann Arbor, Michigan, pp. 247 – 256.

Lund, J.W., Gawell, K., Boyd, T.L., Jennejohn, D., 2010. The United States of America country update 2010, in: PROCEEDINGS,. Presented at the Thirty-Fifth Workshop on Geothermal Reservoir Engineering, Standford University, Stanford, California, p. 19.

Majer, E.L., Baria, R., Stark, M., Oates, S., Bommer, J., Smith, B., Asanuma, H., 2007. Induced seismicity associated with Enhanced Geothermal Systems. Geothermics 36, 185 – 222. doi:http://dx.doi.org/10.1016/j.geothermics.2007.03.003

Malate, R.C.M., Buiing, B.C., Momlina, P.O., Yglopaz, D.M., A.M. Lacanilao, 2000. SK-2D: A case history on geothermal wellbore enhancement, Mindanao geothermal production field, Philippines, in: Proceedings. Presented at the World Geothermal Congress, Kyushu-Tohoku, Japan, p. 6.

Malate, R.C.M., Yglopaz, D.M., Austria, J.J.C., Sarmiento, Z.F., 1997. Acid stimulation of injection wells in the Leyte geothermal power project, Philippines, in: PROCEEDINGS,. Presented at the Twenty-Second Workshop on Geothermal Reservoir Engineering, Stanford University, Stanford, California, p. 6.

Malibiran, M.A.O., Leyrita, J.L., Sambrano, B.G., Nogara, J.B., 2013. Well permeability enhancement through hydraulic stimulation conducted in the Mt. Apo geothermal project, in: Proceedings. Presented at the Thirty-Eighth Workshop on Geothermal Reservoir Engineering, Stanford University, Stanford, California, p. 4.

McClure, M.W., 2012. Modeling and characterization of hydraulic stimulation and induced seismicity in geothermal and shale gas reservoirs. Stanford University, Stanford, California.

McClure, M.W., Horne, R., 2012. Opening mode stimulation or shear stimulation? GRC Trans. 36, 5.

McCourt, W.J., Cobbing, E.J., 1993. The geochemistry, geochronology and tectonic setting of granitoid rocks from southern Sumatra, western Indonesia. South. Sumatra Geol. Miner. Explor. Proj. Report Series 9.

McCourt, W.J., Crow, M.J., Cobbing, E.J., Amin, T.C., 1996. Mesozoic and Cenozoic plutonic evolution of SE Asia: evidence from Sumatra Indonesia. Geol. Soc. Lond. Spec. Publ., Tectonic Evolution of SE Asia 106, 321–335.

Milicich, S.D., Clark, J.P., Wong, C., Askari, M., 2015. A review of the Kawerau Geothermal Field, New Zealand. Geothermics. doi:10.1016/j.geothermics.2015.06.012

Mulyadi, 2010. Case study: “Hydraulic fracturing experience in the Wayang Windu Geothermal field,” in: Proceedings. Presented at the World Geothermal Congress, Bali, Indonesia, p. 9.

Murray, L.E., Rohrs, D.T., Rossknecht, T.G., Aryawijaya, R., Pudyastuti, K., 1995. Resource evaluation and development strategy, Awibengkok field., in: Proceedings. Presented at the World Geothermal Congress, Florence, pp. 1525–1529.

Nitsuma, H., Nakatsuka, K., Takahashi, H., Chubachi, N., Yokoyama, H., Sato, K., 1985. Long-distance acoustic emission monitoring of hydraulically induced subsurface cracks in nigorikawa geothermal field, Japan. Geothermics 14, 539–551. doi:10.1016/0375-6505(85)90005-7

Nitters, G., 2015. Personal communication.

Omenda, P.A., 2012. Geothermal development in Kenya: a country update - 2012, in: Proceedings. Presented at the ARGeo, p. 5.

O’Sullivan, M.J., Pruess, K., Lippmann, M.J., 2001. State of the art of geothermal reservoir simulation. Geothermics 30, 395–429. doi:10.1016/S0375-6505(01)00005-0

Pasikki, R.G., Gilmore, T., G., 2006. Coiled tubing acid stimulation: the case of AWI 8-7 production well in Salak geothermal field, Indonesia. Presented at the Thirty - first workshop on geothermal reservoir engineering, Stanford University, Stanford, California.

Pasikki, R.G., Libert, F., Yoshioka, K., Leonard, R., 2010. Well stimulation techniques applied at the Salak Geothermal field., in: Proceedings. Presented at the World Geothermal Congress, Bali, Indonesia, p. 11.

Perkins, T.K., Gonzalez, J.A., 1985. The effect of thermoelastic stresses on injection well fracturing. Soc. Pet. Eng. J. 25, 78–88.

Portier, S., André, L., Vuataz, F.-D., 2007. Review on chemical stimulation techniques in oil industry and applications to geothermal systems. (Technical Report), WP4: Drilling, stimulation and reservoir assessment. CREGE, Neuchatel - Switzerland.

Purnomo, B.J., Pichler, T., 2014. Geothermal systems on the island of Java, Indonesia. J. Volcanol. Geotherm. Res. 285, 47–59.

Sánchez Luviano, M., Flores-Armenta, M., Ramírez Montes, M., 2015. Thermal stimulation to improve the permeability of geothermal wells in Los Humeros geothermal field, Mexico, in: Proceedings. Presented at the World Geothermal Congress, Melbourne, Australia, p. 10.

Sanjuan, B., Brach, M., 2000. Bouillante geothermal field (Guadeloupe, West Indies): Geochemical monitoring during a thermal stimulation operation, in: PROCEEDINGS,. Presented at the Twenty-Fifth Workshop on Geothermal Reservoir Engineering, Standford University, Stanford, California, p. 8.

Scali, M., Maurizio, C., Tarquini, S., Romagnoli, P., 2013. The Larderello - Travale and Amiata geothermal fields: case histories of enineered geothermal systems since the early 90’s, in: Proceedings. Presented at the European Geothermal Congress, Pisa, Italy, pp. 1–99.

Schulte, T., 2008. Drilling Stimulation and Reservoir Assesment- State of the art and challenges ahead, in: Engine, Best Practice Guide. Presented at the Engine Final Conference, Vilnius, Lithuania, p. 18.

Setijadji, L.D., 2010. Segmented volcanic arc and its association with geothermal fields in Java Island, Indonesia, in:

Proceedings World Geothermal Congress 2010. Bali, Indonesia.

Shemeta, J.E., 1994. Regional tectonic stress orientation in the vicinity of the Awibengkok geotermal field, Java, Indonesia. Unocal Unpubl.

Sherburn, S., Sewell, S.M., Bourguignon, S., Cumming, W., Bannister, S., Bardsley, C., Winick, J., Quinao, J., Wallis, I.C., 2015. Microseismicity at Rotokawa geothermal field, New Zealand, 2008–2012. Geothermics 54, 23–34. doi:10.1016/j.geothermics.2014.11.001

Siega, C.H., Grant, M., Powel, T., 2009. Enhancing injection well performance by cold water stimulation in Rotokawa and Kamerau geothermal fields., in: Proceedings. Presented at the Thirtieth Annual EDC Geothermal Conference, Manila, Philippines.

Sigurdsson, O., 2015. Experimenting with deflagration for stimulating geothermal wells, in: Proceedings. Presented at the World Geothermal Congress, Melbourne, Australia, p. 11.

Simandjuntak, T.O., Barber, A.J., 1996. Contrasting tectonic styles in the Neogene orogenic belts of Indonesia. Geol. Soc. Lond. Spec. Publ., Tectonic Evolution of Southeast Asia 106, 185–201.

Siratovich, P.A., Ingo, S., Hormuth, S., Bjornsson, A., 2011. Thermal stimulation of geothermal reservoirs and laboratory investigation of thermally induced fractures. Geotherm. Resour. Counc. Trans. 35, 9.

Soeparjadi, R., Horton, G.D., Wendt, B.E., 1998. A review of the Gunung Salak geothermal expansion project.l, in: Proceedings. Presented at the 20th New Zealand Geothermal Workshop, University of Auckland, Auckland, New Zealand, pp. 153–158.

Srivastava, R., Guzman-Guzman, A., 1998. Practical approximation of the well function. Ground Water 36, 5.

Stimac, J., Nordquist, G., Suminar, A., Sirad-Azwar, L., 2008a. An overview of the Awibengkok geothermal system, Indonesia. Geothermics, Indonesian geothermal prospects and developments 37, 300–331. doi:10.1016/j.geothermics.2008.04.004

Stimac, J., Nordquist, G., Suminar, A., Sirad-Azwar, L., 2008b. An overview of the Awibengkok geothermal system, Indonesia. Geothermics 37, 300–331.

Stimac, J., Sugiaman, F., 2000. The Awi 1-2 core research program: part I, geologic overview of the Awibengkok geothermal field, Indonesia., in: Proceedings. Presented at the World Geothermal Congress 2000, Kyushu-Tohoku, Japan, p. 6.

Sugiaman, F., 2003. State of stress and welbore stability in the Awibengkok field. Unocal Unpubl.

Theis, C.V., 1935. The relation between the lowering of the Piezometric surface and the rate and duration of discharge of a well using ground-water storage. Eos Trans. Am. Geophys. Union 16, 519–524. doi:10.1029/TR016i002p00519

Thompson, A., 2010. Geothermal development in Canada: country update, in: Proceedings. Presented at the World Geothermal Congress, Bali, Indonesia, p. 3.

Tingay, M., Morley, C., King, R., Hillis, R., Coblentz, D., Hall, R., 2010. Present-day stress field of Southeast Asia. Tectonophysics 482, 92–104.

Tulinius, H., Correia, H., Sigurdsson, O., 2000. Stimulating a high enthalpy well by thermal cracking, in: Proceedings. Presented at the World Geothermal Congress, Kyushu-Tohoku, Japan, p. 6.

Weaver, J.D., Parker, M., van Batenburg, D.W., Nguyen, P.D., 2007. Fracture-Related Diagenesis May Impact Conductivity. SPE J. 12, 272–281. doi:10.2118/98236-PA

Yasuhara, H., Polak, A., Mitani, Y., Grader, A.S., Halleck, P.M., Elsworth, D., 2006. Evolution of fracture permeability through fluid–rock reaction under hydrothermal conditions. Earth Planet. Sci. Lett. 244, 186–200. doi:10.1016/j.epsl.2006.01.046

Yglopaz, D.M., Buiing, B.C., Malate, R.C.M., Ana, F.X.M., Austria, J.J.C., Salera, J.R.M., Lacanilao, A.M., Sarmiento, Z.F., 1998. Proving the Mahanagdong B resource: a case of large scale well stimulation strategy, Leyte geothermal power project, Philippines, in: PROCEEDINGS,. Presented at the Twenty-Thrid Workshop on Geothermal Reservoir Engineering, Stanford University, Stanford, California, p. 6.

Yoshioka, K., Izgec, B., Pasikki, R.G., 2009. Optimization of geothermal well stimulation design using a geomechanical reservoir simulator, in: Proceedings. Presented at the Thirty Third Workshop on Geothermal Reservoir Engineering, Standford University, Stanford, California.

Yoshioka, K., Jermia, J., Pasikki, R., Ashadi, A., 2015. Zonal hydraulic stimulation in the Salak Geothermal field, in: Proceedings. Presented at the World Geothermal Congress, Melbourne, Australia, p. 7.

Zheng, K., Wang, M., 2012. Geothermal resources development in Tibet, China, in: Proceedings. Presented at the New Zealand Geothermal Workshop, Auckland, New Zealand, p. 5.

Appendix A – Details regarding the outcome of stimulated wells in the Salak field, Indonesia

Well	Downhole T (°C)	Pressure (Mpa)	Initial II/PI (kg/s/bar)	Post stim II/PI (kg/s/bar)	Increase (%)	Hydraulic	Thermal	Acid	Notes	Reference
Awi 8-7	260	10	4,68	12,06	61%		1	CT	Well cooled to 100 °C for corrosion inhibitor	Pasikki and Gilmore (2006)
Awi 11-6OH	235	n.a.	2,00	4,00	100%		1		Only initial increase, production values not commercial	Pasikki et al. (2010)
Awi 11-5	280	n.a.	1,10	2,60	136%		1		Only initial increase, production values not commercial	″
Awi 11-6OH	235	n.a.					1	SAS	Acidified condensate injected with T of 26 °C	Pasikki et al. (2010)
Awi 1-9	> 230	n.a.	1,64	5,12	211%		1	CT	Cooled with fresh water for corrosion inhibitor	Pasikki et al. (2010)
Awi 8-7	> 230	n.a.	3,84	9,69	152%		1	CT	Cooled with fresh water for corrosion inhibitor	″
Awi 8-8	250	n.a.	4,20	9,69	130%		1	CT	Cooled with fresh water for corrosion inhibitor	″
Awi 8-10	> 230	n.a.	4,57	21,38	368%		1	CT	Cooled with fresh water for corrosion inhibitor	″
Awi 10-3	> 230	n.a.	4,39	8,04	83%		1	CT	Cooled with fresh water for corrosion inhibitor	″
Awi 11-4	> 230	n.a.	6,40	13,52	111%		1	CT	Cooled with fresh water for corrosion inhibitor	″
Awi 11-5	> 230	n.a.	2,92	6,94	138%		1	CT	Cooled with fresh water for corrosion inhibitor	″
Awi 11-6RD	> 230	n.a.	1,46	6,76	363%		1	CT	Cooled with fresh water for corrosion inhibitor	″
Awi 11-6RD *	> 230	n.a.	6,76	6,76	0%		1	CT	Cooled with fresh water for corrosion inhibitor	″
Awi 19-2	> 230	n.a.	1,10	2,92	167%		1	CT	Cooled with fresh water for corrosion inhibitor	″
Awi 18-1	~ 250	n.a.	0,82	2,21	169%		1		Injectate with T of 38 °C	Pasikki et al. (2010)
Awi 20-1	~ 200	n.a.	1,44	1,29	-11%		1		Injectate with T of 38 °C; WHP dropped during job	″
				average increase	168%					

SAS: Slow Acid Stimulation

CT: Coiled tubing

*) 2nd acid job

Successful

Unsuccessful

Partly successful

APPENDIX B – DETAILS REGARDING THE OUTCOME OF STIMULATED WELLS WORLDWIDE

Country	Field	Stimulated wells	Reservoir lithology	General stress state	Steam/ liquid	Depth Feedzone (m)	Downhole Pi (Mpa)	Downhole T (°C)	PI/II increase (%)	Hydraulic	Thermal	Acid	Reference
New Zealand	Rotokowa	RK-23	Andesite	Extensional	Injection	2790-3100	30	340-200	138%				Siega et al. (2009); Siratovich et al. (2012)
		RK-21	Andesite	Extensional		2350-2500	24,5	340-200	11%				Davidson et al. (2012); Sheburn et al. (2014)
	Ngatamariki	NM-08	Mix of volcanoclastic	Extensional	Injection	3600	35	> 275	575%				Clearwater et al (2015)
		NM-09	intrusive and extrusive	Sh-30-120deg	Injection	3551	35	> 275	131%				
		NM-10	lava's		Injection	2834	28	260	29%				
	Tauhara	1			Liquid	830 - 940	5,7	175	58%			1	
	Kawerau	KA-43	Greywacke	Extensional	Injection	1410-1470; 2290-bt	23	250-310	95%				Siega et al. (2009)
		KA-44	Greywacke	Extensional	Injection	1450 - 2560	24		389%			1	Milicich et al. (2015)
		PK-4A	Greywacke	Extensional	Steam	1408 - 1880	17	55	68%			1	Lim et al. (2011)
Iceland	Krafla**	KJ-14	Basalt	Extensional	Steam	2100	~ 21 (bottom)	210-340	400%				Siratovich et al. (2011); Axelsson et al. (2006)
	Hellisheidi	HE-8	Basalt	Extensional	Injection	1350 - 2200	17,5	275	200%				Bjornsonn et al. (2004); Gunnarsson et al. (2015)
	Reykanes (+)	RN-14	Basalt	Extensional	Steam	2310	23	290	17%				Axelsson et al. 2009
		RN-15	Basalt	Extensional	Steam	2510	25	280	14%				
		RN-16	Basalt	Extensional	Steam	2630	26	220	67%				
		RN-18	Basalt	Extensional	Steam	1820	18	> 285	8%				
		RN-19	Basalt	Extensional	Steam	2250	22	250 - 260	0%				
		RN-21	Basalt	Extensional	Steam	1710	17	275	117%				
		RN-22	Basalt	Extensional	Steam	1680	16	305	0%				
Japan	Sumikawa	SA-1	Andesite	Extensional	Liquid	1610	11	305	64%				Kitao et al. (1995)
		SA-2	Andesite	Extensional	Liquid	1800	12	300	17%				Ariki et al. (2000)
		SA-4	Andesite	Extensional	Liquid	1150	8,3	290	22%				
		S-4	Andesite	Extensional	Liquid	n.a.	n.a.	n.a.	296%				
		SB-1	Andesite	Extensional	Liquid	n.a.	n.a.	n.a.	493%				
		SB-2	Andesite	Extensional	Liquid	n.a.	n.a.	n.a.	-26%				
		SB-3	Andesite	Extensional	Liquid	n.a.	n.a.	n.a.	27%				
	Nirogikawa/ Mori	n.a.	n.a.	n.a.	Liquid	500-2000	Variable	~ 250	n.a.				(Fukuda et al., 2010; Nitsuma et al., 1985)
	Matsukawa	TG-2	n.a.	n.a.	Steam	710 - 1298	n.a.	n.a.	n.a.				Hyodo et al. (1995)
	Kakkonda	42	Granite/andesite	Strike slip/ reverse	Steam	1353 - 1370	15	242-246	22%				Kizaki & Sato (1996)
		47	Granite/andesite	Strike slip/ reverse	Steam	1156 - 1416	14	~ 200 -220	n.a.				Kato et al. (2000)
		7	Granite/andesite	Strike slip/ reverse	Steam	1313	13	197 - 220	n.a.				
		13	Granite	Strike slip/ reverse	Steam	2345	23	> 330	n.a.				
		2	Granite/andesite	Strike slip/ reverse	Steam	977; 1144	0,96; 1,1	206 - 236	n.a.				
Guadeloupe	Bouillante	BO-4	Volcanic tuff	Extensional	Steam	1050	5,1 (?)	250	56%				Tunlinius et al. (2000); Sanjuan and Brach (2000)
Mexico	Los Humeros	H-40	Andesite and Basalt	Strike slip/ extensional	Injection	1610 - 2120 (mult.)	9,5	240	214%				Siratovich et al. 2011
		H-41	Andesite and Basalt	Strike slip/ extensional	Fluid	1250-1600; 1750-1850	8,8; 12,7	150; 200	25%				Luviano et al. (2015)
		H-43	Andesite and Basalt	Strike slip/ extensional	Fluid	1550-1800; 2050-2200		200; 150	n.a.				
		H-44	Andesite and Basalt	Strike slip/ extensional	Fluid	1600-1700		200-240	n.a.				
		H-45	Andesite and Basalt	Strike slip/ extensional	Fluid	1400-1600; 200-2150	6; 9,5	140; 290	n.a.				
	Las Tres Virgines	LV-3	Andesite	Extensional	Steam/Liquid	n.a.	n.a.	n.a.	0%				Flores & Ramirez (2010)
		LV-04	Andesite	Extensional	Steam/Liquid	n.a.	n.a.	n.a.	366%				Gutierrez-Negrin (2015)
		LV-4A	Andesite	Extensional	Steam/Liquid	n.a.	n.a.	n.a.	100%				
		LV-11	Andesite	Extensional	Steam/Liquid	n.a.	n.a.	n.a.	191%				Guillermo et al. (2003)
		LV-13	Andesite	Extensional	Steam/Liquid	1570-1580; 1850-1930;2000-2081	n.a.	n.a.	17%				Guillermo et al. (2003)
		LV-13D	Andesite	Extensional	Steam/Liquid	n.a.	n.a.	n.a.	100%				
	Los Azufres	AZ-7	Andesite	Extensional	Injection	n.a.	n.a.	n.a.	13%				Tello et al. 2010
		AZ-8	Andesite	Extensional	Injection	n.a.	n.a.	n.a.	127%				Flores & Ramirez (2010)
		AZ-9D	Andesite	Extensional	Steam	n.a.	n.a.	n.a.	168%				
		AZ-9AD	Andesite	Extensional	Steam	n.a.	n.a.	n.a.	209%				
		AZ-15	Andesite	Extensional	Injection	n.a.	n.a.	n.a.	32%				
		AZ-25	Andesite	Extensional	Steam	n.a.	n.a.	n.a.	88%				
		AZ-52	Andesite	Extensional	Injection	n.a.	n.a.	n.a.	143%				
		AZ-56R	Andesite	Extensional	Steam	n.a.	n.a.	n.a.	367%				
		AZ-64	Andesite	Extensional	Steam	n.a.	n.a.	n.a.	0%				
		AZ-68D	Andesite	Extensional	Steam	n.a.	n.a.	n.a.	540%				
		AZ-36	Andesite	Extensional	Steam	n.a.	n.a.	n.a.	133%				
		AZ-47D	Andesite	Extensional	Steam	1050-1200; 1300-1400; 1450-1520	12,3	218	500%				
		AZ-51	Andesite	Extensional	Steam	n.a.	n.a.	n.a.	147%				
Costa Rica	Borinquen	PGB-01	Andesite and pyroclastic flows	Extensional	Fluid	1850-2050; 2100	~12,5; 14,0	~250; ~265	295%				Castro-Zúñiga (2015)
	Las Pailas	PGB-08	Andesite and pyroclastic flows	Extensional	Fluid	1042-1065; 1286; 1602-1692	4,7; 6,5; 9,8	232; 243; 243	180%				
Philippines	Palinpion 1	PN31D							n.a.				
		PN27D							n.a.				
		LG4D			Steam				n.a.				Amisoto et al (2005)
		ML2RD			Injection				n.a.				
	Mt. Apo	K6	Andesitic	Extensional	Fluid & Steam	200-2050; 2300-2350		~ 200- 300	950%				Malibran et al. (2013); Esberto et al. (1998)
		SK-2D	Andesitic	Extensional	Fluid & Steam	1450-1500; 1600-1640; 1700-1837	7; 7,5; 8	225; 220; 220	73%				Malate et al. (2000)
	Leyte	MG-7RD	n.a.	Extensional	Injection	1250-1300; 1650-1750; 1800-1815	6; 7; 10	210; 250; 245	13%				Malate et al. (1997)
		4R7D	n.a.	Extensional	Injection	1980; 2260-2492	19,4; 24,4	50; 200	94%				
		4R12D	n.a.	Extensional	Injection	1650-1790; 2550-2624	18; 20	30; 40	59%				
		MN-1	n.a.	Extensional	Wet steam	n.a.	n.a.	300-320	0%				
		MG-8D	n.a.	Extensional	Wet steam	n.a.	n.a.	300-320	44%				Caranto et al. (2010)
		MG-10D	n.a.	Extensional	Wet steam	n.a.	n.a.	300-320	57%				
		MG-26D	Sediments/ ultramafics	Extensional	Wet steam	n.a.	n.a.	290-340	-5%				Yglopaz et al. (1998)
		MG-27D	Sediments/ ultramafics	Extensional	Wet steam	n.a.	n.a.	290-341	157%				
		MG-29D	Sediments/ ultramafics	Extensional	Wet steam	n.a.	n.a.	290-342	6%				
		MG-30D	Sediments/ ultramafics	Extensional	Wet steam	n.a.	n.a.	290-343	500%				
		MG-31D	Sediments/ ultramafics	Extensional	Wet steam	n.a.	n.a.	290-344	319%				
Italy	Larderello	Well A	Metamorphic	Extensional	Dry steam	2245; 3050; 3200; 3700; 3900	38	n.a.	161%				Scali et al. (2013)
		Well B	Metamorphic	Extensional	Dry steam	2110	21	n.a.	159%				
		Well C	Limestone	Extensional	Injection	525	5	n.a.	900%				
	Latera	Ln1	Syenite/ metamorphic	Extensional	Injection	1860	18	230	30%				Barelli et al (1985)
		Ln6	Metamorphic limestone	Extensional	Injection	1720	17	200	n.a.				
USA	Geysers	OS-22	Fractured greywacke	Extensional	Dry Steam	1400-1700	17	230	n.a.				Enting (1999); Hanold et al (1982)
	Bacca	B-23	Fractured Tuff	Extensional		1000-1060	10	230	n.a.				Enting (1999)
		B-20	Fracutred Tuff	Extensional		1490-1550	15	280	n.a.				
	Beowawe	R21-19	Fractured Volcanics	Extensional		1350-2350	23	196	230%				Enting (1999); Morris et al. (1984)

**) Most of the wells in the Krafla field have been stimulated.

(+) Thirtheen wells have been stimulated, but only 7 improvement data

Successful
Unsuccessful
Partly successful